AN ABSTRACT OF THE DISSERTATION OF

Duc Xuan Nguyen for the degree of Doctor of Philosophy in Pharmaceutical Sciences presented on March 14, 2018.

Title: Development of thermosensitive injectable hydrogel and transdermal controlled release formulations for tacrolimus

Abstract approved:

_____

Adam W. G. Alani

TAC is the most commonly used medication in post transplantation maintenance immunosuppression therapy. TAC lipophilicity and its erratic oral absorption especially in the presence of food intake result in great intra- and interpatient pharmacokinetic variations. Complicated dosing and frequent required therapeutic monitoring is thought to be the main cause of non-adherence in the population using this medication. On top of that, being a highly potent drug, it requires a strict control of concentration in whole blood to avoid side effects and graft rejection. Therefore, there is a need to simplify the medication regimen and lower the frequency of medication intake, as such a strategy has been proven to help with increased adherence to medication intake while being less likely to interfere with patient daily schedule. Injectable hydrogels and transdermal drug delivery systems are often employed to deliver drug molecules directly to the blood stream, bypassing GI absorption and hepatic first-pass-effect. This work encompasses the

development of a novel biodegradable/biocompatible polyamino-based polymer library for development of thermosensitive hydrogels, the development of nanoparticle-hydrogel composite formulations that eliminate the burst release commonly seen in current hydrogel formulations on the market, and the development of a matrix type transdermal patch utilizing synergistic enhancers to deliver a large molecule such as TAC.

A library of polyamino-based polymers is synthesized and characterized for their temperature sensitive gelation. Three polyaspartate polymers are identified to be able to undergo thermosensitive gelation, where the transition temperature is dependent on the polymer concentration and hydrophobicity. The gelation mechanism is shown to be due to aggregation of β-sheet formation of the polymer. This phenomenon allows a smaller burst release of TAC from the gel demonstrated both *in vitro* and *in vivo*. The aminoGel formulations show a sustained release profile of TAC over a 7-day period in rats. To investigate the effect of NP on reducing the burst effect of drug release from hydrogels, two NP-hydrogel composite platforms capable of delivering TAC within therapeutic window for up to 7 days are developed. By loading TAC into PEG_{5k}-*b*-PCL_{10k} nanoparticle, the stable formulation allows the incorporation of TAC into the hydrogel solution without using toxic organic solvent. The TAC-NP-hydrogel composites demonstrate no burst effect when compares to the TAC-loaded hydrogel alone.

Another formulation that has been developed for TAC in this is a transdermal patch incorporating synergistic penetration enhancers. TAC is a large molecule beyond the ideal molecular size for transdermal delivery. Here we have demonstrated the feasibility of delivering such molecule across the skin barrier using a pair of synergistic enhancers, phenylpiperazine and TPGS. By incorporating the drug and penetration enhancers into a matrix type transdermal patch using Eudragit RL100 and PVP K30 at 2:8 ratio as matrix formers, the patch is found to deliver TAC across pig ear skin in Franz diffusion experiment at a rate of 5.11±0.71 $\mu g/cm^2/hr$. The release rate is confirmed in rat PK studies. The patch size of 2.5 cm^2 is shown to be able to maintain TAC concentration within the therapeutic

range for up to 7 days. The patch size can be cut to accommodate different release rates, allowing for customized dosing based on weight and scaling to other animal models.

Overall, the formulations developed from our studies would add into the repertoires of available formulations for transplantation clinicians. These formulations can be used to maintain patients who demonstrate difficulties in adhering to their oral TAC regimens or variability in their absorption following TAC administration.

Development of Thermosensitive Injectable Hydrogel and Transdermal Controlled Release Formulations for Tacrolimus

by

Duc Xuan Nguyen

A DISSERTATION

submitted to

Oregon State University

in partial fulfillment of

the requirements for the

degree of

Doctor of Philosophy

Presented March 14, 2018

Commencement June 2018

Doctor of Philosophy dissertation of Duc Xuan Nguyen presented on March 14, 2018

APPROVED:

Major Professor, representing Pharmaceutical Sciences

Dean of the College of Pharmacy

Dean of the Graduate School

I understand that my dissertation will become part of the permanent collection of Oregon State University libraries. My signature below authorizes release of my dissertation to any reader upon request.

Duc Xuan Nguyen, Author

ACKNOWLEDGEMENTS

Firstly, I would like to express my sincere gratitude to my advisor Dr. Adam Alani for the continuous support of my Ph.D. study and related research, for his patience, motivation, and immense knowledge. His guidance helped me in all the time of research and writing of this thesis. I could not have imagined having a better advisor and mentor for my Ph.D study. I feel privileged to be his first Pharm.D./Ph.D. student, and I would like to extend my heartfelt gratitude for the valuable guidance and advices that he continues to provide throughout my career.

Vidhi Shah is the second person I would like to acknowledge. She has helped me a great deal in designing my transdermal studies. Her advices and helps in preparing the formulations and the pig skins are what make this work possible. It is my honor to work closely with her on our liposome formulation project, FRET nanoparticle projects, and many other works. I would like to thank my committee members Dr. Mark Christensen, Dr. Oleh Taratula, Dr. David Lee, and Dr. Natalia Shulzhenko for providing me with valuable insights and for guiding me in completing my projects. I would like to also acknowledge Olena and Canan for our collaboration project. Canan is the primer of many of my novel ideas including the mRNA delivery dendrimers and the entrepreneur adventure. Also other lab colleagues Adel and Brianna for keeping the lab fun and full of curiosity. I would especially like to acknowledge Debra Peters for her support throughout my graduate program and the College of Pharmacy for providing financial support.

A special shout out to my parents and siblings for their continual support of my prolonged education. Also, a big hug to uncle Hiep for repairing my cars and uncle Chat for preparing my tax for free during my time as a poor graduate student.

And last but not least, special thanks to my undergraduate students Rosa, Rohi, Michelle, Mukund, and Yvonne for helping with my experiments.

CONTRIBUTION OF AUTHORS

Chapter 1

Written by Duc Nguyen with editing help from Dr. Adam Alani.

Chapter 2

Dr. Adam Alani and Duc Nguyen designed majority of the experiments. Dr. Gyan Mishra provided technical expertise on synthesizing PEG-PVL-PEG polymers. Dr. Vidhi Shah and Adel Al Fatease helped with animal works. Dr. Deepa Rao helped with suggestions and in preparing the manuscript.

Chapter 3

The experiments were designed by Duc Nguyen, Vidhi Shah, and Dr. Adam Alani. Duc Nguyen did most of the animal work with the help of Vidhi and Adel. Dr. Amira Al-Uzri and Dr. Ali Olyei provided valuable input for tacrolimus immunosuppression therapy.

Chapter 4

Written by Duc Nguyen

TABLE OF CONTENTS

Page

TABLE OF CONTENTS (continued)

Page

TABLE OF CONTENTS (continued)

Page

LIST OF FIGURES

Figures Page

LIST OF FIGURES (continued)

Figures Page

LIST OF TABLES

Tables Page

DEDICATION

For my mother whose love and great food are the fuel of my achievement

For my father, who taught me the art of woodworking

For my late grandmother, who taught me the value of education

Ngọc bất trác bất thành khí, nhân bất học bất tri lý.

Chapter 1.

INTRODUCTION

Duc X. Nguyen

1. INTRODUCTION TO IMMUNOSUPPRESSION THERAPY IN SOLID ORGAN TRANSPLANTS

1.1. History of immunosuppression therapy in solid organ transplant:

Immunosuppressant drugs are a class of drugs that suppress, or reduce, the strength of the body's immune system. Some of these drugs are anti-rejection medications for use post solid organ transplantation to prevent rejection. Other immunosuppressant drugs are often used to treat autoimmune disorders such as lupus, psoriasis, and rheumatoid arthritis. Since the first successful kidney transplant in 1954 solid organ transplantation has evolved from an experimental procedure to a standard-of-care, lifesaving procedure, and cost-effective when compared with nontransplantation management strategies of both chronic and acute end stage organ failures. Prior to the understanding of immune system involvement in graft rejection and the introduction of immunosuppression therapy, early efforts at transplantation were confined to matching donors only or risk fatal rejection[1]. Initially, radiation served as a "proof of concept" that immunosuppression could improve graft survival and that a more refined and titratable modality, such as pharmacologic immunosuppression was much needed. Several antileukemia agents such as cyclophosphamide, methotrexate, and azathioprine were tried during this time. A breakthrough came in 1963 when Thomas Starzl demonstrated that using a combination of high dose prednisone and azathioprine can reverse renal allograft rejection and induce host tolerance. As transplant patient survival increased, a secondary issue appeared. In 1967, Starzl published "Death after Transplantation" summarized the outcome of the first 125 organ recipients at the University of Colorado. The first 60 deaths reported demonstrated a remarkably high rate of opportunistic bacterial, fungal, viral and protozoal infections, the results of global nonselective immune inhibitory effects of early immunosuppressants.

When the FDA approved cyclosporine as "Sandimmune" in 1983, it ushered in the calcineurin era of immunosuppression therapy. Cyclosporine, a natural peptide product of the fungi *Cylindrocarpon lucidum* and *Trichderma polysporum*, the first calcineurin

inhibitor, possesses potent antiproliferative effects toward T-helper lymphocyte and lymphocyte-derived antibody synthesis but without the bone marrow suppressive effect of azathioprine or the broad immune nonlymphocyte inhibitory effects of steroids[2]. Following the introduction of cyclosporine to existing immunosuppression regimen improved graft survival of all solid organ transplant miraculously; the 1-year graft survival for kidney and liver transplants went from 18%-30% to 89%-70% respectivly[1]. However, cyclosporine is not without side effects; they included: neurotoxicity, nephrotoxicity, opportunistic infection, de novo diabetes, and B-cell lymphoma. These complications were only partially responsive to dose-reduction strategies.

In the early 1990s, FK-506 (tacrolimus) started as a clinical investigation in cyclosporine-related liver allograft rejection cases. Converting to tacrolimus rescued 75% of cyclosporine-refractory rejection cases[3]. FK506 exhibited immunosuppressive activity similar to that of CsA but 100 times as potent. The drug forms a complex with FK-binding proteins and selectively binds to and inhibits calcineurin. This process inhibits the translocation of NF-AT, leading to reduced production of IL-2, TNF-α, IL-3, IL-4, CD40L, granulocyte-macrophage colony-stimulating factor, and interferon-gamma[4]. Ultimately, proliferation of T lymphocytes, especially T-helper cells, is reduced. Adverse effects are similar to those of cyclosporine but with a lower incidence of hypertension, hyperlipidemia, skin changes, hirsutism, and gum hyperplasia. However, there are higher incidence of new-onset diabetes mellitus after transplantation and neurotoxicity. The greater potency and equivalent safety of FK-506 compared to that of cyclosporine resulted in significant conversion to FK-506 based immunosuppression for liver, kidney, pancreas and thoracic organ transplantation.

The late 1990s and early 2000s saw the introduction of novel immunosuppressive agents such as antilymphocyte drugs, a new antiproliferative agent (mycophenolate mofetil), interleukin-2 receptor antagonists, and sirolimus. Antilymphocyte antibodies are primarily used in induction phase of immunosuppression, right after transplantation

surgery. Their rate of utilization in induction therapy varies from among different types of solid organ transplantation ranged from lowest use in liver transplant recipients (31.1%) to highest use in pancreas recipients (90.4%)[5]. The reason for such wide range of utilization is because physicians have to weight potential benefits of lower incidence of acute rejection episodes against the increased risk of developing infections and additional medication cost. Sirolimus, an mTOR inhibitor, inhibits the proliferation of T lymphocytes by blocking IL-2 activation and phosphorylation of 70 S6 kinase[6]. The role of sirolimus in immunosuppression after solid organ transplantation is still unclear. Replacing calcineurin inhibitors with mTOR inhibitors during maintenance phase has resulted in non-superior graft-survival rate. However, sirolimus use alone does not have the irreversible nephrotoxicity associated with the use of calcineurin inhibitors. Thus, sirolimus is preserved mostly for patients unable to tolerate calcineurin inhibitors. Mycophenolate mofetil (MMF) is a prodrug that is rapidly metabolised to its active metabolite mycophenolic acid. It inhibits lymphocyte function more selectively than azathioprine by blocking purine biosynthesis via inhibition of the enzyme inosine monophosphate dehydrogenase. Unlike other cells in the body, B and T lymphocytes rely on this pathway to synthesize purines for use in cell division. Because of this, MMF is less hepatotoxic and is not associated with malignancies. MMF has replaced azathioprine in most maintenance immunosuppressive regimens[6].

The development of calcineurin inhibitors, first cyclosporine and later tacrolimus, revolutionized the treatment of solid organ transplant patients. The improvement in both graft and patient survival in solid organ transplantation with the introduction of the calcineurin-inhibitors compared with the precalcineurin immunosuppressive era was impressive. Both have become cornerstones of maintenance immunosuppression (Figure 1-1).

1.2. Current status of immunosuppression therapy in organ transplant:

Nowadays, solid organ transplants are almost-routine surgical procedures in the United States. In 2015, more than 30,000 transplants were performed nationwide, and increase of 4.9% over the previous year. Kidney transplantation continued to be the highest at more than 19,000 operations, followed by liver (7707), heart (2819), lung (2072), pancreas (944), and intestine (141). Following successful organ transplantation, to avoid graft rejection patients are placed on immunosuppression therapy which comprises of 3 phases, induction, maintenance, and treatment of rejection. The selection of immunosuppressive regimen has a goal of maximizing patient and graft survival while minimizing undesired side effects such as infection, malignancy, and drug toxicity. The mainstay of current maintenance immunosuppression, aka "triple-drug regimen", consists of a calcineurin inhibitor, an antiproliferative agent, and a corticosteroid. Tacrolimus, MMF and prednisone have become the most common choices in their respective classes respectively. Across all types of solid organ transplant, tacrolimus is utilized in more than 90% of all maintenance therapies. Transplant recipients generally remain on calcineurin inhibitors for the remainder of their lifetime even if all other immunosuppressives are withdrawn. The reason for tacrolimus gradually supplanting cyclosporine as the backbone calcineurin inhibitor is due to lower acute rejection rates and potentially better graft survival rates demonstrated in several multicenter randomized controlled trials and meta-analyses.

However, as with cyclosporine, tacrolimus exhibits significant inter- and intra-patient pharmacokinetic variability and a narrow therapeutic window, thus requiring therapeutic drug monitoring. When taken orally, TAC is only partially absorbed with large inter- and intra-individual variability, with peak plasma concentration occurs after 1 to 8 hours. TAC oral bioavailability is limited, roughly 20%[7]. The presence of food can decrease the absorption of TAC. Because of its high lipophilicity, TAC undergoes extensive body distribution. In systemic circulation, the drug binds extensively to erythrocytes. In the plasma, TAC binds mainly to albumin and alpha-1-glycoprotein; the plasma protein

binding of tacrolimus is approximately 99 percent and is independent of concentration. Furthermore, TAC is a substrate of p-glycoprotein and is metabolized extensively by hepatic (and to a smaller extend, intestinal) CYP3A enzymes[8,9]. Bile excretion is the primary elimination route for TAC. There is great inter-patient variation in elimination half-life, 12±4 h in children, and 2.1-36 h in adult transplant patients[10]. Moreover, the elimination of TAC is decreased in the presence of liver impairment. To ensure efficacy and avoid toxicity, patients taking TAC typically have their trough concentration before the next dose measured and goals vary by type of organ transplant, time elapsed since transplant, concomitant immunosuppression, and other factors such as history of rejection, and complications. For maintenance immunosuppression in adult transplant recipients, tacrolimus trough concentrations can range from 5 to 15 ng/mL.

Although highly utilized in posttransplantation management, TAC deliver options are very limited. TAC is available commercially as IV formulation, oral immediate release (twice-daily) tablet (Prograf), and oral sustained release (once-daily) tablet (Envarsus XR) or capsule (Astagraf XL). Although the IV formulation of TAC can eliminate the concerns for erratic absorption, there are other concerns regarding side effects and administration safety with this route of administration. There are reports of arrhythmias, nephrotoxicity, and neurotoxicity associated with IV tacrolimus. This is thought to be coming from castor oil derivative, which carries the risk of anaphylactic reaction, in the IV formulation[11]. The risk of nephrotoxicity and neurotoxicity is more frequently associated with bolus dosing and may be reduced if administered over a 24-hour infusion. Furthermore, tacrolimus has been found to adsorb to polyvinyl chloride, commonly used in IV tubing and containers. Extraction of a toxic compound called phthalate can occur if IV tacrolimus is erroneously combined with polyvinyl chloride tubing or container. Therefore, TAC IV formulation should only be used with glass or polyethylene containers and tubing[12]. To sum up, IV TAC is reserved for patients whose enteral or sublingual administration is not an option.

Oral dosage form of TAC is available as either immediate release (Prograf tablet) or sustained release (Envarsus XR tablet and Astagraf XL capsule). Astagraf XL capsule utilizes ethylcellulose to prolong the drug release profile in the gastrointestinal tract via water permeation[13]. Envarsus XR tablet is a newer prolonged-release formulation and uses a proprietary MeltDose drug delivery technology (Veloxis Pharmaceuticals),which breaks the drug particles down into the smallest possible units increasing the drug surface area and thus with greater drug absorption[14]. Patients taking immediate release tablets are required to administer the medication twice or sometime multiple times per day to maintain the trough levels in the therapeutic range. Extended release formulations of TAC were invented to allow for once daily administration and improve PK profiles. Unwanted tacrolimus-associated hematologic and neurologic adverse events have been noted to happen or be most pronounced at peak serum tacrolimus blood concentrations. Both sustained release formulations of TAC, Astagraf XL and Envarsus XR, have shown lower C_{max} levels and a prolonged T_{max} compare with immediate-release tacrolimus. Patients switching from IR TAC to Astagraf XL are recommended by the manufacturer to follow a 1 to 1 dose conversion. However, post market studies have reported low trough levels and AUCs with the extended formulation. Current practice recommended a 10 to 30% increase in dose when convert patients to Astagraf XL[15]. On the other hand, switching from IR TAC to Envarsus XR requires a 30% dose reduction to achieve similar TAC exposure as recommened by manufacturer. Although the two sustained release TAC formulations offer improved PK profiles as compared to IR TAC, they are still taken orally, on empty stomach, and subjected to absorption and first pass metabolism variations as the IR formulation. This is especially true in adolescent and young adult population. As these patients' physiology can change quickly as they grow, it is challenging to adjust the oral dosing to adapt to the new PK.

1.3. Nonadherence is the current pitfall in posttransplantation immunosuppression.

Although short-term (<5 years) patient and graft survival rates continue to improve, long-term graft rejection rates are still high, indicating rooms for improvement. This is especially true in adolescent and young adult population. The graft survival probabilities are 77% and 63% at year 7 and 10 post-transplant, respectively, for recipients of living donor organs. The corresponding estimates for recipients of deceased donor organs are even lowered at 64% and 50%[5,16]. Studies have shown that nonadherence to medication intake is among the most important factors in kidney loss in both adult and pediatric populations. Furthermore, nonadherence in adolescent renal transplant recipients can negatively impact the successful transition to adult care and affect long term graft outcomes. Nonadherence to immunosuppressants is also associated with higher medical costs and increase rate of hospitalization. A recent study in adult kidney transplant recipients showed that each patient in the low-adherence group paid an extra $12000 over a 3-year period versus the well-adherence group[17].

Lifelong immunosuppression is necessary to maintain allograft function in transplant patients. When designing a formulation, treatment adherence is a vital factor that must be taken into account, because nonadherence has been associated with a 7 times increased in graft rejection[13]. This is especially true in adolescent population where nonadherence is at a whooping rate, 41%[18]. Solving nonadherence is a priority in improving adolescent kidney transplant. The immediate release formulation of TAC carries the disadvantages of large inter-/intra-patient variability in absorption, CYP3A5 metabolism, and a poor oral bioavailability causing variable blood drug levels necessitating the need for close therapeutic drug-level monitoring. This standard formulation of TAC also requires twice, sometimes multiple times, a day administration to maintain therapeutic levels. Multiple daily dosing of medications is known to negatively affect treatment adherence. Prolonged release formulations of TAC were designed to relieve the “pill burden” and improve patient adherence. When stable heart and liver transplant patients convert from twice-daily TAC regimen to once-daily regimen, patient

adherence has been shown to improve with no adverse effects[19,20]. Beckebaum et al[19] found a 53% reduction in nonadherence at 12 months post-conversion from TAC-BID to extended release TAC in liver transplant patients using the "Basel Assessment of Adherence Scale to Immunosuppressives." Similarly, Doesch et al[20] found a 49% reduction in nonadherence at 4-month post-conversion in heart transplant patients. Kidney transplantation is by far the largest transplantation population, greater than all other transplantation combined. It is suggested that oral sustained release TAC could improve adherence in this population. Yet, several studies found no significant improvement in patient adherence post conversion[15,21]. However, among those who persisted with the once-daily therapy, the proportion of patients taking the correct daily doses was significantly better than in twice-daily TAC recipients.

1.4. Pharmacokinetics of tacrolimus

Oral dosage forms of TAC are available as Prograf® 0.5 mg, 1 mg, 5 mg, twice-a-day capsule, Astagraf XL® 0.5 mg, 1 mg, 5 mg, once-a-day capsule, Envarsus XR® 0.75 mg, 1 mg, 4 mg, once-a-day capsule. IV TAC is available as 5 mg/mL solution in Cremophor™. Before administration, it should be diluted in normal saline or 5% dextrose to a concentration between 0.004–0.02 mg/L, and the drug should be given as a continuous infusion. Anaphylactic reactions to the castor oil derivative used in the excipients have been reported[11]. The initial dose of tacrolimus varies greatly among various transplant centers with a range of 0.1–0.3 mg/kg/d for orally administered drug and 0.03–0.1 mg/kg/d for intravenously administered drug. Recommended initial oral doses of tacrolimus are 0.2 mg/kg/d for adult kidney transplant patients, 0.10–0.15 mg/kg/d for adult liver transplant patients, 0.15–0.2 mg/kg/d for pediatric hepatic transplant recipients, and 0.075 mg/kg/d for adult heart transplant patients. Oral tacrolimus is usually given in two divided daily doses given every 12 hours[10,15,22].

Following oral intake, TAC bioavailability and rate of absorption have been reported to be highly variable. Generally, mean oral bioavailability is 25% but can range from 4-89%[10,22].

TAC is absorbed rapidly in most subjects, with T_{max} obtained in 0.5-1 h. However, during clinical trials, some patients experienced delayed drug uptake, yielding a flat absorption profile, an extended lag time or secondary peaks. The poor aqueous solubility of TAC, alteration of GI motility during hospitalization, and food interaction may be responsible for poor and erratic drug uptake[23]. To avoid the possible effect of food on tacrolimus bioavailability, the drug should be given on an empty stomach and at a constant time in relation to meals. Another factor influencing interpatient PK variability is CYP3A4 and 3A5 expression differences between patients[9]. TAC is metabolized extensively by CYP3A4 and 3A5 found in both the GI tract and in the liver. Once absorbed, TAC binds extensively to erythrocytes. The volume of distribution is 0.91±0.29 L/kg[10,24]. The volume of distribution has been reported to be 1.8 times higher in pediatric patients than adults due to higher body fat ratio. TAC is eliminated mainly (95%) by the liver and excreted into bile. TAC PK parameters in humans are summarized in (Table 1-1)[10,22]. Throughout our studies, we will be using rat as animal model to investigate the PK of various formulations. The PK parameters of TAC following IV injection into healthy rat are presented in (Table 1-2)[25]

1.5. Summary

The development of immunosuppressants for use in posttransplantation has gone a long way since the first transplants in the 50s. Nowadays, calcineurin inhibitors are the backbone of maintenance regimens often in combination with an antiproliferative and a steroid. TAC is the most commonly used calcineurin inhibitor of more than 95% maintenance transplant patients. Although oral prolonged release formulations of TAC are great improvement in patient adherence and PK compares to standard immediate release TAC, they still exhibit inherent weaknesses associated with oral dosing. Oral extended formulation of TAC still suffers the drawback of erratic pharmacokinetics caused by dietary interaction and changes in patient development. They must be taken on an empty stomach in the same way as standard once-daily TAC tablet. As of 2017, no other controlled release formulation of TAC that can be administered once every 1-2 weeks is

on the market. The development of a new controlled release formulation for TAC that can be administer once every 1-2 weeks is believed to further help improving patient quality of life and long-term graft survival.

2. INTRO TO CONTROLLED AND SUSTAINED RELEASE FORMULATIONS

2.1. A brief history of controlled drug delivery systems.

Since the first controlled release formulation Spansule® was introduced by Smith Kline & French in 1952 for 12-hour delivery of dextroamphetamine, the understanding and evolution of controlled drug delivery have gone a long way[26]. By the end of 1970s, different drug release mechanisms including dissolution-, diffusion-, osmosis-, and ion exchange-based mechanisms were characterized[27]. Knowledge gained during this era was channeled into development of numerous twice-a-day and once-a-day oral delivery systems. The same drug release mechanisms were also used to develop once-a-day and once-a-week transdermal patches.

Starting from the 1980s, significant efforts were devoted into developing zero-order delivery system[27]. Many technical advancements have been made and resulted in new techniques for drug delivery. These techniques are capable of controlling the rate of drug release. An ideal controlled drug delivery system is the one which delivers drug at a predetermined rate, locally or systemically, for a specified period of time[27,28]. Many so-called "smart" polymers and hydrogels were developed with release mechanisms dependent on environmental triggers such as changes in pH, temperature, or glucose concentration. By the turn of the millennium, much effort has been put on the development of nanocarriers and "smart" targeting delivery systems as a result of intensive support from the governmental funding agencies. This is based on the idea that the ideal medical therapy, especially tumor treatment and gene therapy, depends entirely on the ability of drug delivery systems to reach their intended targets without causing offsite effects. Although all nanoparticle drug delivery systems showed improved efficacy over the control in shrinking the tumor size in small animal models, none of the nanoparticle formulations have been successfully translated into clinical applications[27].

2.2. Why controlled release drug delivery systems matter?

Due to the difficulty of new drug discovery and development, more and more emphasis has been given to advancing drug delivery systems for existing drugs. The release of active ingredients from a controlled release drug delivery advances at a rate profile that is not only predictable kinetically, but also reproducible from one unit to another.

The clinical advantages of controlled release dosage forms are[28]:

- Reduction in frequency of drug administration
- Improved patient adherence
- Reduction in drug level fluctuation in blood
- Reduction in total drug usage when compared with conventional therapy
- Reduction in drug accumulation with chronic therapy
- Reduction in drug toxicity
- Stabilization of medical condition (because of more uniform drug levels)
- Improvement in bioavailability of some drugs because of spatial control

However, they are not without limitation such as[24]:

- Delay in onset of drug action
- Possibility of dose dumping in the case of a poor formulation strategy
- Possibility of less accurate dose adjustment in some cases
- Cost per unit dose is higher when compared with conventional doses
- Not all drugs are suitable for formulating into controlled release dosage form

Whether or not a drug molecule is suitable for formulating into controlled release dosage forms is depending on its physicochemical properties and biological factors. Although the requirements are different with various dosage forms, generally speaking, the dosage size, drug metabolism, and therapeutic window are important factors in considering whether a drug molecule is suitable for formulating into controlled release formulation[24–26]. A drug that requires large daily bulk dose, in grams, is often impractical to formulate into a controlled release form. When other excipients are incorporated, the final formulation can easily increase more than twice in size making administering such dosage form, whether orally, subcutaneously, or transdermal, uncomfortable for patients. Another factor to consider is the metabolism of the drug. Drugs with very short half-life are poor candidate due to the high rate of absorption required to maintain the effective level in the blood stream. Similarly, drugs that induce or inhibit their own metabolism in chronic administration are poor candidates for controlled delivery systems due to difficulty in maintaining uniform blood levels. Therapeutic window is another factor influencing the choice of formulating a drug into controlled release form. Although it is tempting and often considered advantageous to formulate a controlled release formulation for a drug with narrow therapeutic window, it is challenging to maintain the drug plasma concentration in the favorable range. Furthermore, dose dumping or formulation breakage can cause significant toxicity if the formulation cannot be retrieved.

2.3. Controlled release formulations:

Controlled release drug delivery systems can be formulated for oral such as tablets/capsules, parenteral such as injectable hydrogels, and transdermal patches. In the following section, we will review the current technology development of the three controlled release dosage forms.

Oral controlled release dosage forms:

Oral dosage forms are the oldest and most common route of the delivery. Today's oral controlled delivery is quite mature since their development in the 60s[26]. Polymeric matrix

tablets, coated multi-particulates, and oral osmotic pump tablets are all in use today. Recently polymeric microspheres constructed from ethylcellulose and polyethylene glycol were investigated for oral controlled delivery of metoprolol, an antihypertensive drug[31]. The release rate of the drug can be controlled by varying the proportion of ethylcellulose and polyethylene glycol. The mechanism of release was described as diffusion rate limited, and zero-order release was achieved[31]. However, in spite of recent advances in rate control and polymer fabrication, oral controlled release systems still face similar challenges as previous generations such as changes in absorption as the drug move down the GI tract, food effects, first pass effect, and etc[30]. Furthermore, oral dosage form is not suitable for weekly sustained release due to the emptying of the GI content daily. Thus, they are limited to delivering TAC as daily sustained release formulation only.

Injectable controlled release dosage forms:

Injectable hydrogels are most commonly employed as controlled release dosage form for subcutaneous administration. Hydrogels are gels that as the name suggest can swell in water. Hydrogels are a three dimensional network of natural and/or synthetic polymers capable of absorbing and retaining significant amounts of water [32]. As such these gels offer the ability to release drugs solubilized in the gel network in a controlled manner [33]. Thermogels are a subset of hydrogels that are temperature sensitive and undergo sol-gel transition at a specific temperature[32,33]. Thermogel polymers capable of undergoing sol-gel transition are composed of hydrophobic and hydrophilic segments and the molecular weight of each segment as well as the temperature dictate the sol-gel transition process.

Thermogel polymers exhibit a critical solution transition temperature at which the polymer goes from being a fully miscible sol to a gel. When the polymers are in the sol state at higher temperatures and undergo transition to the gel state at lower temperature, the polymer is said to exhibit an upper critical solution temperature (UCST) [32,33]. Conversely, when a polymer is in the sol state at lower temperatures and undergoes gelation at higher temperature it is said to exhibit a lower critical solution temperature

(LCST). Biologically, polymers that exhibit LCST are of greater interest due to limitations on the temperature at which a drug delivery system can be introduced into the body. The sol-gel transformation is generally governed by the balance of hydrophilic and hydrophobic moieties on the polymer chain and the free energy of mixing [34]. Other factors affecting polymer gelation transition include nanoassembly, stereochemistry, and polymer topology.

Biologically, polymer sols that can undergo gelation at body temperatures offer three main advantages, the first being, the ease of handling and manufacturing, secondly, syringeability, the ability to inject these formulations, and lastly, the ability to "tailor" synthetic polymers for specific applications. Additionally, injectable gel-forming matrices offer several advantages over traditional implants. For example, injectable materials do not require a surgical procedure for placement (and retrieval if not biodegradable), and various therapeutic agents can be incorporated by simple mixing. When they are used to fill a cavity or a defect, their flowing nature enables a good fit. *In situ* gelation can occur as a result of either a physical or chemical change of the system. In general, hydrogels are classified into 4 main groups based on their polymer construction. They are Pluronic/Pluronic derivatives, polyesters, chitosans and derivatives, and polypeptides.

Pluronic/Pluronic derivatives

Pluronics® (BASF) or Poloxamers (ICI) are triblock copolymers composed of poly(ethylene oxide)-*b*-poly(propylene oxide)-*b*-poly(ethylene oxide) (PEO-PPO-PEO). They are widely used as non-ionic surfactants, solubilizers, and drug delivery systems. They can undergo reversible gelation above their critical gelation concentration (CGC) as the temperature is raised. The gelation mechanism is postulated to occur through micellar packing and entanglement as temperature increases [35]. The polymers are synthesized by condensation of ethylene oxide and propylene oxide.

Although the unique sol-gel-sol transition behavior has made Pluronics® a very attractive injectable platform, these thermogels suffer from poor gel durability, weak mechanical strength, and a rapid drug release profile [36,37]. Thus, derivatives of Pluronics® are being investigated to retard erosion *in vivo*. Various functional groups such as urethane (hexamethylene diisocyanate), carbonate (phosgene/triphosgene), ester (terephthaloyl chloride), disulfide, acetal, stereocomplex, silane, and polypeptide have been attached to the hydroxyl end group of Pluronic® [38–47]. The resulting multiblock copolymer significantly prolongs the duration of the gel from a few days to several weeks. It is speculated that the multiblock polymers may be capable of forming intermicellar bridges between the micelles, thereby strengthening the gel network and retarding erosion. For example, disulfide-connected Pluronics® shows thiol-based degradation and drug release, extending the degradation of these polymers from 6 hours to 12 days [45]. Paclitaxel (PTX) in an in-situ-formed Pluronic® disulfide multiblock copolymer gel releases in a glutathione concentration-dependent manner [45]. Pluronic® triblock copolymers (Pluronic® P85 and P104) linked with di-(ethylene glycol) divinyl ether polymers are acid labile and can direct drug release from the matrix in a pH-sensitive manner [48].

Polyesters

The individual monomers in polyester-based polymers are linked by an ester bond which allowed for digestion by endogenous enzymes such as esterases. Poly(ethylene glycol)-*b*-poly(D,L- lactide-co-glycolide)-*b*-poly(ethylene glycol) (PEG-PLGA-PEG) triblock copolymers containing shorter PEG blocks are designed to undergo sol-gel transition as temperature increases with the LCGT being around the body temperature[33]. Poly(ethylene glycol) (PEG) and poly(ethylene oxide) (PEO) are often used to refer to the same chemical structure. However, Materials with Mw <100,000 are usually called PEGs, while higher molecular weight polymers are classified as PEOs. PEG-polyester aqueous solutions display a sol-gel transition as the temperature increases when the PEG moiety is 1000 Daltons or less [49]. A library of polymers capable of undergoing sol-gel transition

have been developed by varying the molecular weight and composition of PEG and PLGA. In general, an increase in the hydrophobic moiety decreases the gelation concentration and temperature and vice versa. In addition, the gel strength is mainly determined by the hydrophobic block length[33]. The gelation temperature is also influenced by additives, such as NaCl, NaSCN, and free PEG [49–51]. These polymers are biocompatible and biodegradable with degradation products of PEG, lactic acid, and glycolic acid [49].

The reverse platform of PLGA-PEG-PLGA triblock developed after the PEG-PLGA-PEG platform came into existence. The synthesis scheme for the newer platform is simpler and does not require a coupling agent [52,53]. PLGA-PEG-PLGA show lower LCGT compared to PEG-PLGA-PEG. Furthermore modifying the hydroxyl end groups into other functional groups such as alkyl or carboxylic acid, can alter the sol-gel transition [54]. Changing the topology of these polymers also effect the gelation behavior. For example PEG– graft-PLGA (PEG–g-PLGA) and PLGA–graft-PEG (PLGA–g-PEG) while having a similar chemical composition have different topology and therefore exhibit different gelation behavior[55]. The major drawbacks of PLGA-based thermogels is their low solubility requiring hours to dissolve, difficult to handle due to their paste-like nature and cannot be freeze dried into powder form.

Polycaprolactone (PCL) polymers are hydrophobic polymers which are both biocompatible and biodegradable. They are also used as a common excipient in several FDA- approved products [56]. Triblock polymers of PEG–PCL–PEG and PCL–PEG–PCL have been synthesized and characterized[57,58]. These polymers are crystalline in nature and thus can be lyophilized into a powder form. Furthermore, due to the crystalline nature of polymer and its ability to be lyophilized it can be reconstituted to form a thermogel in minutes. All the process needed is to heat the reconstituted aqueous suspension to the polymer's melting point (45-55 ^{o}C) followed by immediate cooling on ice. However, one of the drawbacks of the high crystallinity of the PCL based polymers is that in general the

sol-gel transition is irreversible and the transition can occur within an hour even if the polymer solution is kept below its LCST[57,58].

Copolymers of mPEG-PCL with short mPEG block (M_n=750 g/mol) are capable of undergoing a sol-gel transitions[59]. However, when injected subcutaneously in rats, the mPEG-PCL thermogel erosion occurs too slowly resulting in a gel lasting more than 10 months. Incorporation of hydroxy groups along the polymer backbone by copolymerization of caprolactone and 3-benzyloxymethyl lactide, followed by deprotection of the benzyl groups may be a strategy to increase gel erosion[60]. These hydroxy groups can be further converted into carboxylic acid groups which can accelerate the degradation further resulting in a gel with a duration of upto 6 weeks. Incorporating pH sensitive groups like, sulfonylamine, poly(β-amino ester), and poly(β-amino ester) into PCL-PEG-PCL copolymers introduces pH sensitivities to gelation behavior [61]. By adjusting the pKa of these groups, the sol-gel transition temperature and phase diagram of the polymers can be sensitively affected by small changes in environmental pH.

Chitosan and its derivatives

Chitosan is a linear polysaccharide synthesized by partial deacetylation of insoluble naturally available chitin, obtained from exoskeletons of crustaceans and insects[62]. Due to hydrogen interactions between acetamide groups and hydroxyl groups and low solubility, chitin is structurally rigid and not readily adaptable to formulate for drug delivery purposes[63]. Chitosan on the other hand is non-toxic, biodegradable, biocompatible, and approved by the FDA for medical use[64]. However, application of unmodified chitosan has been limited due to it being soluble only at acidic pH.

Chitosan and β-glycerolphosphate (GP) thermoresponsive hydrogel has been developed by Chenite and colleagues[65]. To prepare, a chilled GP solution is added dropwise to a cold chitosan in hydrochloric acid solution with stirring. The chitosan/GP solution forms a clear liquid at room temperature and gels rapidly at around body temperature. The

thermogelation of the chitosan/GP aqueous solution is the result of decreased hydrogen bonding interactions and increased hydrophobic interactions. The gelation temperature of the chitosan/GP solution decreases as the degree of deacetylation increases. The gelation rate is affected by the degree of deacetylation, concentration of GP, pH, and temperature of chitosan/GP solution[66].

Bhattarai and colleagues have developed a chitosan-graft-PEG by grafting monohydroxy PEG onto the chitosan backbone using a Schiff base and sodium cyanoborohydride[67]. The thermogel behavior of the polymers is controlled by optimizing the PEG content. When 45-55 wt% of PEG is grafted to chitosan chains the resultant polymer is soluble in water without dissolving chitosan at low pH and transformed to a semisolid hydrogel at body temperature. However, the chitosan-g-PEG gel is very soft and has low viscosity <10 Pa at 37°C. To improve the mechanical properties of the gel, chemical crosslinking by genipin has been attempted[67]. Genipin reacts with the remaining amine groups on chitosan-g-PEG copolymer and the crosslinked copolymer forms a thermos-irreversible blue-colored hydrogel with substantially reduced the initial burst release. When loaded with albumin, the crosslinked hydrogel substantially decreases release rate as compared to the unlinked PEG-g-chitosan hydrogel.

Hydroxybutyl chitosan is prepared by reacting chitosan and 1,2-butane oxide[68]. The hydroxyl and amino groups of the polymer increase the solubility in water at low temperature through the hydrogen bonding of these groups with water. As the temperature increases, hydrogen bonds are broken and dehydrated hydroxyl butyl groups associate to form a gel. At 3% concentration, the gelation process is reversible and occurs at 26 °C. This novel material is shown to promote the growth of Human Umbilical Vein Endothelial Cells (HUVEC) causing no harm to the nitric oxide synthesis function of HUVECs. The reversible phase transformation of process of the hydrogel is also appropriate for the survival of the cells. Hydroxybutyl chitosan has the potential for use in 3D cell culture without the use of trypsin.

Polypeptides

Synthetic polypeptides are a versatile biodegradable platform with great potential in drug delivery applications. These polymers can also be designed to undergo sol-gel transition as the temperature increases[69–73]. The gelation process of these polymers is controlled by the ratio of hydrophilic to hydrophobic blocks in the polymer like all synthetic polymers. These ratios are adjusted by regulating the number and the type of amino acids building block as well as by inserting hydrophilic block such as PEG in the synthesized polymer.

Two methods have been designed to prepared synthetics polypetide-based hydrogels, which include gene expression recombinant technology and/or solid-phase peptide synthesis. Synthetic hydrogels can contain sequences mimicking those of natural proteins. Additional functional groups can be added to change the biological or mechanical properties of these hydrogels. Modifications in the peptide sequences can be made to improve the features of the hydrogels[74–76].

Elastin-like polypeptides (ELP) containing a pentapeptide repeat VPGXG, in which X can be any natural amino acid except proline can form thermogels[74,75]. At low temperatures, a soluble ELP aqueous solution forms due to the hydration of the hydrophobic residues by ordered water. As the temperature increases and approaches the transition temperature (T_t) the surrounding water becomes less-ordered and bulky, which leads to the collapse of the polymer. As the polymer collapses, it folds and self-assembles to form a gel[74,75]. Major advantages of ELP include its biocompatibility and biodegrability as manifested by degradation products of natural amino acids[77].

Di- or tri-block copolymers of polypeptides and PEG can be prepared by ring-opening polymerization of N-carboxy anhydrides of amino acids and using an amino group end-capped PEG as an initiator[76]. These di- or tri-block thermogels can be tailored by adjusting the ratio between the hydrophobic polypetide blocks and hydrophilic PEG blocks. Sol-gel transition temperature can be lowered by increasing the hydrophobic block or decreasing

the PEG molecular weight[76]. Unlike the polyester thermogels, polypeptide-PEG thermogels are not reversible once formed even at temperatures of 70 ^{o}C or higher[76].

Transdermal controlled release dosage forms:

Transdermal delivery is an attractive alternative to oral and injectable routes of drug administration. The idea of placing medications on the skin has been practiced for thousands of years. The first transdermal patch approved in the United States in 1979 was a three-day patch that delivers scopolamine to treat motion sickness[78]. Until recently, the use of transdermal patches for pharmaceuticals has been limited because only a few drugs have proven effective delivered through the skin typically cardiac drugs such as nitroglycerin and hormones such as estrogen[79]. It is considered to be an important alternate route for delivery of drugs which require chronic and sustained delivery of treatment[78].

Compared to oral drug delivery, transdermal route offers several advantages[79,80]. In particular, it allows avoiding gastrointestinal drug absorption difficulties caused by

gastrointestinal pH, enzymatic activity and drug interactions with food, drink and

other orally administered drugs. It is used to overcome the first-pass effect that can prematurely metabolize drugs, yet does not have pain associated with parenteral injection. Inter- and intra-patient variation, therefore, is minimized. Transdermal patches can substitute for oral administration of medication when that route is unsuitable, as with vomiting and diarrhea. They also provide extended therapy with a single application, improving patient compliance over other more frequently administered dosage forms. In case of emergency, the therapy can be terminated rapidly by removal of the application from the surface of the skin. They are used for drugs with narrow therapeutic window. Accurate dosing can be achieved through controlled release, and zero order release may be achieved[78,79].

Transdermal drug delivery is not without challenges. Only a limited number of drugs are amenable to administration by this route. Suitable candidates for transdermal delivery are small molecule drugs, usually no more than 500 Da. The delivery system cannot be used for drugs requiring high blood levels; daily dose is limited to a few milligrams or less. Some patients may develop skin irritation at the site of application from one or more of the components. The use of transdermal patches may not be economical[78,79].

Broadly speaking, there are two types of TDDS, reservoir and matrix systems. The design of a reservoir TDDS has the drug dissolved in liquid or gel stored in a "pouch". The release rate of the drug is controlled by a membrane positions between the skin and the reservoir. The rate controlling membrane can be either a microporous or a non-porous polymeric membrane. Adhesion to skin surface is provided by a thin layer of drug compatible, hypoallergenic pressure sensitive adhesive polymer. The drug release rate of the reservoir system is optimized by varying the composition of drug reservoir and thickness of rate controlling membrane[78].

In the matrix system, the drug is dispersed homogenously in a hydrophilic or lipophilic polymer matrix and then the medicated polymer is molded into medicated disks with defined surface area and thickness. Skin adhesion is provided either from self-adhesive polymer or by applying along the circumference of the patch to form a strip of adhesive rim surrounding the medicated disk. Drug release rates are controlled by the matrix composition. An advantage that the reservoir system has over the matrix one is that release rate of drug remain constant[79]. However, the largest drawback of the reservoir TDDS is a risk of formulation breakage and complicated design.

The backbone of a TDDS is the drug reservoir/matrix. It consists of drug particles dissolved or dispersed in the matrix. The choice of polymers and patch design are not only to meet fabrication criteria but also to optimize the drug release, adhesion cohesion balance,

physicochemical properties, compatibility and stability with other components of the system as well as with skin. Acrylic acids are among the most commonly utilized matrix formers. Some of the common polymers that have been reported are Eudragit RL/RS 100, Eudragit S-100, Eudragit E-100. These matrices are often combined with plasticizers to make flexible drug-polymer matrix films for transdermal delivery systems. These polymers are self-adhesive[74,75].

Ethyl cellulose (EC) and polyvinylpurrolidone (PVP) matrix with 30% dibutyl phthalate as a plasticizer have been used to deliver diltiazem hydrochloride and indomethacin. By adding the hydrophilic PVP to a hydrophobic EC the release-rate constant is increased. As the matrix is hydrated, the hydrophilic PVP component swells, leading to the formation of pores and thus decrease the decrease the diffusion path length of drug molecules to release into the skin[81].

Hydroxypropyl methylcellulose (HPMC), widely used in formulating oral controlled release formulations, is also used as a matrix former in the design of propranolol transdermal patch. HPMC matrices without rate-controlling membranes exhibited a burst effect during dissolution testing because the hydrophilic polymer is hydrated easily, leading to the fast release of the drug[82].

To enhance the permeation flux of a drug across the stratum corneum, various means are employed. In general, permeation enhancers are categorized into either chemical or physical enhancers. Chemical enhancers are incorporated into the reservoir/matrix of the patch. They alter the barrier property of the stratum corneum. An ideal permeation enhancer should not interact with the drugs and matrices, pharmacologically inert, non-toxic, non-irritant, and non-allergenic. Penetration enhancers can enhance the skin permeability by a variety of mechanisms. One primary mechanism is by interaction with intercellular lipids, leading to disruption of their organization and fluidity. Another mechanism is delipidization of stratum corneum. Surfactants such as Tween, Span, and

SLS work this way. Another way is through interaction with intercellular proteins and keratin denaturation.

Physical enhancers, as the name suggested, it involve physically or mechanically altering the skin to enhance the permeability. Iontophoresis has been studied for enhancing permeation of small charged molecules. This method involves applying a low level electric current to the skin, providing the driving force to enable the penetration of substances into the skin[83]. Charged molecules are moved via electrophoresis, while weakly charged and uncharged compounds can be moved by electroosmotic flow of water[84]. Ultrasound is another example of using mechanical mean to enhance the skin permeability. In this case, ultrasonic energy is use either pre-treatment or simultaneously at the time of application. Skin ablation using laser, short heat shock, or mechanical friction is another method of physically enhancing drug permeation by removing the stratum corneum. Recently microneedles have been employed to physically enhance the permeation of large molecules such as protein and DNA. Microneedles are thin microscopic projectiles hundreds of micrometers in length. They are long enough to pierce the stratum corneum without injuring the underlying pain nerve in the skin[85].

Table 1-1: TAC PK parameters in human

	Kidney transplant	Liver transplant	Heart transplant
V_d (L/kg)	1.58±0.45	0.91±0.29	2.4±0.79
Cl (L/h/kg)	0.103±0.04	0.054±0.02	0.2±0.08

Table 1-2: TAC PK parameters in healthy rat

V_d (L/kg)	0.266±0.002
Cl (L/h/kg)	2.52±0.078

Figure 1-1: Patient and liver allograft survival in the azathioprine (AZA), cyclosporine (CYA), and tacrolimus (TAC) eras[1]

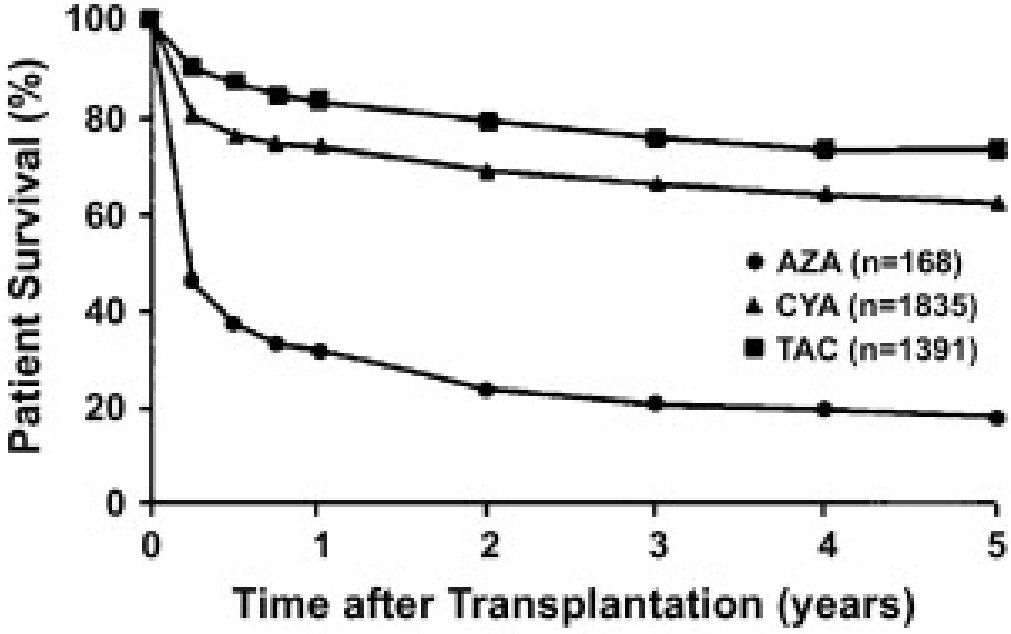

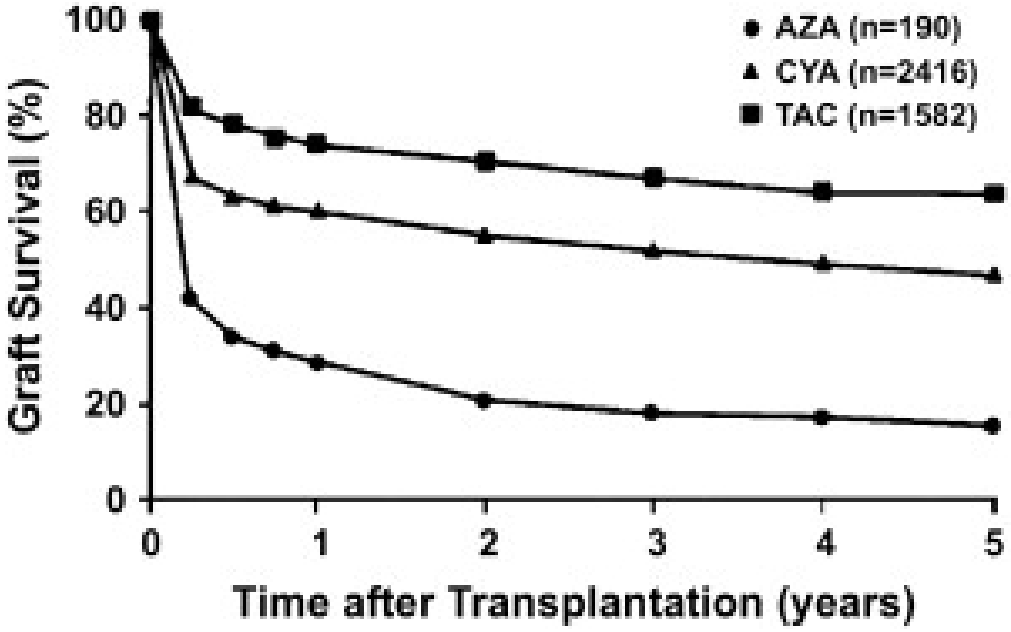

Figure 1-2: General structure of poly(ethylene oxide)-b-poly(propylene oxide)-b-poly(ethylene oxide) polymers

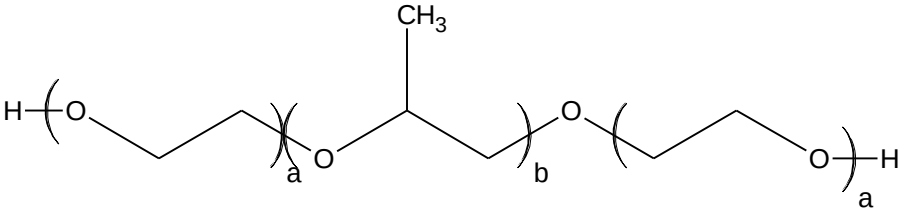

Figure 1-3: Chemical structures of PLGA-based polymers. A: PEG-PLGA-PEG; B: PLGA-PEG-PLGA

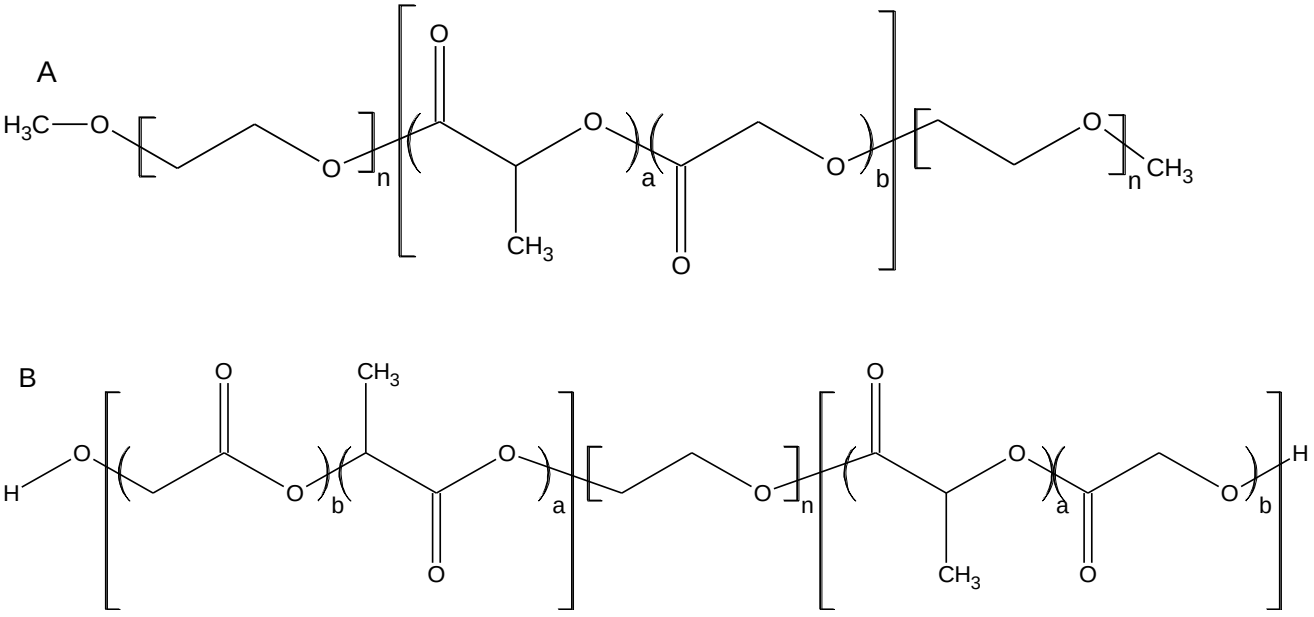

Figure 1-4: General structure of mPEG-PCL polymer

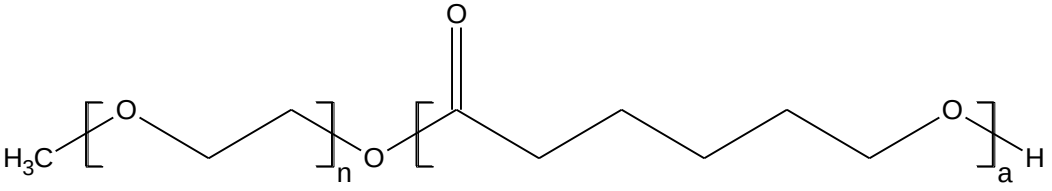

3. REFERENCES:

1 1 Linden PK. History of solid organ transplantation and organ donation. *Crit Care Clin* 2009;**25**:165–184, ix. https://doi.org/10.1016/j.ccc.2008.12.001.

2 Borel JF, Feurer C, Gubler HU, Stähelin H. Biological effects of cyclosporin A: a new antilymphocytic agent. 1976. *Agents Actions* 1994;**43**:179–86.

3 Fung JJ, Todo S, Tzakis A, Demetris A, Jain A, Abu-Elmaged K, *et al.* Conversion of liver allograft recipients from cyclosporine to FK 506-based immunosuppression: benefits and pitfalls. *Transplant Proc* 1991;**23**:14–21.

4 Wiederrecht G, Lam E, Hung S, Martin M, Sigal N. The mechanism of action of FK-506 and cyclosporin A. *Ann N Y Acad Sci* 1993;**696**:9–19.

5 2010 Annual Report of the U.S Organ Procurement and Transplantation Network and the Scientific Registry of Transplant Recipients: Transplant Data 1999-2008. US Department of Health and Human Services, Health Resources and Services Administratio, Healthcare Systems Bureau, Division of Transplantatio, ROckville, MD n.d.

6 Masri MA. The mosaic of immunosuppressive drugs. *Mol Immunol* 2003;**39**:1073–7.

7 Staatz CE, Tett SE. Clinical Pharmacokinetics of Once-Daily Tacrolimus in Solid-Organ Transplant Patients. *Clin Pharmacokinet* 2015;**54**:993–1025. https://doi.org/10.1007/s40262-015-0282-2.

8 Yokogawa K, Takahashi M, Tamai I, Konishi H, Nomura M, Moritani S, *et al.* P-glycoprotein-dependent disposition kinetics of tacrolimus: studies in mdr1a knockout mice. *Pharm Res* 1999;**16**:1213–8.

9 Hu Y-F, Qiu W, Liu Z-Q, Zhu L-J, Liu Z-Q, Tu J-H, *et al.* Effects of genetic polymorphisms of CYP3A4, CYP3A5 and MDR1 on cyclosporine pharmacokinetics after renal transplantation. *Clin Exp Pharmacol Physiol* 2006;**33**:1093–8. https://doi.org/10.1111/j.1440-1681.2006.04492.x.

10 Venkataramanan R, Swaminathan A, Prasad T, Jain A, Zuckerman S, Warty V, *et al.* Clinical pharmacokinetics of tacrolimus. *Clin Pharmacokinet* 1995;**29**:404–30. https://doi.org/10.2165/00003088-199529060-00003.

11 Kang S-Y, Sohn K-H, Lee J-O, Kim S-H, Cho S-H, Chang Y-S. Intravenous tacrolimus and cyclosporine induced anaphylaxis: what is next? *Asia Pac Allergy* 2015;**5**:181–6. https://doi.org/10.5415/apallergy.2015.5.3.181.

12 Jasiak NM, Park JM. Immunosuppression in Solid-Organ Transplantation: Essentials and Practical Tips. *Crit Care Nurs Q* 2016;**39**:227–40. https://doi.org/10.1097/CNQ.0000000000000117.

13 Patel N, Cook A, Greenhalgh E, Rech MA, Rusinak J, Heinrich L. Overview of extended release tacrolimus in solid organ transplantation. *World J Transplant* 2016;**6**:144–54. https://doi.org/10.5500/wjt.v6.i1.144.

14 Rostaing L, Bunnapradist S, Grinyó JM, Ciechanowski K, Denny JE, Silva HT, *et al.* Novel Once-Daily Extended-Release Tacrolimus Versus Twice-Daily Tacrolimus in De Novo Kidney Transplant Recipients: Two-Year Results of Phase 3, Double-Blind, Randomized

Trial. *Am J Kidney Dis Off J Natl Kidney Found* 2016;**67**:648–59. https://doi.org/10.1053/j.ajkd.2015.10.024.

15 Ho ETL, Wong G, Craig JC, Chapman JR. Once-daily extended-release versus twice-daily standard-release tacrolimus in kidney transplant recipients: a systematic review. *Transplantation* 2013;**95**:1120–8. https://doi.org/10.1097/TP.0b013e318284c15b.

16 North American Pediatric Renal Trials and Collaborative Studies, 2014 Annual Report. Available from: https://www.naprtcs.org. An overview of the current state of pediatric kidney transplantation across the United States. The data provide future directions for changing practices and guiding research to improve outcomes in pediatric kidney transplantation. n.d.

17 Pinsky BW, Takemoto SK, Lentine KL, Burroughs TE, Schnitzler MA, Salvalaggio PR. Transplant outcomes and economic costs associated with patient noncompliance to immunosuppression. *Am J Transplant Off J Am Soc Transplant Am Soc Transpl Surg* 2009;**9**:2597–606. https://doi.org/10.1111/j.1600-6143.2009.02798.x.

18 Akchurin OM, Melamed ML, Hashim BL, Kaskel FJ, Del Rio M. Medication adherence in the transition of adolescent kidney transplant recipients to the adult care. *Pediatr Transplant* 2014;**18**:538–48. https://doi.org/10.1111/petr.12289.

19 Beckebaum S, Iacob S, Sweid D, Sotiropoulos GC, Saner F, Kaiser G, *et al.* Efficacy, safety, and immunosuppressant adherence in stable liver transplant patients converted from a twice-daily tacrolimus-based regimen to once-daily tacrolimus extended-release formulation. *Transpl Int Off J Eur Soc Organ Transplant* 2011;**24**:666–75. https://doi.org/10.1111/j.1432-2277.2011.01254.x.

20 Doesch AO, Mueller S, Konstandin M, Celik S, Erbel C, Kristen A, *et al.* Increased adherence after switch from twice daily calcineurin inhibitor based treatment to once daily modified released tacrolimus in heart transplantation: a pre-experimental study. *Transplant Proc* 2010;**42**:4238–42. https://doi.org/10.1016/j.transproceed.2010.09.074.

21 Kuypers DRJ, Peeters PC, Sennesael JJ, Kianda MN, Vrijens B, Kristanto P, *et al.* Improved adherence to tacrolimus once-daily formulation in renal recipients: a randomized controlled trial using electronic monitoring. *Transplantation* 2013;**95**:333–40. https://doi.org/10.1097/TP.0b013e3182725532.

22 Staatz CE, Tett SE. Clinical pharmacokinetics and pharmacodynamics of tacrolimus in solid organ transplantation. *Clin Pharmacokinet* 2004;**43**:623–53.

23 Steiner RW, Feist AA. The 'generic' effect of food on tacrolimus pharmacokinetics. *Clin Transplant* 2011;**25**:334–5. https://doi.org/10.1111/j.1399-0012.2010.01387.x.

24 Andrews LM, Li Y, De Winter BCM, Shi Y-Y, Baan CC, Van Gelder T, *et al.* Pharmacokinetic considerations related to therapeutic drug monitoring of tacrolimus in kidney transplant patients. *Expert Opin Drug Metab Toxicol* 2017;**13**:1225–36. https://doi.org/10.1080/17425255.2017.1395413.

25 Okabe H, Hashimoto Y, Inui KI. Pharmacokinetics and bioavailability of tacrolimus in rats with experimental renal dysfunction. *J Pharm Pharmacol* 2000;**52**:1467–72.

26 Helfand WH, Cowen DL. Evolution of pharmaceutical oral dosage forms. *Pharm Hist* 1983;**25**:3–18.

27 Park K. Controlled drug delivery systems: past forward and future back. *J Control Release Off J Control Release Soc* 2014;**190**:3–8. https://doi.org/10.1016/j.jconrel.2014.03.054.

28 Siepmann J, Siegel RA, Rathbone MJ, Controlled Release Society, editors. *Fundamentals and applications of controlled release drug delivery*. New York: Springer : Controlled Release Society; 2012.

29 Mishra MK, editor. *Handbook of encapsulation and controlled release*. Boca Raton: CRC Press, Taylor & Francis Group, CRC Press is an imprint of the Taylor & Francis Group, an Informa business; 2016.

30 Wilson CG, Crowley PJ, editors. *Controlled release in oral drug delivery*. New York: Springer; 2011.

31 Malipeddi VR, Awasthi R, Dua K. Formulation and evaluation of controlled release ethylcellulose and polyethylene glycol microspheres containing metoprolol tartrate. *Interv Med Appl Sci* 2016;**8**:60–7. https://doi.org/10.1556/1646.8.2016.2.6.

32 Moon HJ, Ko DY, Park MH, Joo MK, Jeong B. Temperature-responsive compounds as in situ gelling biomedical materials. *Chem Soc Rev* 2012;**41**:4860–83. https://doi.org/10.1039/c2cs35078e.

33 Jeong B, Kim SW, Bae YH. Thermosensitive sol-gel reversible hydrogels. *Adv Drug Deliv Rev* 2002;**54**:37–51.

34 Heskins M, Guillet JE. Solution Properties of Poly(N-isopropylacrylamide). *J Macromol Sci Part - Chem* 1968;**2**:1441–55. https://doi.org/10.1080/10601326808051910.

35 Rassing J, Attwood D. Ultrasonic velocity and light-scattering studies on the polyoxyethylene—polyoxypropylene copolymer Pluronic F127 in aqueous solution. *Int J Pharm* 1982;**13**:47–55. https://doi.org/10.1016/0378-5173(82)90141-7.

36 Chen P-C, Kohane DS, Park YJ, Bartlett RH, Langer R, Yang VC. Injectable microparticle-gel system for prolonged and localized lidocaine release. II. In vivo anesthetic effects. *J Biomed Mater Res A* 2004;**70**:459–66. https://doi.org/10.1002/jbm.a.30101.

37 Lin HR, Sung KC. Carbopol/pluronic phase change solutions for ophthalmic drug delivery. *J Control Release Off J Control Release Soc* 2000;**69**:379–88.

38 Sosnik A, Cohn D. Ethoxysilane-capped PEO-PPO-PEO triblocks: a new family of reverse thermo-responsive polymers. *Biomaterials* 2004;**25**:2851–8. https://doi.org/10.1016/j.biomaterials.2003.09.057.

39 Ahn JS, Suh JM, Lee M, Jeong B. Slow eroding biodegradable multiblock poloxamer copolymers. *Polym Int* 2005;**54**:842–7. https://doi.org/10.1002/pi.1780.

40 Cohn D, Lando G, Sosnik A, Garty S, Levi A. PEO-PPO-PEO-based poly(ether ester urethane)s as degradable reverse thermo-responsive multiblock copolymers. *Biomaterials* 2006;**27**:1718–27. https://doi.org/10.1016/j.biomaterials.2005.10.035.

41 Loh XJ, Goh SH, Li J. New biodegradable thermogelling copolymers having very low gelation concentrations. *Biomacromolecules* 2007;**8**:585–93. https://doi.org/10.1021/bm0607933.

42 Loh XJ, Goh SH, Li J. Hydrolytic degradation and protein release studies of thermogelling polyurethane copolymers consisting of poly[(R)-3-hydroxybutyrate], poly(ethylene glycol), and poly(propylene glycol). *Biomaterials* 2007;**28**:4113–23. https://doi.org/10.1016/j.biomaterials.2007.05.016.

43 Loh XJ, Tan YX, Li Z, Teo LS, Goh SH, Li J. Biodegradable thermogelling poly(ester urethane)s consisting of poly(lactic acid) – Thermodynamics of micellization and hydrolytic degradation. *Biomaterials* 2008;**29**:2164–72. https://doi.org/10.1016/j.biomaterials.2008.01.016.

44 Niu G, Zhang H, Song L, Cui X, Cao H, Zheng Y, *et al.* Thiol/Acrylate-Modified PEO-PPO-PEO Triblocks Used as Reactive and Thermosensitive Copolymers. *Biomacromolecules* 2008;**9**:2621–8. https://doi.org/10.1021/bm800573e.

45 Sun KH, Sohn YS, Jeong B. Thermogelling poly(ethylene oxide-b-propylene oxide-b-ethylene oxide) disulfide multiblock copolymer as a thiol-sensitive degradable polymer. *Biomacromolecules* 2006;**7**:2871–7. https://doi.org/10.1021/bm060512r.

46 Chung HJ, Lee Y, Park TG. Thermo-sensitive and biodegradable hydrogels based on stereocomplexed Pluronic multi-block copolymers for controlled protein delivery. *J Control Release Off J Control Release Soc* 2008;**127**:22–30. https://doi.org/10.1016/j.jconrel.2007.12.008.

47 She Z, Wang C, Li J, Sukhorukov GB, Antipina MN. Encapsulation of Basic Fibroblast Growth Factor by Polyelectrolyte Multilayer Microcapsules and Its Controlled Release for Enhancing Cell Proliferation. *Biomacromolecules* 2012;**13**:2174–80. https://doi.org/10.1021/bm3005879.

48 Garripelli VK, Kim J-K, Namgung R, Kim WJ, Repka MA, Jo S. A novel thermosensitive polymer with pH-dependent degradation for drug delivery. *Acta Biomater* 2010;**6**:477–85. https://doi.org/10.1016/j.actbio.2009.07.005.

49 Jeong B, Bae YH, Kim SW. Thermoreversible Gelation of PEG−PLGA−PEG Triblock Copolymer Aqueous Solutions. *Macromolecules* 1999;**32**:7064–9. https://doi.org/10.1021/ma9908999.

50 Jeong B, Windisch, CF, Park MJ, Sohn YS, Gutowska A, Char K. Phase Transition of the PLGA- *g* -PEG Copolymer Aqueous Solutions. *J Phys Chem B* 2003;**107**:10032–9. https://doi.org/10.1021/jp027339n.

51 Zhang H, Yu L, Ding J. Roles of Hydrophilic Homopolymers on the Hydrophobic-Association-Induced Physical Gelling of Amphiphilic Block Copolymers in Water. *Macromolecules* 2008;**41**:6493–9. https://doi.org/10.1021/ma7026484.

52 Lee DS, Shim MS, Kim SW, Lee H, Park I, Chang T. Novel Thermoreversible Gelation of Biodegradable PLGA-block-PEO-block-PLGA Triblock Copolymers in Aqueous Solution. *Macromol Rapid Commun* 2001;**22**:587–92. https://doi.org/10.1002/1521-3927(20010501)22:8<587::AID-MARC587>3.0.CO;2-8.

53 Shim MS, Lee HT, Shim WS, Park I, Lee H, Chang T, *et al.* Poly(D,L-lactic acid-co-glycolic acid)-b-poly(ethylene glycol)-b-poly (D,L-lactic acid-co-glycolic acid) triblock copolymer and thermoreversible phase transition in water. *J Biomed Mater Res* 2002;**61**:188–96. https://doi.org/10.1002/jbm.10164.

54 Gong C, Qi T, Wei X, Qu Y, Wu Q, Luo F, *et al.* Thermosensitive polymeric hydrogels as drug delivery systems. *Curr Med Chem* 2013;**20**:79–94.

55 Jeong B, Lee KM, Gutowska A, An YH. Thermogelling biodegradable copolymer aqueous solutions for injectable protein delivery and tissue engineering. *Biomacromolecules* 2002;**3**:865–8.

56 Labet M, Thielemans W. Synthesis of polycaprolactone: a review. *Chem Soc Rev* 2009;**38**:3484–504. https://doi.org/10.1039/b820162p.

57 Bae SJ, Suh JM, Sohn YS, Bae YH, Kim SW, Jeong B. Thermogelling Poly(caprolactone- *b* -ethylene glycol- *b* -caprolactone) Aqueous Solutions. *Macromolecules* 2005;**38**:5260–5. https://doi.org/10.1021/ma050489m.

58 Hwang MJ, Suh JM, Bae YH, Kim SW, Jeong B. Caprolactonic poloxamer analog: PEG-PCL-PEG. *Biomacromolecules* 2005;**6**:885–90. https://doi.org/10.1021/bm049347a.

59 Kim MS, Hyun H, Khang G, Lee HB. Preparation of Thermosensitive Diblock Copolymers Consisting of MPEG and Polyesters. *Macromolecules* 2006;**39**:3099–102. https://doi.org/10.1021/ma052713d.

60 Kim JI, Kim DY, Kwon DY, Kang HJ, Kim JH, Min BH, *et al.* An injectable biodegradable temperature-responsive gel with an adjustable persistence window. *Biomaterials* 2012;**33**:2823–34. https://doi.org/10.1016/j.biomaterials.2012.01.004.

61 Shim WS, Yoo JS, Bae YH, Lee DS. Novel injectable pH and temperature sensitive block copolymer hydrogel. *Biomacromolecules* 2005;**6**:2930–4. https://doi.org/10.1021/bm050521k.

62 Bhattarai N, Gunn J, Zhang M. Chitosan-based hydrogels for controlled, localized drug delivery. *Adv Drug Deliv Rev* 2010;**62**:83–99. https://doi.org/10.1016/j.addr.2009.07.019.

63 Murakami K, Aoki H, Nakamura S, Nakamura S, Takikawa M, Hanzawa M, *et al.* Hydrogel blends of chitin/chitosan, fucoidan and alginate as healing-impaired wound dressings. *Biomaterials* 2010;**31**:83–90. https://doi.org/10.1016/j.biomaterials.2009.09.031.

64 Baldrick P. The safety of chitosan as a pharmaceutical excipient. *Regul Toxicol Pharmacol RTP* 2010;**56**:290–9. https://doi.org/10.1016/j.yrtph.2009.09.015.

65 Chenite A, Chaput C, Wang D, Combes C, Buschmann MD, Hoemann CD, *et al.* Novel injectable neutral solutions of chitosan form biodegradable gels in situ. *Biomaterials* 2000;**21**:2155–61.

66 Chenite A. Rheological characterisation of thermogelling chitosan/glycerol-phosphate solutions. *Carbohydr Polym* 2001;**46**:39–47. https://doi.org/10.1016/S0144-8617(00)00281-2.

67 Bhattarai N, Ramay HR, Gunn J, Matsen FA, Zhang M. PEG-grafted chitosan as an injectable thermosensitive hydrogel for sustained protein release. *J Control Release Off J Control Release Soc* 2005;**103**:609–24. https://doi.org/10.1016/j.jconrel.2004.12.019.

68 Wei YN, Wang QQ, Gao TT, Kong M, Yang KK, An Y, *et al.* 3-D culture of human umbilical vein endothelial cells with reversible thermosensitive hydroxybutyl chitosan hydrogel. *J Mater Sci Mater Med* 2013;**24**:1781–7. https://doi.org/10.1007/s10856-013-4918-1.

69 Yokoi H, Kinoshita T, Zhang S. Dynamic reassembly of peptide RADA16 nanofiber scaffold. *Proc Natl Acad Sci* 2005;**102**:8414–9. https://doi.org/10.1073/pnas.0407843102.

70 Petka WA, Harden JL, McGrath KP, Wirtz D, Tirrell DA. Reversible hydrogels from self-assembling artificial proteins. *Science* 1998;**281**:389–92.

71 Nowak AP, Breedveld V, Pakstis L, Ozbas B, Pine DJ, Pochan D, *et al.* Rapidly recovering hydrogel scaffolds from self-assembling diblock copolypeptide amphiphiles. *Nature* 2002;**417**:424–8. https://doi.org/10.1038/417424a.

72 Hartgerink JD. Self-Assembly and Mineralization of Peptide-Amphiphile Nanofibers. *Science* 2001;**294**:1684–8. https://doi.org/10.1126/science.1063187.

73 Klok H-A. Protein-Inspired Materials: Synthetic Concepts and Potential Applications. *Angew Chem Int Ed* 2002;**41**:1509–13. https://doi.org/10.1002/1521-3773(20020503)41:9<1509::AID-ANIE1509>3.0.CO;2-K.

74 Wright ER, Conticello VP. Self-assembly of block copolymers derived from elastin-mimetic polypeptide sequences. *Adv Drug Deliv Rev* 2002;**54**:1057–73.

75 Lao UL, Sun M, Matsumoto M, Mulchandani A, Chen W. Genetic Engineering of Self-Assembled Protein Hydrogel Based on Elastin-like Sequences with Metal Binding Functionality. *Biomacromolecules* 2007;**8**:3736–9. https://doi.org/10.1021/bm700662n.

76 Jeong Y, Joo MK, Bahk KH, Choi YY, Kim H-T, Kim W-K, *et al.* Enzymatically degradable temperature-sensitive polypeptide as a new in-situ gelling biomaterial. *J Control Release Off J Control Release Soc* 2009;**137**:25–30. https://doi.org/10.1016/j.jconrel.2009.03.008.

77 Bessa PC, Machado R, Nürnberger S, Dopler D, Banerjee A, Cunha AM, *et al.* Thermoresponsive self-assembled elastin-based nanoparticles for delivery of BMPs. *J Control Release Off J Control Release Soc* 2010;**142**:312–8. https://doi.org/10.1016/j.jconrel.2009.11.003.

78 Pastore MN, Kalia YN, Horstmann M, Roberts MS. Transdermal patches: history, development and pharmacology. *Br J Pharmacol* 2015;**172**:2179–209. https://doi.org/10.1111/bph.13059.

79 Prausnitz MR, Langer R. Transdermal drug delivery. *Nat Biotechnol* 2008;**26**:1261–8. https://doi.org/10.1038/nbt.1504.

80 Aggarwal G. Development, Fabrication and Evaluation of Transdermal Drug Delivery- A Review. *PharmainfoNet* 2009.

81 Rao PR, Diwan PV. Formulation and in vitro evaluation of polymeric films of diltiazem hydrochloride and indomethacin for transdermal administration. *Drug Dev Ind Pharm* 1998;**24**:327–36. https://doi.org/10.3109/03639049809085627.
82 Guyot M, Fawaz F. Design and in vitro evaluation of adhesive matrix for transdermal delivery of propranolol. *Int J Pharm* 2000;**204**:171–82.
83 Kalia YN, Naik A, Garrison J, Guy RH. Iontophoretic drug delivery. *Adv Drug Deliv Rev* 2004;**56**:619–58. https://doi.org/10.1016/j.addr.2003.10.026.
84 Pikal MJ. The role of electroosmotic flow in transdermal iontophoresis. *Adv Drug Deliv Rev* 2001;**46**:281–305.
85 Lee JW, Han M-R, Park J-H. Polymer microneedles for transdermal drug delivery. *J Drug Target* 2012. https://doi.org/10.3109/1061186X.2012.741136.

Chapter 2.

DEVELOPING AND ASSESSING SUSTAINED RELEASE THERMOSENSITIVE HYDROGEL FORMULATIONS OF TACROLIMUS

Duc X. Nguyen, Vidhi Shah, Rosa Woo, Reid Kinser, Bhuvana S. Doddapaneni, Amira Al-Uzri and Adam WG Alani

(to be submitted to ACS Chemistry of Material)

1. ABSTRACT

Tacrolimus is one of the most commonly prescribed immunosuppressants in renal transplants. However, the current oral dosage forms exhibit large intra- and interpatient PK variability due to erratic absorption and nonadherence. Developing an injectable sustained release formulation can help improving patient adherence and drug PK. Thermosensitive hydrogels are often utilized to develop subcutaneous depot injection dosage form. However, they often suffer from burst release of the drug. In this study, we develop and characterized a novel polyamino-based polymer family capable of undergoing thermosensitive gelation. Three polyaspartate polymers are identified to be able to undergo thermosensitive gelation, where the transition temperature is dependent on the polymer concentration and hydrophobicity. The gelation mechanism is shown to be due to aggregation of β-sheet formation of the polymer. The PPLA-PEG-PPLA polymer with 16 repeating units of the aspartate group is found to undergo gelation at 37°C. We have also developed a TAC-loaded nanoparticle platform utilizing PEG_{5k}-*b*-PCL_{10k} polymer. The drug loaded nanoparticles are loaded into a PVL-based hydrogel and polyaspartate hydrogel for investigation in rat. The aminoGel formulation has a smaller burst release than the pvlGel formulation. Also, incorporation of drug loaded nanoparticles significantly reduces the burst effect seen in pvlGel without nanoparticle. The two TAC-NP gel composite formulations developed in this study are able to maintain TAC concentration within therapeutic window over a 7-day period.

2. INTRODUCTION

Kidney transplantation is the treatment of choice for kidney failure in children. However, the long-term graft and patient survival in pediatric renal transplant recipients remains suboptimal in spite of newer and improved immunosuppression therapy [1]. Tacrolimus (TAC) is one of the most commonly prescribed immunosuppressants in renal transplants. Pediatric patients taking this immunosuppressant have to undergo frequent therapeutic monitoring to ensure TAC levels remain within the therapeutic window to avoid side effects or graft rejection. Complicated oral dosing, food-drug interaction, and interference with daily schedule lead to non-adherence to medication intake especially in adolescents and young adults. Medication non-adherence is the most important factor in kidney rejection in this population [2]. The 10-year kidney allograft survival for adolescents ages 12-18 years is the lowest among all age groups, averaging 50% for deceased donor and 64% for living donor recipient [3]. Furthermore, non-adherence in adolescent renal transplant recipients can negatively impact the successful transition to adult care and affect long term graft outcomes. The introduction of sustained release oral TAC has helped with increasing medication adherence by simplifying the regimen and reducing medication intake [4]. Sustained release formulation is also less likely to interfere with daily schedule and activities of adolescents and young adults. Thus, formulation of TAC in a 7-day sustained injectable formulation has the potential for decreasing the monitoring requirements and improving patient compliance.

We are interested in using thermosensitive hydrogel for formulating sustained injectable formulation of TAC. Thermosensitive hydrogels are often made of block co-polymers that are biocompatible and biodegradable. Upon hydration at room or refrigerated temperature, they remain in solution and convert into a gel at an elevated temperature, usually close to 37°C. The building block copolymers are primarily composed of a combination of biodegradable hydrophilic and hydrophobic segments giving the gel an ability to swell in water and create a physical network capable of trapping and releasing

hydrophobic drugs in a controlled manner. Furthermore, a subset of hydrogels can undergo thermosensitive sol-gel transition at close to body temperature. Thus, in addition to the aforementioned properties, these hydrogels are ideal for formulating into a dosage form that remains in solution at room temperature and upon administration can form an *in situ* slow release depot.

Synthetic polypeptides are a versatile biodegradable platform with great potential in drug delivery applications. These polymers can also be designed to undergo sol-gel transition as the temperature increases[5–9]. The gelation process of these polymers is controlled by the ratio of hydrophilic to hydrophobic blocks in the polymer like all synthetic polymers. These ratios are adjusted by regulating the number and the type of amino acids building block as well as by inserting hydrophilic block such as poly(ethylene) glycol (PEG) in the synthesized polymer. Di- or tri-block copolymers of polypeptides and PEG can be prepared by ring-opening polymerization of N-carboxy anhydrides of amino acids and using an amino group end-capped PEG as an initiator[10]. These di- or tri-block thermogels can be tailored by adjusting the ratio between the hydrophobic polypetide blocks and hydrophilic PEG blocks. Sol-gel transition temperature can be lowered by increasing the hydrophobic block or decreasing the PEG molecular weight. Unlike the polyester thermogels, polypeptide-PEG thermogels have been shown to be not reversible once formed even at temperatures of 70 ^{o}C or higher[10].

TAC is a low molecular weight hydrophobic molecule with narrow therapeutic windows. In whole blood, a trough concentration between 5-15 ng/ml is required to prevent graft rejection. To avoid nephrotoxicity, neurotoxicity, and cardiovascular side effects, the peak blood concentration should not rise above 30 ng/ml. The challenges in this work is to design sustained drug delivery systems in a hydrogel platform that will maintain the therapeutic window and have minimal burst effect. Thus, we employed two different formulation strategies, one a thermosensitive hydrogel, and a second, a drug loaded nanoparticles dispersed in the hydrogel.

Here we are reporting the synthesis and characterization of a reverse thermal gelling polypeptide block copolymer consisting of PEG and poly(aspartate-propylamine). The material characteristics, the mechanism of the sol-to-gel transition, *in vitro/in vivo* degradation, and the feasibility of the novel hydrogel as an injectable drug delivery system for TAC are investigated. Another arm of this work will be to develop an injectable formulation using our recently designed polyester based polymer. Previously, our colleagues Mishra et al successfully developed a polyvalerolactone (PVL) based polymer capable of forming a thermosensitive hydrogel that exhibits sol-gel conversion at 37 º C [11]. When injected subcutaneously, the gel maintains its integrity for 21 days, and fully hydrolyzed and cleared from the site of injection after 28 days. We hypothesize that the drug loaded NP in the hydrogel will have a sustained release with a lower burst effect as compared to the drug in hydrogel alone. The specific objectives for this work included preparing and characterizing the nanoparticles and *in vivo* assessing the pharmacokinetics of the two formulations for further preclinical testing.

3. MATERIAL AND METHODS:

3.1. Reagents, mice, and rats

TAC is purchased from LC Laboratories (Woburn, MA). β-Benzyl L-aspartate (BLA) and γ-benzyl L-glutamate (BLG) are purchased from Alfa Aesar (Tewksbury, MA). α-Aminopropyl-ω-aminopropoxy-polyoxyethylene (NH_2-PEG-NH_2) (M_n = 2000 g/mol, PDI = 1.03) and α-aminopropyl-ω-methoxy-polyoxyethylene (PEG-NH_2) (M_n = 2000 g/mol, PDI = 1.03) are purchased from NOF America Corporation (White Plains, NY). Polymers for nanoparticle synthesis are purchased from either Sigma-Aldrich Inc. (Milwaukee, WI) or Advanced Polymer Materials Inc. (Montreal, CAN) (Table 2-1). Monomethoxy poly(ethylene glycol) (mPEG) (M_w = 550), δ-Valerolactone, and stannous octoate, are received from Sigma-Aldrich Inc (Milwaukee, WI). Hexamethylene diisocyanate (HDI) is obtained from Acros Organics-Thermo Fisher Scientific (Fairlawn, NJ). Slide-A-Lyzer dialysis cassettes (with a MWCO of 20 000 Da) are obtained from Thermo Scientific Inc.

(Fairlawn, NJ). All other reagents were of analytical grade and purchased from VWR International, LLC (Radnor, PA) or Fisher Scientific Inc. (Fairlawn, NJ). 6-8 weeks old female Swiss-Webster mice and Sprague-Dawley rats were purchased from NCI Charles River.

3.2. Synthesis of polyamino polymers

The schematic for the synthesis is presented in (Figure 2-1). Step one is the synthesis of β-benzyl aspartate N-carboxy anhydrides (BLA-NCA) and γ-benzyl glutamate N-carboxy anhydrides (BLG-NCA) using triphosgene. Followed by step two, which is the polymerization of BLA-NCA or BLG-NCA using either PEG-NH_2 (M_w = 2000) or NH_2-PEG-NH_2 (M_w = 2000) as initiator. And finally, step three is the replacement of the benzyl sidechain by an alkylamine.

BLA-NCA and BLG-NCA are synthesized according to the Fuchs-Farthing method[12]. Briefly, 10 g of either BLA (44.8 mmol) or BLG (42.5 mmol) is dried under vacuum for 3 h and is mixed with 0.4 equivalence of triphosgene (5.3 g for BLA and 5 g for BLG). The dried mixture is then suspended in 60 ml of anhydrous THF with stirring at 40°C. The entire reaction is performed under argon atmosphere for at least 4 h. The formation of BLA-NCA and BLG-NCA is indicated by the formation of a clear pale-yellow solution. Then the solution is let cool to room temperature followed by stepwise addition of 150 ml anhydrous hexane. The solution is stored at -20°C overnight to facilitate the precipitation of white NCA crystal which is then purified by recrystallization from THF and hexane.

The synthesis of di-/tri-block PBLA and PBLG copolymers using PEG-NH_2 and NH_2-PEG-NH_2 as initiators are based on previously described method[13]. The BLA-NCA or BLG-NCA are polymerized by ring opening initiated by the terminal primary amine group of PEG-NH_2, for di-block copolymer, or of NH_2-PEG-NH_2, for tri-block copolymer (Figure 2-1, step 2). The amount of each ingredient is found in (Table 2-2). The process starts with freeze-drying of the initiator, either PEG-NH_2 or NH_2-PEG-NH_2, from benzene, followed by the addition of 10 ml anhydrous DMF. Freshly prepared BLA-NCA at various amounts,

calculated to achieve 8, 16, or 24 repeating units, are dissolved in 10 ml anhydrous DMF and transferred to the initiator solution. The reactions are carried out at 45°C under argon atmosphere for 48 hr. The resulting polymers are precipitated in cold diethyl ether then freeze-dried from benzene.

The last step in the synthesis scheme is the replacement of the benzyl sidechain with either n-propylamine or n-butylamine by the aminolysis reaction (Figure 2-1, step 3). The collected polymers from step 2 are dissolved in anhydrous DMF (100 mg/ml) followed by the addition of n-propylamine or n-butylamine (5 equivalence of the benzyl repeating unit). The reactions are run at room temperature for 48 hr. Upon completion, the synthesized polymers are collected by triple washing the solution with cold diethyl ether followed by freeze-drying from benzene.

3.3. Synthesis of poly(ethyleneglycol)-poly(valerolactone)-poly(ethyleneglycol) (PEG-PVL-PEG)

PEG-PVL-PEG triblock copolymer is synthesized according to a previously described method (Gyan et al) (Figure 2-2). Briefly, 1 g (1.8 mmol) of mPEG (M_w = 550) is added to 2.5 g (25 mmol) of δ-Valerolactone and heated for 6 hours at 130°C to remove moisture. Then stannous octoate (0.05% w/w) is added to the mixture as a catalyst for the ring opening polymerization reaction. The reaction is carried out for 24 hr at 130°C under argon atmosphere. The final PEG-PVL-PEG product is synthesized by reacting 2 g of the collected PEG-PVL with 0.02 g of HDI (2:1 molar ratio) at 60°C for 6 hr. Then polymer mixture is allowed to cool to room temperature, and 30 ml methanol is added to the to terminate the crosslinking reaction. The final product is collected after evaporating the methanol under reduced pressure.

3.4. Characterization of synthesized polymers

The ^{1}H NMR spectra of the synthesized polyamino and PVL polymers are recorded using a Bruker 400 MHz Advance III spectrometer using deuterated DMSO and chloroform

respectively. The molecular weight and chemical composition are determined from the resulting spectra. The FTIR spectra of synthesized polyamino polymers are obtained using a Nicolet-100 Infrared Spectrophotometer. The resolution is set at 4 sec^{-1}, and 16 scans per sample. The samples are dissolved in methylene chloride and casted on KBr plates.

Gel permeation chromatography (GPC) is performed on a Viscotek system with a Viscotek GPC Max VE 2001 solvent sample module, column oven 90-225 revH, VE 3500 RI detector, and Viscotek 279 Dual Detectors (Malvern, UK). The samples are resolved on a dual Styragel HR1 and HR2 columns kept at 40°C (Waters, Milford, MA). Polyamino and PVL polymers are dissolved in DMF and THF respectively. After filtered through a 0.2-micron filter, 100 μL of the sample is injected to the GPC for analysis. The mobile phase for polyamino polymers is DMF with 0.05 M LiBr. THF is used as mobile phase for PVL polymer. The flow rate is set at 0.5 mL/min. Molecular weight and distribution are computed using universal calibration curve plotted with narrow PMMA standards for the analysis of polyamino polymers and polystyrene standards for PVL polymer.

The critical micelle concentration (CMC) of the synthesized polyamino polymers is determined by DPH (1,6-diphenyl-1,3,5-hexatriene) solubilization method. The synthesized polymers are dissolved in water at various concentrations to which 50 μL of DPH solution (0.4 mM) is added. The solutions are kept at 25°C for 12 hr followed by fluorescence measurement at excitation and emission wavelength of 358 and 430 nm, respectively using Cary Eclipse Fluorescence Spectrophotometer (Agilent Technologies, Santa Clara, CA). CMC values are computed from the plot of the fluorescence intensity against polymer concentration.

Sol-gel transition behaviors of each synthesized polymer are determined by the inverted tube method. Polymer solutions in PBS at concentrations ranging from 5% to 40% are prepared by gentle mixing overnight at 4°C. The copolymer solution (0.5 mL) is transferred to a test tube with an inner diameter of 11 mm. The test tube is incubated in

a water bath, and the temperature is increasing from 25 to 60°C at a rate of 1 degree every 5 minutes. Gelation is assessed by inverting the incubated tubes and observing the flow. Gelation is defined as no flow observed within 30 s. The results are plotted to create the phase diagrams.

Rheological measurements are performed on a AR2000 rheometer (TA instruments, Texas). The polymer solution is placed between parallel plate geometry of 25 mm diameter and a Peltier heat pump. The loading gap is set at 1000 micron. Temperature dependent change in viscosity is measured in the temperature range of 10-60°C at a heating rate of 1°C/min and a controlled shear rate of 0.1 s^{-1}.

3.5. Cryogenic Transmission Electron Microscopy (Cryo-TEM)

The synthesized polyamino polymer is dissolved in cold double distilled water at 0.1, 0.5, 1, and 5%. The solution (3 µl) is pipetted on copper Quantifoil holey carbon support grids (Ted Pella 658-300-CU) and vitrified on liquid ethane using a Mark IV Vitrobot. The conditions utilized are 100% humidity, blot force 0 and blotting times between 2-4 seconds. Images are acquired on low-dose conditions using a FEI Krios-Titan equipped with a Falcon II direct electron detector (FEI, Hillsboro, OR) and a FEI Eagle 4k x 4k CCD camera (FEI). The operating voltage set at 120 keV. Cryo-TEM images are collected with a defocus range of 2-4 µm and 2 s bolting time.

3.6. In vitro gel duration.

Tris-HCl buffer solution (0.05 M, pH 7.4) containing 0.2 mg/mL proteinase K, 10 mM $CaCl_2$, and 0.2% NaN_3 is used as the degradation medium. The Tris-HCl buffer solution with proteinase (3.0 mL) is added into a test tube containing 0.5 mL polyamino hydrogel at 37°C. The buffer solution is replaced daily, and the weight of the hydrogel is recorded. The experiment is performed in triplicate.

3.7. Cytotoxicity studies

The cytotoxicity of the polyamino polymers are evaluated on RAW 264.7 cells. Cells are grown in 75 cm^2 tissue culture flask in 5% CO_2 at 37°C in Dulbecco's Modified Eagle medium. The cells are plated into 96-well plates at a density of 10,000 cells/well and incubated for 24 hr before exposed to either PBS or different concentrations of the testing polyamino polymer. After 48 hr, the cell viability is determined by adding 20 μL of CellTiter-Blue® reagent followed by 1 hr of incubation at 37°C. Fluorescence ($560_{ex}/590_{em}$) signal is measured with BioTek synergy HT (Winooski, VT). All measurements are performed in quadruplicate. One-way analysis of variance (one-way ANOVA) is used to evaluate the statistical differences between treatment group means.

3.8. In vivo gelation studies

Three male Swiss-Webster mice are injected subcutaneously with 0.5 mL aqueous hydrogel solution. At different time points (1, 7, and 14 days) post injection, the gel integrity is assessed, and animal weight is monitored for acute toxicity. The animal work is conducted in compliance with NIH guideline and Institutional Animal Care and Use Committee policy in Oregon State University for End-Stage Illness and Pre-emptive Euthanasia based on Humane Endpoints Guidelines.

3.9. in vitro drug release of TAC-load hydrogels:

TAC stock solution 10 mg/ml in ethanol is prepared to spike into the hydrogel solutions. For each hydrogel platform, polyamino and PVL, TAC solution is spiked into the polymer solution to achieve either 1.0 mg/mL or 0.5 mg/mL concentration. The polymer solution (0.5 mL) is transferred to a 15-mL polypropylene test tube and allowed to gel at 37°C for 5 minutes. Then 10 mL of a pre-warmed 37°C PBS (pH 7.4) is added into the tube. The release is performed at 37°C in a shaker bath adjusted to 60 rpm. At predetermined intervals, the release medium is replaced with fresh pre-warmed buffer to maintain sink condition, and 1 mL sample is kept for later analysis by LC-MS/MS to determine TAC concentrations. The cumulative amount and percent of drug release are determined and

fitted into either first-order kinetic or Higuchi model[14] using GraphPad Prism (GraphPad Softwares Inc, CA).

$$1st\ order: \ln C = \ln C_0 - k \times t$$

C is the percent of drug remaining at time t. C_0 is the initial concentration of drug. K is the release rate constant.

$$Higuchi\ model: Q = k \times t^{1/2}$$

Q is the cumulative drug released at time t. K is the Higuchi constant.

3.10. Preparation and characterization of TAC-loaded nanoparticles:

TAC-loaded nanoparticles (TAC-NP) are prepared using a solvent evaporation method[15]. First, the polymers are dissolved in 2 mL of acetone at 3, 4, or 5 mg/mL concentration. TAC is then added into each polymer solution to achieve a final concentration of 1 mg/mL. Following dropwise addition of 2 ml normal saline, the organic solvent is evaporated using a IKA RV10 rotary evaporator (IKA Works, Wilmington, NC) under gradient reduced pressure condition at 550 mBar for 10 minutes then 400 mBar for 10 minutes then 300 mBar for 5 minutes. The bath temperature is set at 40°C, and rotation is set at 100 rpm. The final volume is then adjusted to 2 mL with saline. The nanoparticles are collected in a 1.5-ml centrifuge tube, spun at 5,000 rpm for 3 minutes, and filtered using a 0.2 µm filter prior to use. Seven different biodegradable/biocompatible polymers with different molecular weight are chosen to characterize the stability of TAC with different core compositions (Table 2-1).

Particle size and drug retention in the nanoparticles at refrigerated temperature (4°C) are investigated over a one-week period. Nanoparticles are characterized for size by Dynamic Light Scattering (DLS). DLS measurements are performed on a Malvern Nano ZS (Malvern Instruments Inc, U.K.) in triplicate. Data is presented as the mean Z-average diameter ± SD (nm) and polydispersity index (PDI). Drug loading is assessed using reversed phase

liquid chromatography using a Shimadzu HPLC system consisting of LC-20 AT pump and SPD M20 a diode array detector. The analysis is performed on a Zorbax C18 Column (4.6×75 mm, 3.5 µm) in isocratic mode with acetonitrile/water (85/15) containing 0.1% phosphoric acid and 1% methanol at a flow rate of 0.5 ml/min and an injection volume of 10 µL. Column temperature is maintained at 40°C. TAC peak is monitored at 254 nm at retention time of 4 minutes. All measurements are performed in triplicate and loading data is presented as mean drug loading ± SD for the various time points.

3.11. In vitro drug release of TAC nanoparticles:

The most stable nanoparticles are selected for the *in vitro* drug release study. The TAC-loaded nanoparticles prepared as described above are loaded into a Slide-A-Lyzer® (Thermo Scientific Inc.) dialysis 3.0 mL cassette with a MWCO of 20,000 g/mol. Four cassettes are used in each experiment (n = 4). The cassettes were placed in 2.5 L of 10 mM phosphate buffer at pH 7.4, which is changed every 3 hr to ensure sink conditions and the temperature is maintained at 37°C. The sampling time intervals are 0, 0.5, 1, 2, 3, 6, 9, 12, 24, 48, and 72 h. A volume of 50 µL at each time point is withdrawn and replaced with an equal volume of buffer. Samples are analyzed by HPLC for drug content. The drug release data is curve-fitted using a one phase exponential association equation which assumes that the drug released occurs by simple diffusion. The curve fitting analysis is performed with GraphPad Prism version 5.04 for Windows, GraphPad Software, San Diego California USA.

3.12. Preparation of the TAC hydrogel formulations:

The PVL hydrogel solution (pvlGel) is prepared by dissolving the PVL polymer in sterile normal saline at 25% (w/v) concentration. The polymer aqueous mixture is run through several heat cold cycles to facilitate the dissolution of the polymer. The polyamino hydrogel solution (aminoGel) is prepared by dissolving the polymer in pre-chilled sterile normal saline at 25% (w/v) concentration under constant stirring. The solution is allowed to fully hydrate overnight under refrigerated temperature 4°C. The hydrogel solutions are

sterilized by UV irradiation for 45 minutes then stored at 4 °C for future use. To prepare the TAC loaded hydrogel formulation, 50 μL of sterile TAC ethanol solution of 10 mg/mL is added to achieve a final TAC concentration of 0.5 mg/mL. A similar process is used to prepare TAC-loaded NP hydrogel composite by adding 100 μL of TAC-NP solution at 5 mg/mL to the hydrogel solution. All formulations are prepared fresh prior to use in animal studies.

3.13. Pharmacokinetic study in rats:

The pharmacokinetic (PK) profile of the TAC hydrogel and TAC-NP hydrogel composite formulations injected subcutaneously is evaluated in 6 to 8-week-old Sprague-Dawley rats (Charles River). To assess the influence of formulation design on the initial burst effect, four groups of rats (n = 4 each) are injected subcutaneously at 0.31 mg/kg dose with either TAC-NP, pvlGel, aminoGel, or TAC-NP pvlGel composite. This dose is estimated based on allometric scaling of TAC daily dose from human to rat in which daily dose for an adult is 0.05 mg/kg, assuming average adult human weight is 60 kg, and average rat weight is 0.25 kg[16,17].

$$Rat\ dose \frac{mg}{kg} = Human\ dose \div (W_{animal} \times W_{human})^{0.33}$$

Another two group of rats (n = 4 each) are injected with either TAC-NP pvlGel or TAC-NP aminoGel composite at 1 mg/kg dose to assess the sustained release profile of the NP hydrogel composites. For all animal groups, blood is collected at 1, 2, 4, 8, 12, and 24 hr, then every day thereafter. Approximately 100 μl whole blood is collected from the saphenous vein and analyzed by LC-MS/MS for TAC concentrations.

Weights, grooming, and feeding behaviors are monitored daily as indicators of toxicity. Acute toxicity is described a s weight loss of ≥15%. WinNonLin software is used to analyze pharmacokinetic parameters. All animal work is conducted in compliance with NIH

guidelines and Institutional Animal Care and Use Committee policy at Oregon Health and Sciences University.

3.14. LC-MS/MS analysis

TAC and creatinine are analyzed using AB Sciex Triple Quad 3500 LC-MS/MS based on methods described by Koop et al[18]. TAC samples are processed by adding 200 mcl of 0.1 mM $ZnSO_4$ solution, vortexing for 4 seconds, followed by adding 500 mcl of acetonitrile containing 4 ng/ml ascomycin. The mixture is mixed for 1 minutes then centrifuged for 5 minutes at 16,000 g. A 10 mcl aliquot of the clear supernatant is injected into LC-MS/MS for analysis. Creatinine is extracted by adding 15 mcl of whole blood sample to methanol:acetonitrile 80:20 mixture containing 3 mcg/ml creatinine-d3. After 5 minutes centrifugation at 16,000 g, 10 mcl of the clear supernatant is added into 390 mcl acetonitrile with 0.3 mM HCl. 5 mcl is injected into LC-MS/MS for analysis.

TAC and ascomycin are resolved on a Thermo C18 Accucore™ column (30 mm x 2.1 mm, 30 Å, 2.6 μm) maintained at 40 °C. The gradient mobile phase is consisted of two solvents: A, 2 mM ammonium acetate with 0.1% formic acid in water and B, 2 mM ammonium acetate with 0.1% formic acid in methanol. The gradient is 50% B for 0.3 min, increase to 100% B in 0.7 min and hold for 2 min, return to 50% B for 0.1 min, re-equilibrate at 50% B for 3 min. The flow rate is 0.4 mL/min. The LC system is interfaced to an AB Sciex 3500 triple-quadrupole (Foster City, CA) with multiple raction monitoring. The equipped TurboIonSpray® ESI source is operated in positive mode with the following setting: source voltage 2500 V, GS1 60 psi, GS2 60 psi, CUR 30, TEM 550°C. The MRM transitions monitored are *m/z* 821 -> 768.5, amd 821 -> 718.5 for TAC, and *m/z* 809 ->756.2, and 809 -> 564.1 for ascomycin[18]. The DP is 80 V for both TAC and ascomycin. The dwell time is 150 ms. The optimal instrument parameters for the 4 MRM transitions are: EP, 10 V; CXP (V), 20, 20, 15, and 15; CE (V), 30, 35, 30, and 34 respectively. The transitions used for quantification are *m/z* 821 -> 768.5 for TAC and 809 -> 756.2 for ascomycin. Instrument control and data acquisition are done with Analyst® Software.

3.15. Statistical analyses

The data are analyzed using descriptive statistics and presented as mean values ± standard deviation (SD) from 3-5 independent measurements. The comparison among groups is performed by the nonparametric unpaired t-test. The difference between variants is considered significant at $p < 0.05$. All linear regression and statistical analyses are performed with GraphPad Prism version 5.04 for Windows, GraphPad Software, San Diego California USA.

4. RESULTS & DISCUSSION

4.1. Synthesis and characterization of polyamino and PVL polymers:

Tri- block copolymers are synthesized successfully using PEG-NH_2 or NH_2-PEG-NH_2 as initiators. BLA-NCA and BLG-NCA at different feed ratios is added to have final polymers with 8, 16, and 24 repeating units (Table 2-2).The structures of the synthesized polymers in step 2 are confirmed with ^{1}H NMR spectra. ^{1}H NMR spectra show methylene protons of PEG (-CH_2CH_2O- : δ 3.60 ppm, resonance *a*), allyl protons of β-benzyl aspartate (-*R*-CH_2-*C=O*- : δ 2.5 ppm, resonance *b*) (Figure 2-3 and 4), allyl protons of γ-benzyl glutamate (-*R*-CH_3-CH_2-*C=O*- : δ 2.2 ppm, resonance *b*) (Figure 2-5 and 6), benzylic proton (-CH_2-C_6H_5 : δ 5.0 ppm, resonance *c*) and aromatic proton (C_6H_5- : δ 7.30 ppm, resonance *d*) (Figure 2-3, 4, 5, and 6). The number of BLA or BLG repeating units in the synthesized copolymers are calculated from the peak ratio of the PEG's methylene protons (-CH_2CH_2O- : δ 3.60 ppm, resonance *a*) relative to the aromatic protons of the BLA and BLG groups (C_6H_5- : δ 7.60 ppm, resonance *d*). Successful ring opening polymerization of step 2 synthesis is also confirmed by the appearance of ester peaks (C=O, 1740 cm^{-1}) as observed in FTIR spectra (Figure 2-9 and 10).

$$\#\, repeating\ unit = \ resonance\ d / resonance\ a \ \times \ 36.2$$

To optimize the step 3 nucleophilic replacement of the phenolic group with the desired alkylamine (Figure 2-1), 1 mL sample of the PPLA-PEG-PPLA synthesis reaction is

precipitated and triple washed with cold diethyl ether at 1, 3, 24, and 48 hr. Progress of the reaction is monitored by observing the disappearance of benzylic and aromatic protons (resonance *a* and *b*) and the occurrence of alkane protons (resonance *c* and *d*) (Figure 2-7). The aminolysis reaction progresses quickly following the addition of an alkylamine at room temperature and comes to completion at 48 hr. The complete disappearance of the aromatic proton at 7.30 ppm on ^{1}H NMR spectra confirms the completion of the reactions (Figure 2-7 and 8). FTIR spectra also confirm the reaction completion. The replacement of the ester peak (C=O, 1740 cm^{-1}) by the sharp amide peaks (C=O at 1640 cm^{-1} and N-H at 1540 cm^{-1}) is observed on FTIR spectra (Figure 2-11 and 12).

The PVL polymer is synthesized successfully according to method described by Gyan et al[11]. The triblock copolymer PEG-*b*-PVL-*b*-PEG is synthesized by ring opening polymerization of δ-Valerolactone using stannous octoate as catalyst and PEG as initiator. The 1H NMR of the synthesized polymer is shown in (Figure 2-13). The number of VL repeating unit is computed from the peak ratio of the methylene protons of PEG (-*CH2CH2O*- : δ 3.60 ppm, resonance *a*) ratio relative to methylene protons of VL (-*CH2OOC*- : δ 4.06 ppm, resonance *d*). The number of VL repeating unit in the synthesized polymer is 60. FTIR analysis further confirms the structure of the triblock copolymer (Figure 2-14). The formation of ester bond is confirmed by a weak C=O stretch at 1724 cm^{-1}. Furthermore, the absence of absorbance peaks at 2200-2280 cm^{-1} indicates the complete reaction of -NCO group in HDMI. Finally, N-H bending vibration at 1540 cm^{-1} confirms the formation of urethane group in the PEG-PVL-PEG copolymer (Figure 2-14).

GPC analysis shows that the weight average molecular weight (M_w) and polydispersity index (PDI) of the synthesized PVL polymer is 7428 and 1.47, respectively (Figure 2-15). The unimodal GPC distribution of the polymer suggested successful coupling of PEG-PVL by HDMI. The PVL polymer solution at 25% w/v in PBS undergoes thermosensitive gelation at 37°C similar to that reported by Mishra et al[11]. The copolymer is stored at -20°C for later use.

The synthesis of the polyamino polymer family has great advantage over other methods which required toxic metal catalysts and linkers as in the case of polyester-based polymers[11]. Triphosgene and excess alkylamine are the only toxic concern in our polyamino synthesis (Figure 2-1). However, as the polymers are triple washed after each step of synthesis, the unreacted residues should not remain in any significant quantity. This polymer family provides versatile configurations for customization of the polymer properties. First, the arrangement of hydrophobic and hydrophilic blocks is selected by initiating the synthesis with either PEG-NH_2 for A-B configuration, or NH_2-PEG-NH_2 for B-A-B configuration, where A is hydrophilic and B is hydrophobic block. A-B-A configuration can be achieved by crosslinking two A-B copolymers. Second, the length of the hydrophobic block can be controlled by changing the amount of NCA used in the ring polymerization process. The longer the amino units the more hydrophobic the polymer becomes. This has been observed in our synthesized polymers, as their repeating unit increases, the polymer's CMC decreases indicating the influence of amino block length on overall hydrophobic/hydrophilic balance of the polymer (Table 2-3). Furthermore, the amino acid repeating unit can be switched out for other amino acid derivative such as γ-benzyl glutamate, O-benzyl tyrosine, or phenylalanine[19]. Our work has shown that glutamate-based polymers are less soluble and have lower CMC than their aspartate counterparts (Table 2-3). And lastly, for fine tuning of the hydrophobicity of the polymer, the benzyl sidechain can be replaced with an alkylamine group of different length such as propylamine or butylamine. Alkylamine of longer carbon sidechain increases the polymer's hydrophobicity. Other than propylamine and butylamine, a variety of other alkylamines such as diethylenetriamine or ethanolamine can be explored as functional group to further tailor the properties of the final polymer to suit the ultimate needs of the chemist.

Overall, 26 polyamino polymers are synthesized in either di- or tri- block configuration (Table 2-3). Three aspartate-based polymers, PPLA-PEG-PPLA 8, 16, and 24 repeating

units, have demonstrated thermosensitive gelation at various concentrations. The effects of polymer concentration (%w/v in PBS) on gelation temperature are investigated using the inverted method. The three PPLA-PEG-PPLA polymers at increasing concentrations are incubated at increasing temperatures until the solution becomes gel. Sol-gel phase diagrams of the three tri-block copolymers are constructed based on the recorded gelation temperatures (Figure 2-16). All three polymers show distinct sol-gel transition temperatures, which are inversely proportional to increasing repeating unit. The polymer with 24 aspartate repeating units, PPLA-PEG-PPLA24, has the lowest transition temperatures, while the 8 repeating unit polymer, PPLA-PEG-PPLA8, requires much higher heat to undergo gelation (Figure 2-16). PPLA-PEG-PPLA8, at 35% w/v concentration in PBS, shows a high sol-gel transition temperature at 47°C. Such a high temperature will cause discomfort for patients in order to induce *in situ* gelation. Furthermore, at concentration higher than 40%, the polymer swells and forms a thick slurry unsuitable for further development as an injectable vehicle. PPLA-PEG-PPLA16 and PPLA-PEG-PPLA24, at 25% and 10% w/v in PBS, demonstrate gelation temperatures at 35°C and 30°C respectively. This finding is consistent with previous studies, where sol-gel transition has been shown to be dependent on the hydrophobicity/hydrophilicity balance of the polymer[20]. Furthermore, the gelation temperatures for all three polymers are shown to be concentration dependent. The gelation temperature decreases as the concentration of polymer in solution increases. This is due to an increase in polymer interaction and configuration change at high concentrations. Thus, the gelation process requires less heat to form than at lower concentration. However, unlike other ester-based hydrogels our polyamino hydrogels do not exhibit an upper transition temperature. Ester-based hydrogel when heated beyond its gelation temperature would result in the gel turning into a turbid solution[21,22]. Also for our polyamino hydrogels, once gelation has occurred, it is irreversible even when the temperature has decreased. The mechanism of gelation of polyester hydrogels is thought to be driven by micellar aggregation triggered by an increase in temperature[11,21–24]. This process by nature is reversible. The irreversible

gelation of our synthesized hydrogels means the mechanism is a different process. We hypothesize that the temperature driven gelation is a result of the aspartate blocks aggregating and adopting the β-sheet conformation. Cryo-TEM images reveal a continuous network of fibers throughout the hydrogel sample, even at concentrations as low as 0.1% (Figure 2-17). The increasing adoption of β-sheet conformation by hydrophobic amino block as temperature increases above 30°C has been shown in other studies[10,19,25,26]. This phenomenon promotes better intermolecular interaction and hydrogelation. And unlike micellar aggregation gelation process of polyester polymers, β-sheet aggregation of polyamino polymers are irreversible once formed[10,19,25,26].

The temperature driven viscosity change from solution to gel state and the strength of the formed gel are studied with rheological measurements of PPLA-PEG-PPLA16 and PPLA-PEG-PPLA24 at 25% and 10% w/v in PBS buffer (Figure 2-18). Over the range of measurement, from 10-60°C, the viscosity of PPLA-PEG-PPLA16 rises sharply as the temperature increases pass 35°C. From 10-30°C, the viscosity is ~10-20 Pa.s, the polymer solution is a syringible free flowing liquid. PPLA-PEG-PPLA16 at 25% in PBS has a transition temperature (Tg) of approximately 37°C. As the peltier plate temperature rises above 35°C, the storage modulus increases sharply from 325 Pa.s (37°C) and to 1071 Pa.s (40°C). It reaches a maximum of 1450 Pa.s at 45°C. These results confirm the transition from liquid to gel at the physiological temperature range. Similarly, PPLA-PEG-PPLA24 10% in PBS exhibits rapid gelation as the temperature rises above 22°C. However, the gel strength is inferior to the gel formed by polymer 2. The maximum viscosity of PPLA-PEG-PPLA24 gel is 600 Pa.s at 37°C. As temperature increases pass 37°C, the gel integrity begins to compromise indicated by dropping in viscosity. This present a problem in formulating an injectable hydrogel because the injected gel can break resulting in dose dumping of the loaded drug. In contrast, PPLA-PEG-PPLA16 gel does not compromise until the temperature is raised above 45°C. Even then the gel still retains its viscosity above 400 Pa.s. Base on the obtained characteristics, PPLA-PEG-PPLA16 25% in PBS possesses

desirable properties for a biomedical hydrogel because, at room temperature, a drug-loaded liquid polymer solution could be administered by injection, followed by *in situ* gelling at body temperature, avoiding the need for surgical implantation.

Cytotoxicity of PPLA-PEG-PPLA16 polymer is evaluated with the RAW 264.7 macrophage cell line. The cell viability following incubation with different concentrations of the copolymer is not affected in comparison to PBS (negative control) (Figure 2-19). Relative cell viability remains above 80% for all concentrations in the range of 0.15-10 mg/ml of PPLA-PEG-PPLA16 polymer. These synthesized polyamino copolymers are composed of PEG and aspartate blocks which are well known for biocompatible nature[25,27]. Our findings further confirm that hydrogels composed of PEG and PPLA block copolymers are biocompatible and can be further explored for drug delivery platforms.

In vitro gel degradation is studied using proteinase K buffer. Proteinase K has been shown in to hydrolyze the peptide bonds of polyamino polymers and simulate *in vivo* degradation[25]. Compares to control samples, the presence of proteinase K slowly degrades the polyamino hydrogel daily. After day 10, the degradation speeds up as the bulk gel has been degraded to smaller masses and becomes more water-soluble (Figure 2-20). It is an important property for an injectable hydrogel to be degradable by enzymes present in the body. The resulting monomers after degradation such as PEG and aspartate would be absorbed and excreted renally.

In situ gelation is confirmed in mice (Figure 2-21). PPLA-PEG-PPLA16 solution at 25% w/v in PBS is injected subcutaneously into mice. Gelation site is observed on days 1, 7, 14, and 21 to determine gel degradation. A few minutes after injection, the gel can be palpated at injection site. The size of the injected hydrogel decreases gradually and reduces to a thin smear on day 14. It is completely gone by day 21. Our observations are consistent with previous *in vitro* gel degradation experiment in enzymatic buffer[25]. All injected mice

show no acute toxicity which is defined by lost in the median body weight by ≥15% and causes either remarkable change in general appearance or behavior.

4.2. Development of TAC-loaded nanoparticles:

One obstacle in incorporating highly hydrophobic drugs such as TAC into the hydrogel is the use of organic solvents such as acetone and ethanol to prepare the spiking solution of the drug. Nanoparticles have been used successfully to formulate sustained released formulation for hydrophobic drugs for injection [28,29]. A wide range of diblock copolymers can be used to develop drug-loaded nanocarriers with different *in vitro* drug release profiles. Seven different polymers of different molecular weights and block lengths are selected to form TAC-loaded nanoparticles (Table 2-1). Drug loading, particle size, stability, and *in vitro* drug release are assessed to determine the best polymer for TAC encapsulation.

We find the two polymers PEG_{5k}-*b*-PCL_{10k} and PEG_{5k}-*b*-PLA_{10k} demonstrate highest drug loading efficiencies (Figure 2-22). Under refrigerated conditions, both formulations are stable at up to 5 days with more than 98% drug being retained in solution and with minimal change in size and PDI (data not shown). However, data indicate that at room temperature, PEG_{5k}-*b*-PCL_{10k} nanoparticles are stable for up to 24 hr, while PEG_{5k}-*b*-PLA_{10k} retained less than 50% of the initial loading at 24 h. Based on our results, PEG_{5k}-*b*-PCL_{10k} and PEG_{5k}-*b*-PLA_{10k} nanoparticles demonstrate longer shelf-life at refrigerated temperature presumably due to better drug-polymer compatibility which may result in sustained release. Thus, future characterization is limited to these polymers.

4.3. In vitro drug release of TAC nanoparticles

The release profiles of TAC from PEG_{5k}-*b*-PCL_{10k}, and PEG_{5k}-*b*-PLA_{10k} nanoparticles are evaluated in pH 7.4 PBS buffer at 37 °C over 72 hr dialysis. As depicted in (Figure 2-23), TAC released fromPEG_{5k}-*b*-PLA_{10k} nanoparticles follows a biphasic profile characterized by a fast burst followed by a slow release phase. The initial burst is where 40% of the drug is

released by 24 hr. The drug is observed to have precipitated out of the nanoparticle formulation following the burst phase as the solution inside the cassettes turns cloudy. The release of TAC from PEG_{5k}-*b*-PCL_{10k} is much slower with only 25% TAC released by 24 hr. Curve fitting of the *in vitro* data indicates that half-time ($t_{1/2}$) values as calculated by Graph Pad Prism are 8.71 hr and 38.5 h for PEG_{5k}-*b*-PLA_{10k} and PEG_{5k}-*b*-PCL_{10k} respectively. Based on the release profile we hypothesize that the release of TAC from the PEG_{5k}-*b*-PLA_{10k} nanoparticles is strongly driven by diffusion as most of the drug is pushed from the crystalline core to the particle corona resulting in rapid drug depletion and precipitation. Furthermore, when it comes to drug retention stability at room temperature, the PEG_{5k}-*b*-PCL_{10k} nanoparticle outperforms the PEG_{5k}-*b*-PLA_{10} nanoparticle. This indicates a better compatibility between the drug and PEG_{5k}-*b*-PCL_{10k} polymer. We decided to incorporate PEG_{5k}-*b*-PCL_{10k} nanoparticle into our final formulations.

4.4. In vitro drug release from hydrogels

To understand how drug loading affects the release rate of TAC from the hydrogels, we load each hydrogel platform with either 0.5 or 1 mg/ml TAC. At each predetermined sampling time point, the entire buffer is exchanged with fresh solution to maintain sink condition. The drug release kinetics of the two hydrogels are shown in (
Figure 2-24). The release profile of TAC from pvpGel exhibits a large burst at 1 hr when more than 10% of the total drug content is release into the medium. In contrast, the aminoGel shows significantly smaller burst effect with less than 5% of total loaded drug released. Such a stark contrast in burst release of the two hydrogels are due to their different gelation mechanism and matrix configuration. As discussed earlier, the pvlGel gelation is by micellar aggregation and rearrangement of the PEG-PVL-PEG polymers in aqueous solution. Polymers of similar building blocks such as PEG-PCL-PEG and PCL-PEG-PCL have been shown to undergo recrystallization of the PCL core during gelation process[21–23]. Differential scanning calorimetry and X-ray diffraction analysis of the PVL block in PEG-PVL-PEG copolymer have shown the crystalline nature of the PVL block[11]. Therefore, as the PEG-PVL-PEG polymer solution undergo thermosensitive gelation, the PVL core also recrystallizes in similar manner as the PCL-based hydrogels. We hypothesize

that as the PEG-PVL-PEG polymers undergo conformational changes, a fraction of the loaded drug is pushed out of the crystalline core onto the gel surface. Upon contacting with the release medium, the surface bound TAC is immediately dissolved. In contrast, the aminoGel internal structure is a fiber like network formed by PPLA block β-sheet aggregate of the PPLA-PEG-PPLA polymer as previously discussed (Figure 2-17). Lipophilic drugs such as TAC could be trapped in the hydrophobic matrix allowing for prolonged released from the formulation.

After the initial burst phase, the release kinetics of both hydrogel platforms follow a steady and slow release path. To characterize the release mechanism of TAC from the hydrogel matrix, we fit the release data to first order and Higuchi model. The summarized data are organized in (Table 2-4). Higuchi model is found to be best fitted for the both pvlGel and aminoGel data (Figure 2-25). This indicates that the fraction of drug released from the gels is a function of the square root of time. The release of TAC is a diffusion process from the hydrogel core to the interfacial surface[14]. As the drug deposited on the superficial layers of the hydrogel is released, it takes progressively longer for the drug molecules from the gel core to diffuse outward through the polymer matrix. For each hydrogel, the Higuchi constant k, which is related to the release rate of the drug from the gel matrix, is similar between the two different drug loading concentrations. Thus, by changing the loading concentration we can tailor the input rate of TAC from the hydrogel formulations allowing convenient scaling to different animal models in future studies.

4.5. In vivo Pharmacokinetic studies in rats:

The first part of our PK study is to understand how each formulation platform behaves *in vivo* before embarking on investigating extended release formulations. For this we loaded 0.5 mg/ml TAC in hydrogels by either spiking the hydrogels with a concentrated TAC in ethanol or NP solution. Healthy rats are injected subcutaneously at 0.31 mg/kg dose with either TAC-loaded pvlGel, aminoGel, TAC-NP, or TAC-NP-pvpGel composite. A large burst is observed in pvlGel group at 1 hr post dose ($p<0.05$) (Figure 2-26). The burst does not

last long as the blood concentration quickly returns to below 10 ng/ml by 2 hr. The blood level remains steady between 5-10 ng/ml and gradually tapers off toward 48h. This is in accordance with the *in vitro* release profile of pvlGel observed in previous section which also exhibits a burst release followed by a slow release phase. The TAC-NP and aminoGel formulations also show an initial burst albeit at a much lower magnitude. Similarly, the TAC concentrations in blood gradually taper off toward 48h, indicating a sustained release phase. When we combine the TAC-loaded NP into the PVL hydrogel to form the TAC-NP-pvlGel composite, the burst release is eliminated. The drug is released in a controlled manner and reach an apparent C_{max} (15 ng/ml) by 12h. By 48h the drug is eliminated from the system (Figure 2-26).

Current research on hydrogels for sustained drug delivery often show a burst release following the hydration and swelling of the gels after injection[30]. This present a major obstacle in formulating hydrogels for injectable prolonged release of highly potent drugs like TAC. The incorporation of TAC-loaded PEG_{5k}-b-PCL_{10k} NP into our pvlGel platform has eliminated the burst phase. It is possible that the interaction between the pvlGel polymeric network and the PEG_{5k}-*b*-PCL_{10k} stabilizes the NP allowing for a slower release of the drug from the composite matrix[31]. The incorporation of drug loaded NP into a hydrogel network has been shown to provide an additional diffusion barrier and strengthen the diffusion resistance of drugs from the NP-gel composite, thus, moderating or eliminating the burst release[32].

We then formulate two composite formulations by combining PEG_{5k}-b-PCL_{10k} NP to pvlGel and aminoGel and increase our dosing 1 mg/kg to achieve prolonged release of TAC. Another group of rats (n = 4) is injected with TAC-loaded aminoGel formulation at 1 mg/kg. Both NP-gel composite formulations show biphasic release profile with no observable burst effect (Figure 2-27). A rapid initial release of TAC from the injected formulation allows the drug to accumulate to ~15 ng/ml. However, the drug levels do not rise any further but rather exhibits a second release phase. We hypothesize that the first

pulse of drug release is due to breakage of drug-loaded NPs. The hydrogel phase acts as a second diffusional barrier and reduces the drug release rate, thus, lessening the burst effect. The effect of NP on retarding the burst release can be contrasted with the TAC-loaded aminoGel formulation, which does not incorporate NP in the drug loading process. A small but significant burst is observed at 2 hr post injection. The burst raises the TAC concentration significantly higher than the other two composite formulation groups ($p<0.05$). The composite NP hydrogel formulations exhibit a second release phase that is most likely due to degradation or erosion in combination with drug diffusion out of the hydrogels. The drug gradually tapers off after reaching the second Cmax and completely eliminated from the body by day 9. The aminoGel platform shows a much less visible biphasic profile and demonstrates a much tighter control of drug release.

5. CONCLUSION

In the period following kidney transplantation, it is important to keep the concentration of TAC in the range of 5-15 ng/ml to avoid rejection of the new organ. When administered orally, the main common route of TAC administration for chronic immunosuppression post transplantation, high fluctuations of TAC concentrations in whole blood are often observed[33,34]. Such fluctuations endangers patients for toxicity, when TAC level is above 30 ng/ml, and graft failure/rejection when the level is too low[35]. One of the main causes of the circulating TAC variability within each patient is the different individual ability for gastrointestinal absorption of TAC, which is further affected by the presence of food. Therefore, it is empirical that patients administering TAC orally should take the medication on time and consistently without food. This presents a great barrier to patient adherence which in turn further jeopardizes graft health post transplantation.

In this study, two TAC-NP aminoGel composite formulation are successfully prepared by dispersing TAC loaded PEG_{5k}-b-PCL_{10k} NP to PEG grafted poly(aspartate-propylamine) and PVL-based thermogels. The NP-gel composite demonstrates a prolonged sustained release of TAC without burst effect, and maintains clinically relevant TAC concentrations for up to 7 days. The developed formulations, especially the NP-aminoGel composite, have a potential as sustained delivery system of TAC for the prevention of graft rejection. The significance of this finding when translated to human remained to be determined in future clinical trials.

Table 2-1: Polymers assessed for TAC nanoparticle preparation

Name	Manufacturer	Polymer Type	Avg.Molecular Weight (Dalton)
RG502	Sigma	Poly(lactic-co-glycolic acid) 50:50	12,000
RG505	Sigma	Poly(lactic-co-glycolic acid) 50:50	61,500
RG756S	Sigma	Poly(lactic-co-glycolic acid) 75:25	96,000
PLA	Advanced Polymer Materials, Inc.	Poly(lactic acid)	10,000
PCL	Advanced Polymer Materials, Inc.	Polycaprolactone	10,000
PEG5k-b-PLA10k	Advanced Polymer Materials, Inc.	mPEG-b-Poly(lactic acid)	15,000
PEG5k-b-PCL10k	Advanced Polymer Materials, Inc.	mPEG-b-Polycaprolactone	15,000

Table 2-2: Amount of ingredients in step 2 and 3 of polyamino synthesis

	BLA-NCA amount			BLG-NCA amount		
	8 units	16 units	24 units	8 units	16 units	24 units
PEG-NH2 or NH2-PEG-NH2 1 g, 0.5 mmol	1.25 g 5 mmol	2.5 g 10 mmol	5 g 15 mmol	1.32 g 5 mmol	2.64 g 10 mmol	5.28 g 15 mmol
Propylamine	1.48 g 25 mmol	2.96 g 50 mmol	5.92 g 100 mmol	1.48 g 25 mmol	2.96 g 50 mmol	5.92 g 100 mmol
Butylamine	1.84 g 25 mmol	3.68 g 50 mmol	7.36 g 100 mmol	1.84 g 25 mmol	3.68 g 50 mmol	7.36 g 100 mmol

Table 2-3: Gelation properties of synthesized polymers

Type	Initiator	Hydrophobic block	Side chain (R-group)	Repeating unit	CMC mg/ml	Gelation
A-B	PEG-NH2	Glu	Propylamine	8	0.25	X
	PEG-NH2	Glu	Propylamine	16	0.25	X
	PEG-NH2	Glu	Propylamine	24	0.2	X
	PEG-NH2	Glu	Butylamine	8	0.2	X
	PEG-NH2	Glu	Butylamine	16	0.1	X
	PEG-NH2	Glu	Butylamine	24	0.1	X
	PEG-NH2	Asp	Propylamine	8	0.8	X
	PEG-NH2	Asp	Propylamine	16	0.8	X
	PEG-NH2	Asp	Propylamine	24	0.4	X
	PEG-NH2	Asp	Butylamine	8	0.5	X
	PEG-NH2	Asp	Butylamine	16	0.4	X
	PEG-NH2	Asp	Butylamine	24	0.3	X
A-B-A	PEG-NH2	Asp	Propylamine	48	0.4	X
	PEG-NH2	Asp	Propylamine	32	0.6	X
B-A-B	NH2-PEG-NH2	Glu	Propylamine	8	0.22	**X**
	NH2-PEG-NH2	Glu	Propylamine	16	0.2	X
	NH2-PEG-NH2	Glu	Propylamine	24	0.1	X
	NH2-PEG-NH2	Glu	Butylamine	8	0.2	X
	NH2-PEG-NH2	Glu	Butylamine	16	0.1	X
	NH2-PEG-NH2	Glu	Butylamine	24	0.01	X
	NH2-PEG-NH2	Asp	Propylamine	8	2	Yes
	NH2-PEG-NH2	Asp	Propylamine	16	1.6	Yes
	NH2-PEG-NH2	Asp	Propylamine	24	0.25	Yes
	NH2-PEG-NH2	Asp	Butylamine	8	0.4	X
	NH2-PEG-NH2	Asp	Butylamine	16	0.4	X
	NH2-PEG-NH2	Asp	Butylamine	24	0.2	X

Table 2-4: pvlGel and aminoGel kinetic model fitting parameters

Model name	pvlGel 0.5 mg/ml			aminoGel 0.5 mg/ml		
	R^2	Slope	Intercept	R^2	Slope	Intercept
1st order	0.976	-0.0099	5.40	0.961	-0.0030	5.47
Higuchi	0.996	16.76		0.987	7.64	
Model name	pvlGel 1 mg/ml			aminoGel 1 mg/ml		
	R^2	Slope	Intercept	R^2	Slope	Intercept
1st order	0.958	-0.0092	6.08	0.941	-0.0040	6.13
Higuchi	0.998	33.04		0.998	19.61	

Figure 2-1: Polyamino polymer synthesis scheme

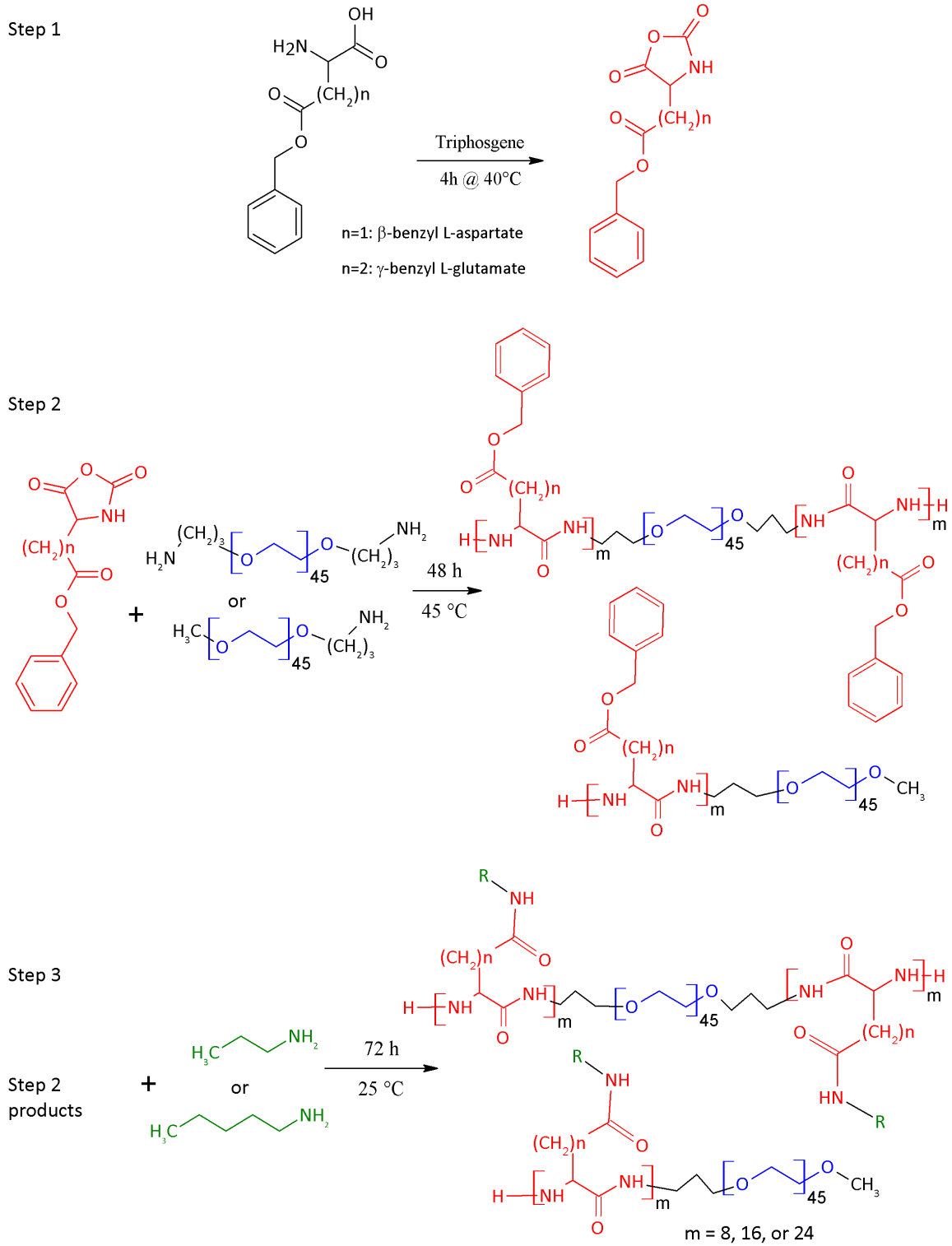

Figure 2-2: PVL polymer synthesis scheme

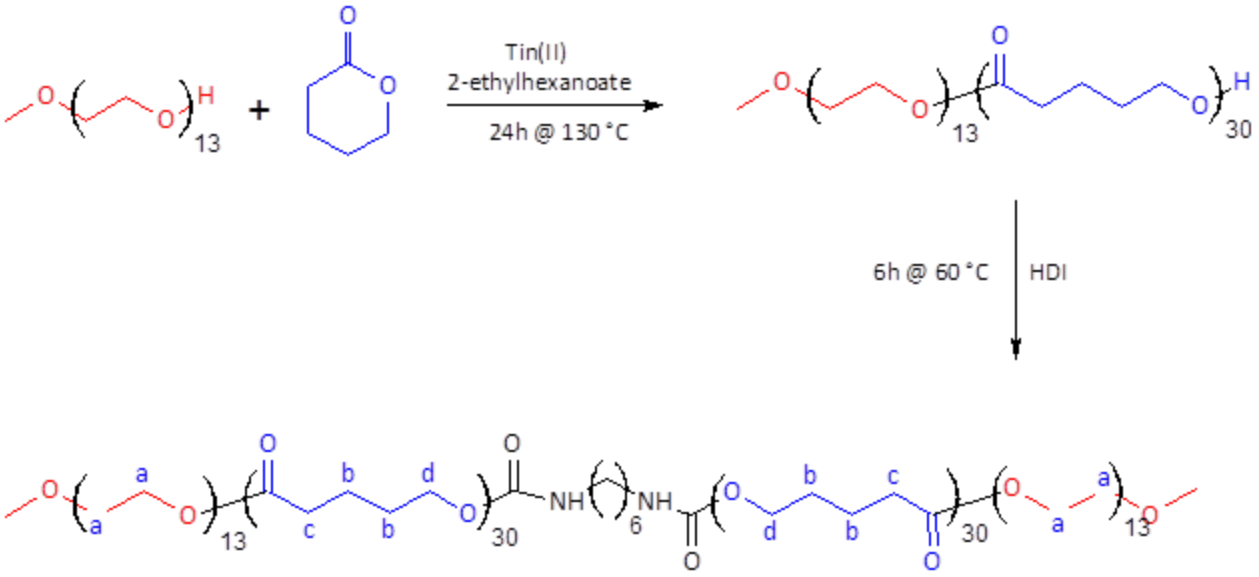

Figure 2-3: ^{1}H NMR Spectra of PBLA-PEG-PBLA polymers. A: 24 repeating units; B: 16 repeating units; C: 8 repeating units of benzyl-aspartate

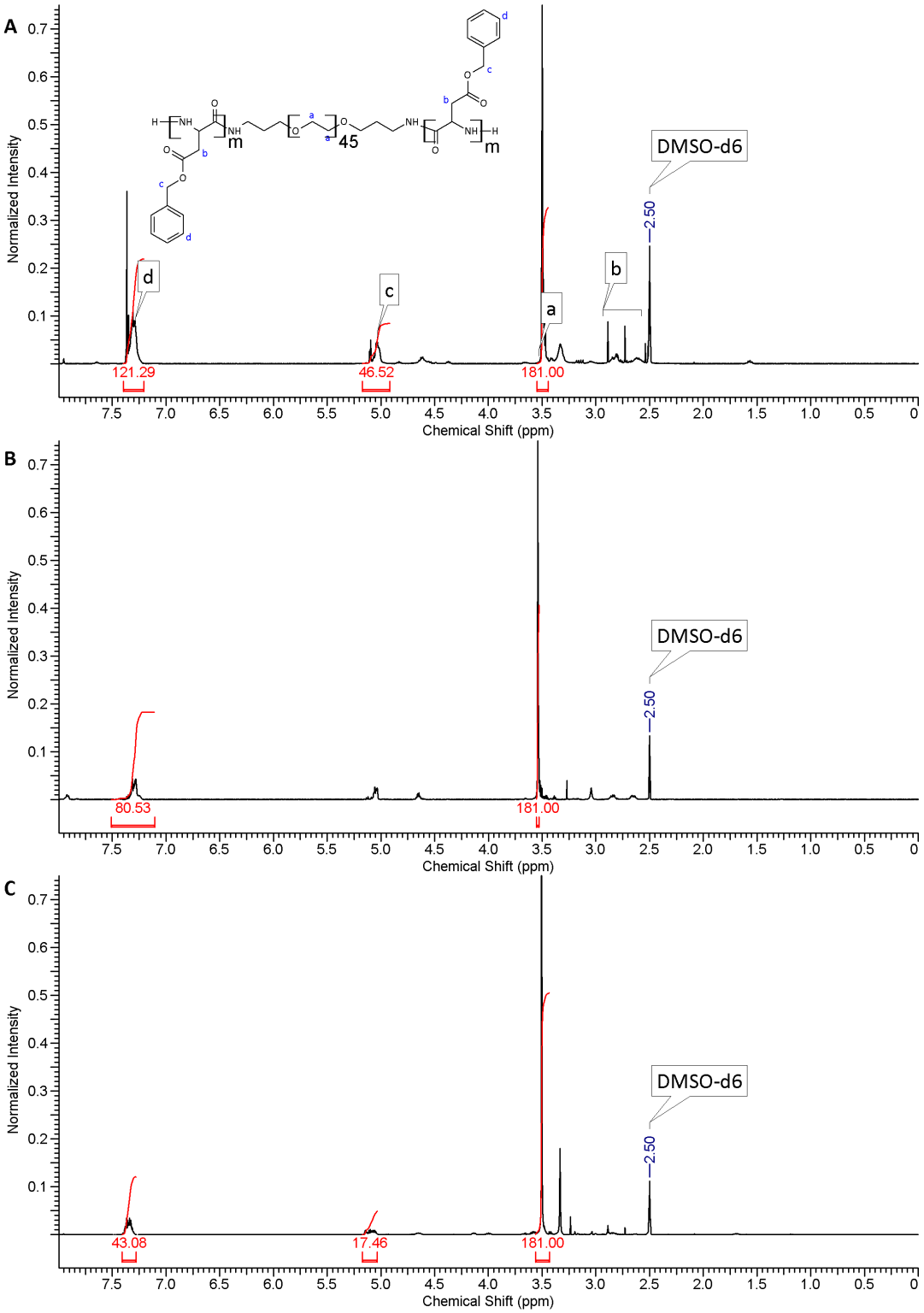

Figure 2-4: ^{1}H NMR spectra of PEG-PBLA polymers. A: 24 repeating units; B: 16 repeating units; C: 8 repeating units of benzyl-aspartate

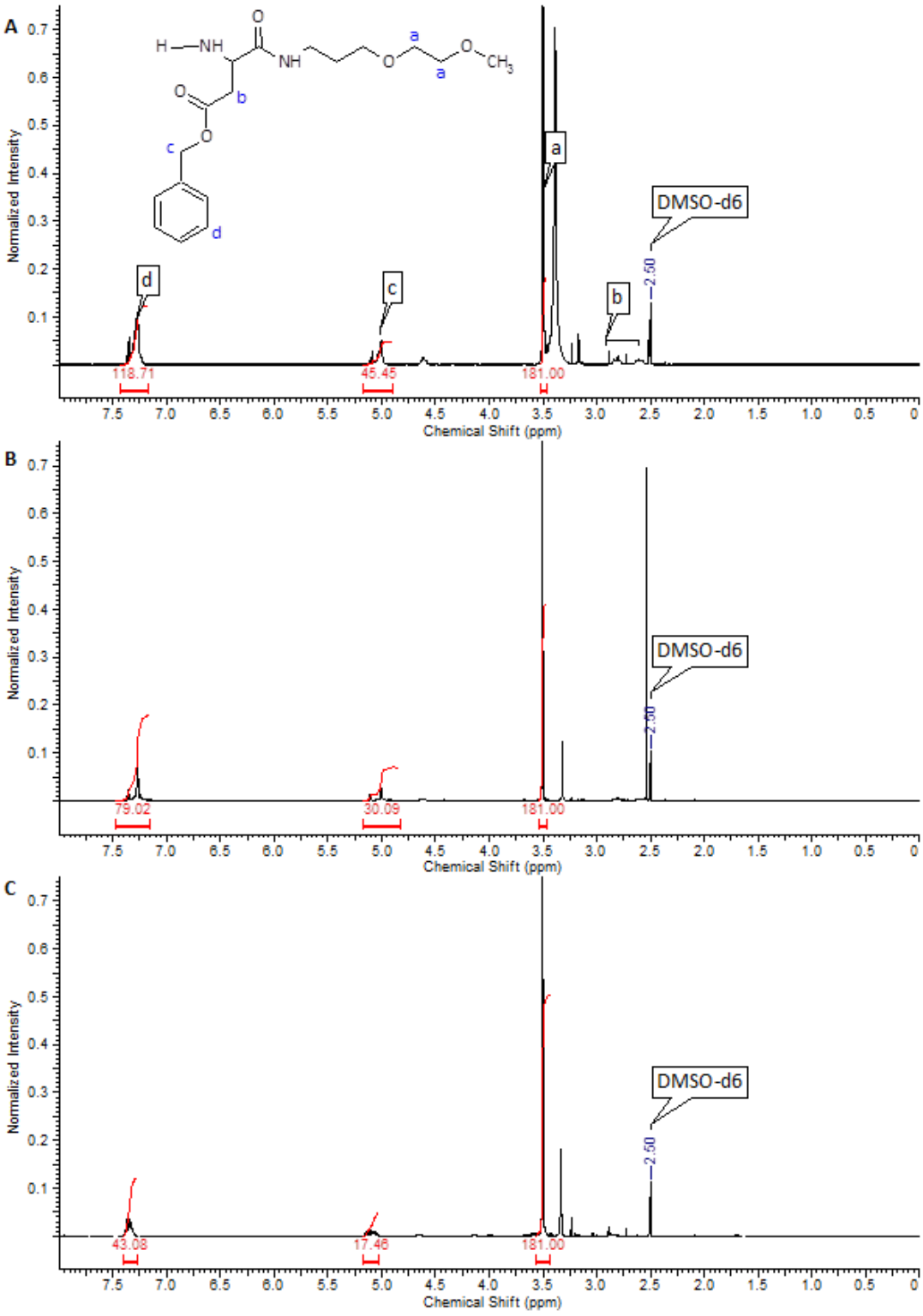

Figure 2-5: ^{1}H NMR spectra of PBLG-PEG-PBLG polymers. A: 24 repeating units; B: 16 repeating units; C: 8 repeating units of benzyl-aspartate

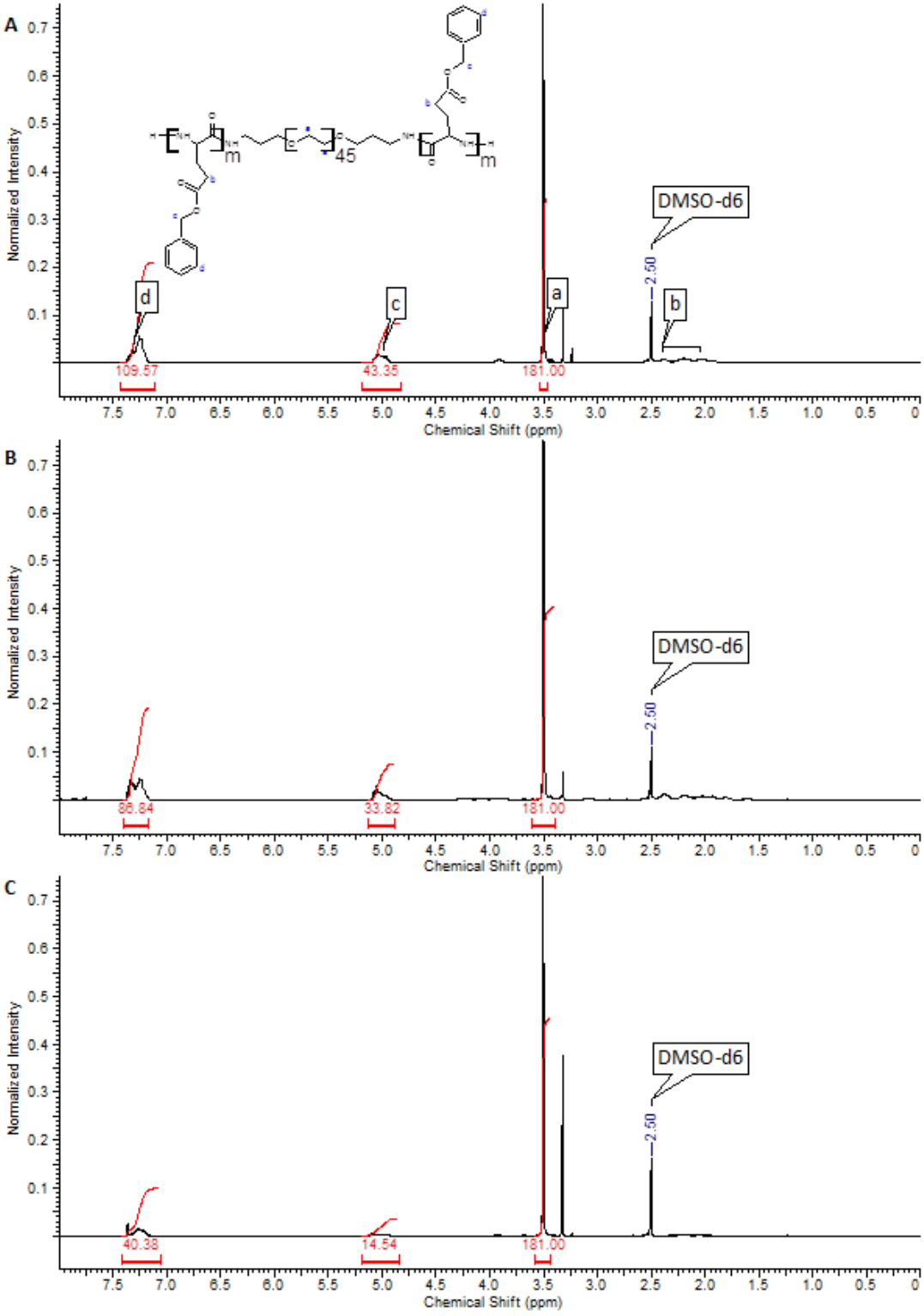

Figure 2-6: ^{1}H NMR spectra of PEG-PBLG polymers. A: 24 repeating units; B: 16 repeating units; C: 8 repeating units of benzyl-aspartate

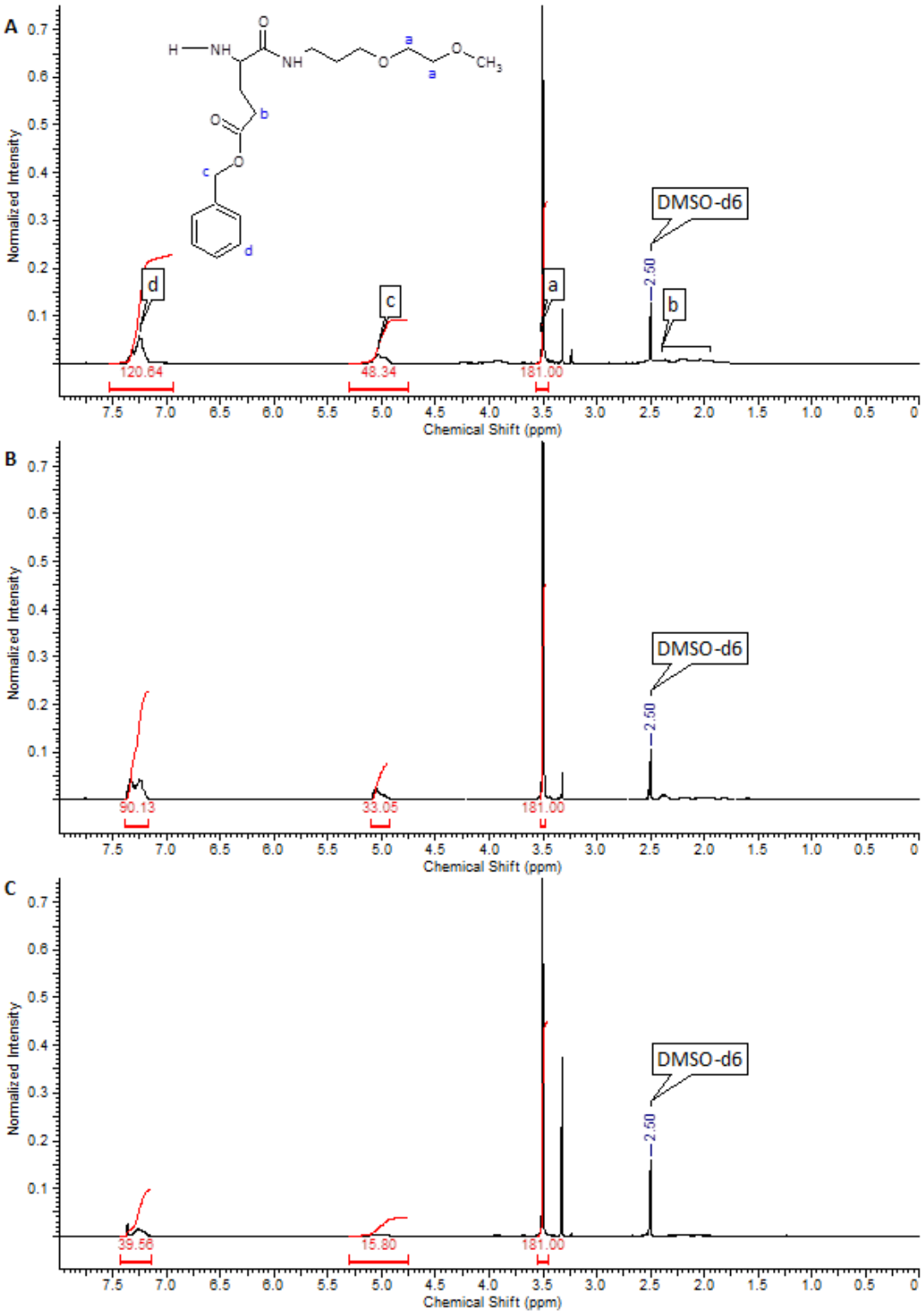

Figure 2-7: ^{1}H NMR spectra of PPLA-PEG-PPLA polymer conversion kinetic. A: 1 hr; B: 3 hr; C: 24 hr; D: 48 hr.

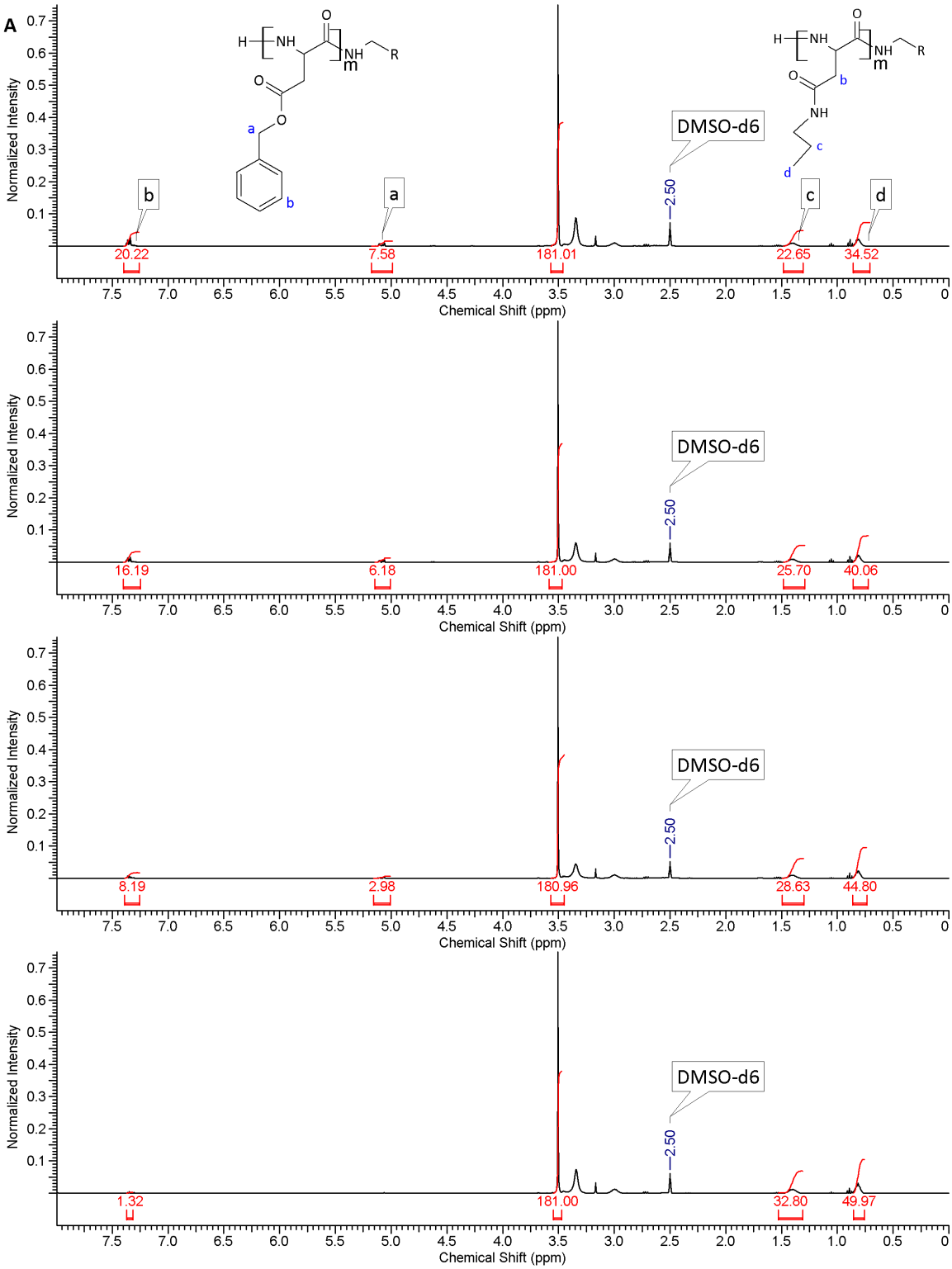

Figure 2-8: ^{1}H NMR spectra of PPLA-PEG-PPLA. A: 24 repeating units; B: 16 repeating units; C: 8 repeating units

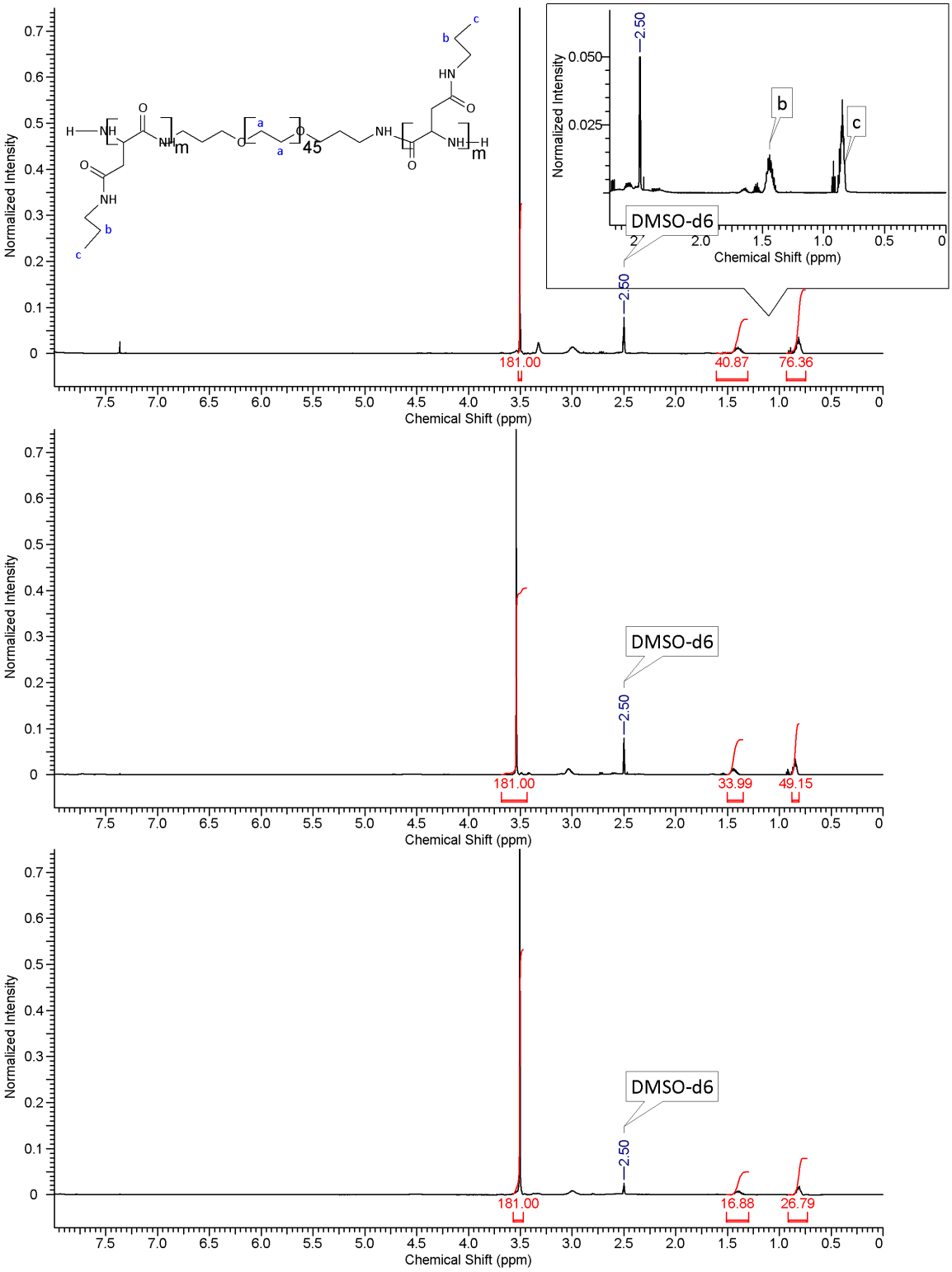

Figure 2-9: ^{1}H NMR spectra of PBuLA-PEG-PBuLA. A: 24 repeating units; B: 16 repeating units; C: 8 repeating units

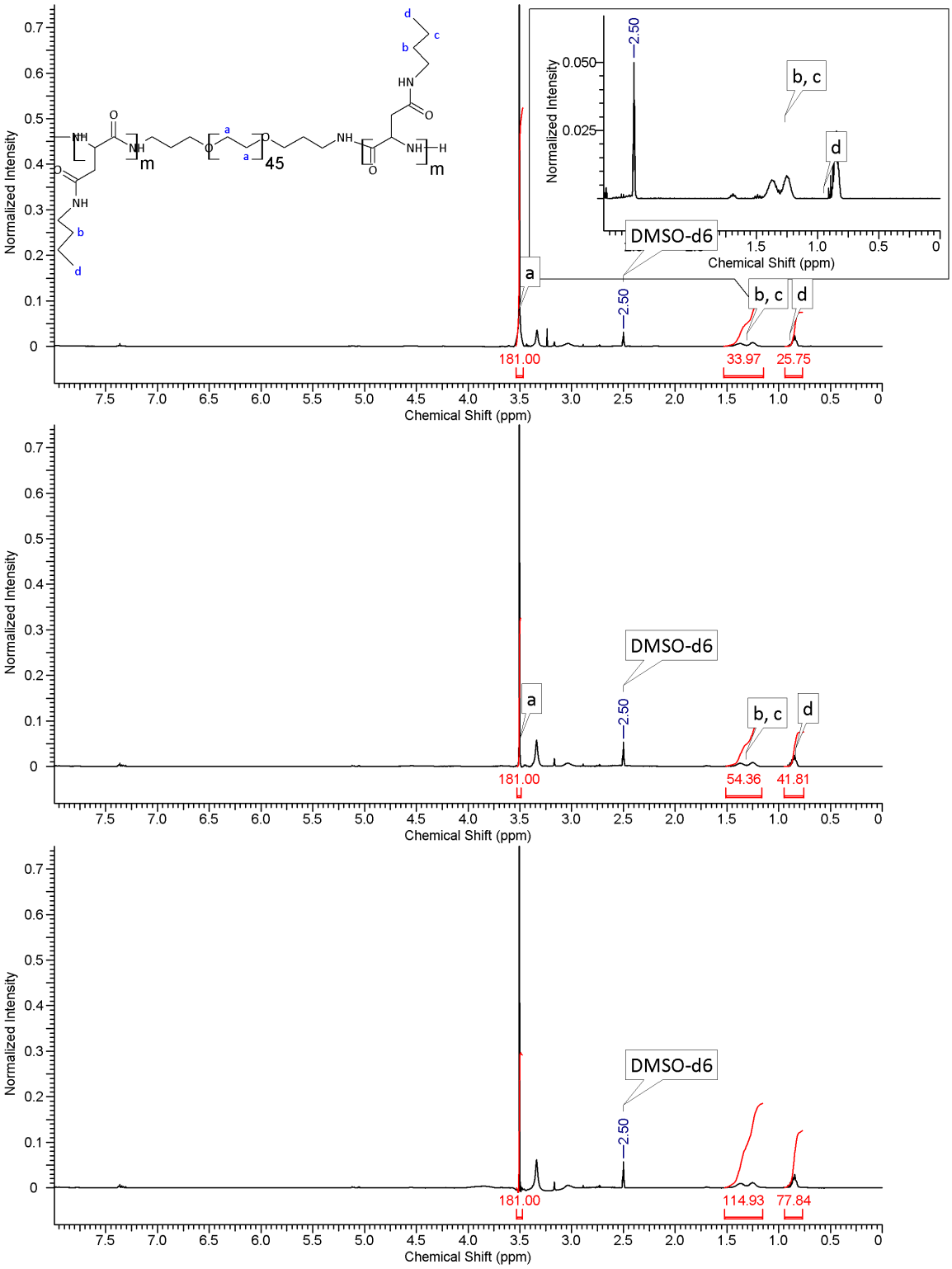

Figure 2-10: ^{1}H NMR spectra of PPLG-PEG-PPLG 8 repeating units

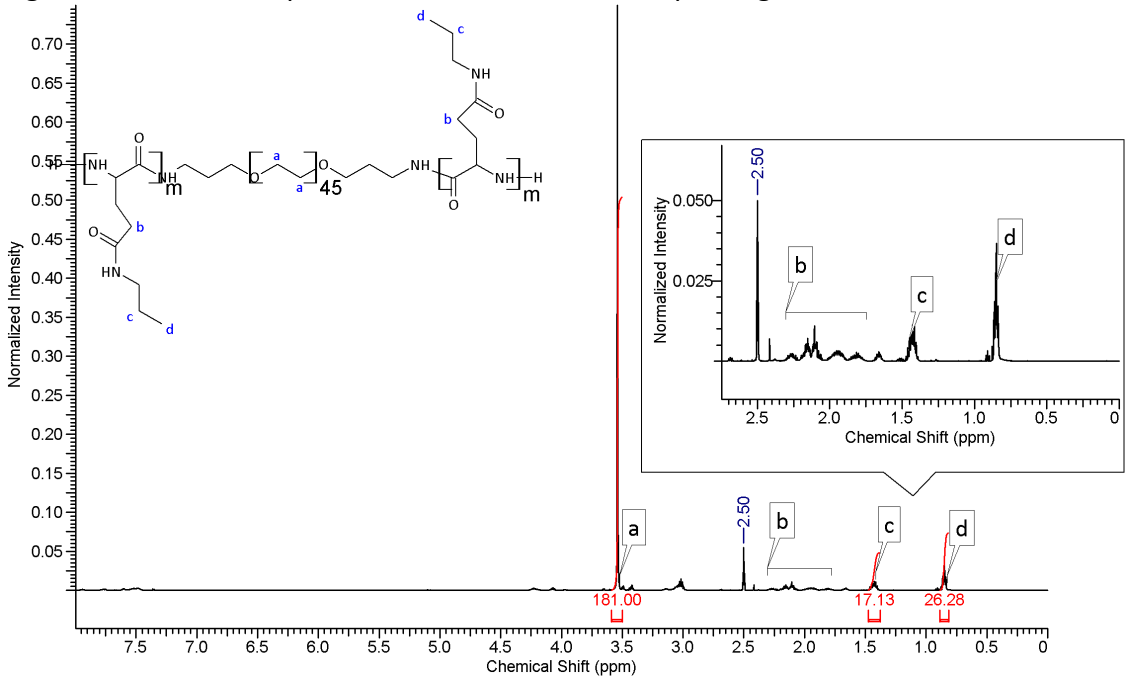

Figure 2-11: FTIR Spectra of PPLA-PEG-PPLA

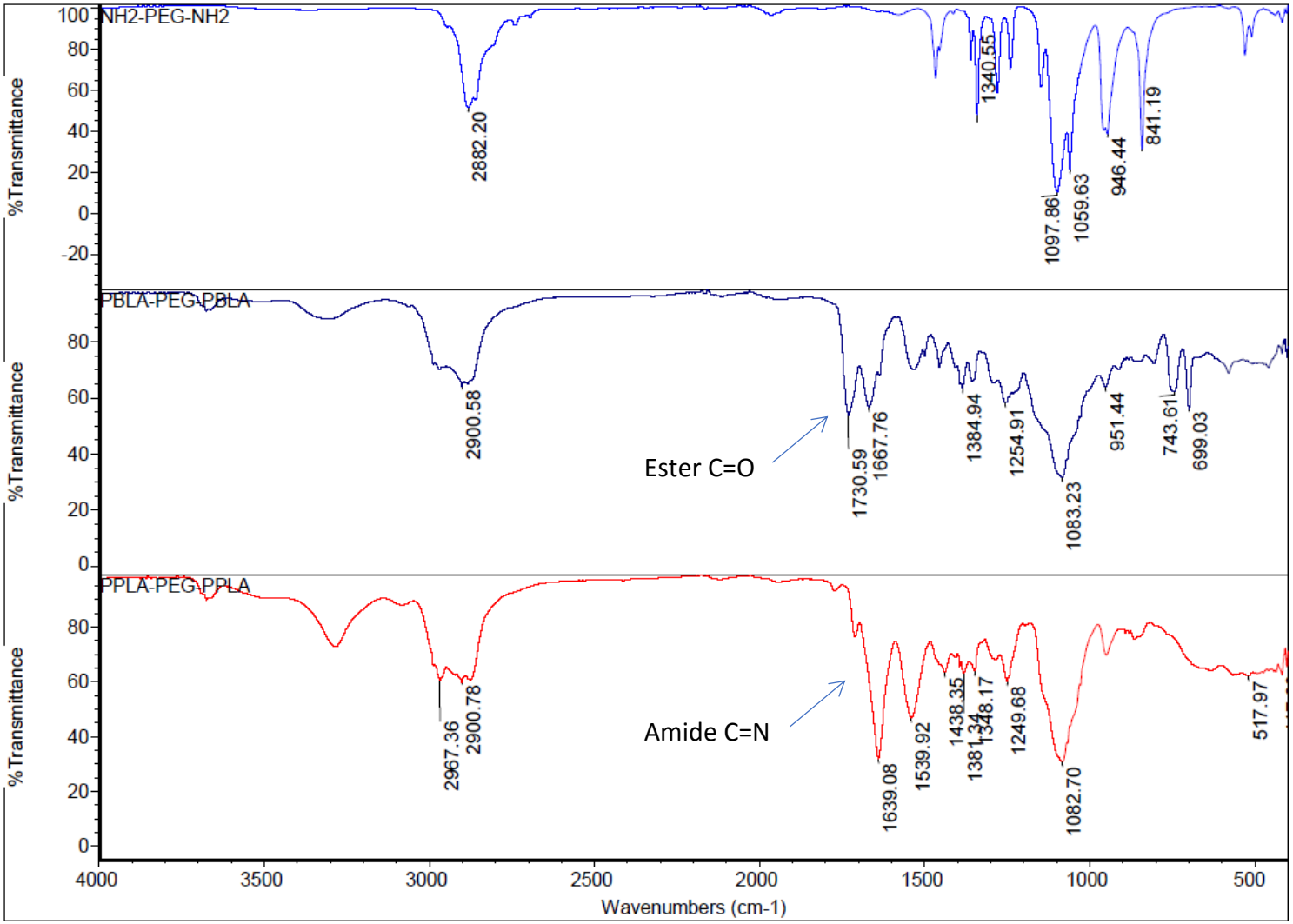

Figure 2-12: FTIR spectra of PPLG-PEG-PPLG

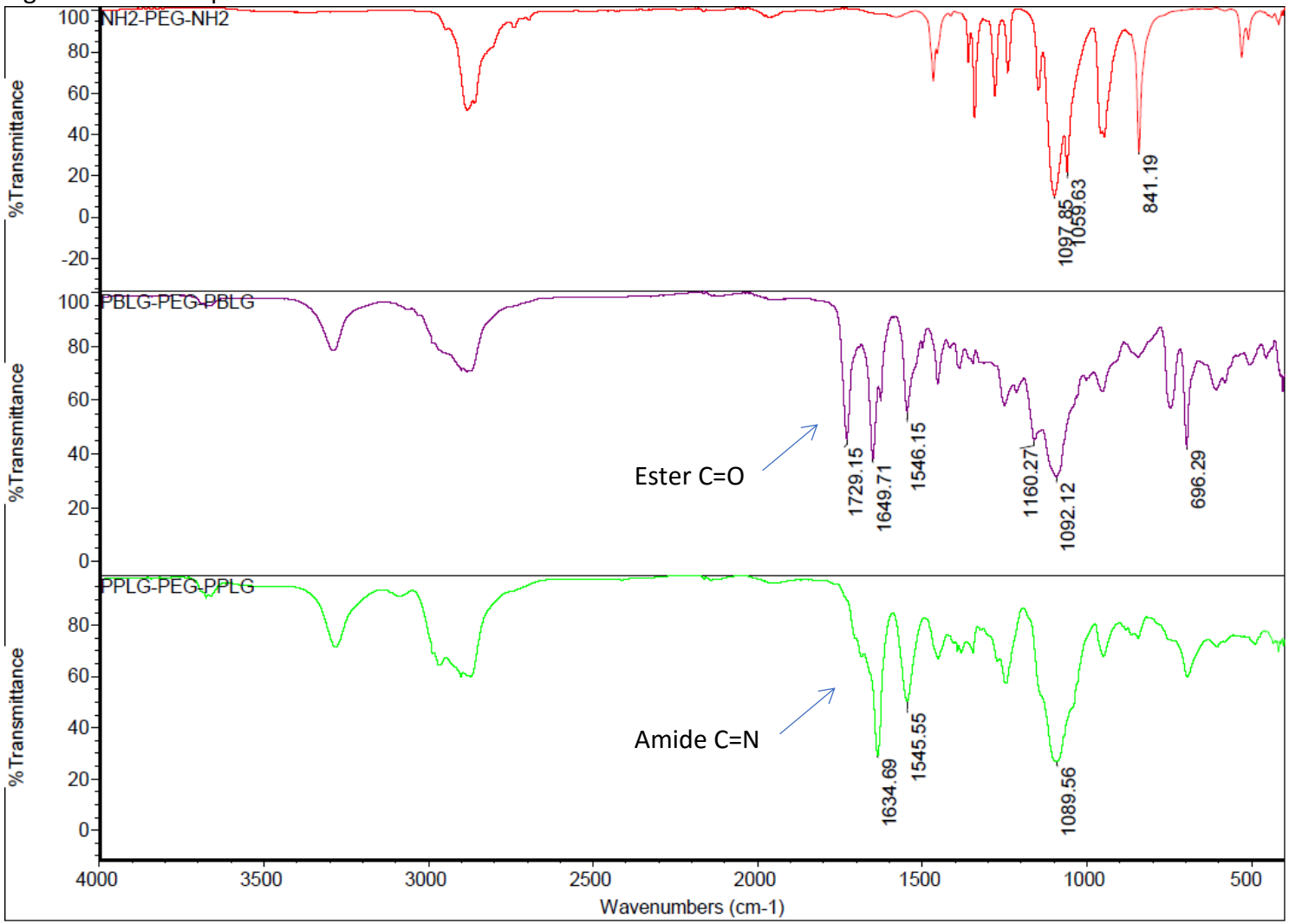

Figure 2-13: ^{1}H NMR spectrum of PEG-PVL-PEG polymer

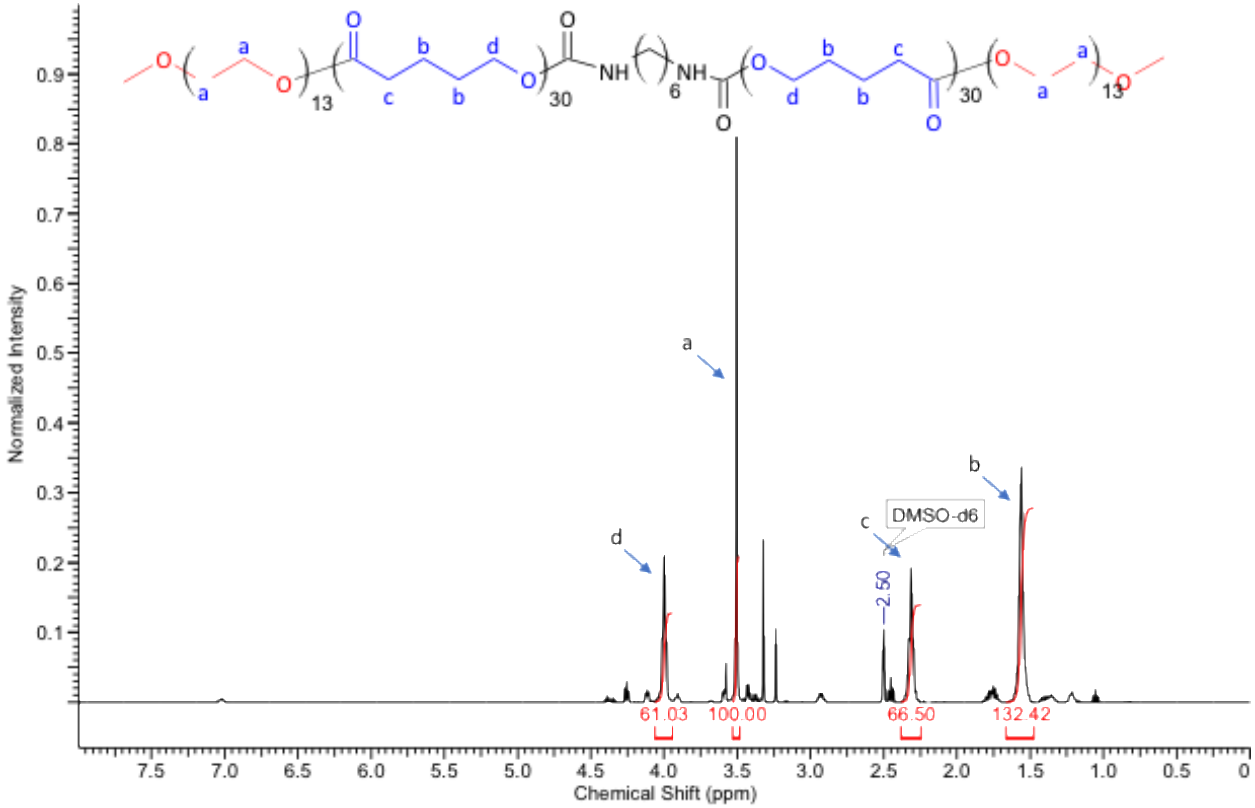

Figure 2-14: FTIR spectrum of PEG-PVL-PEG polymer

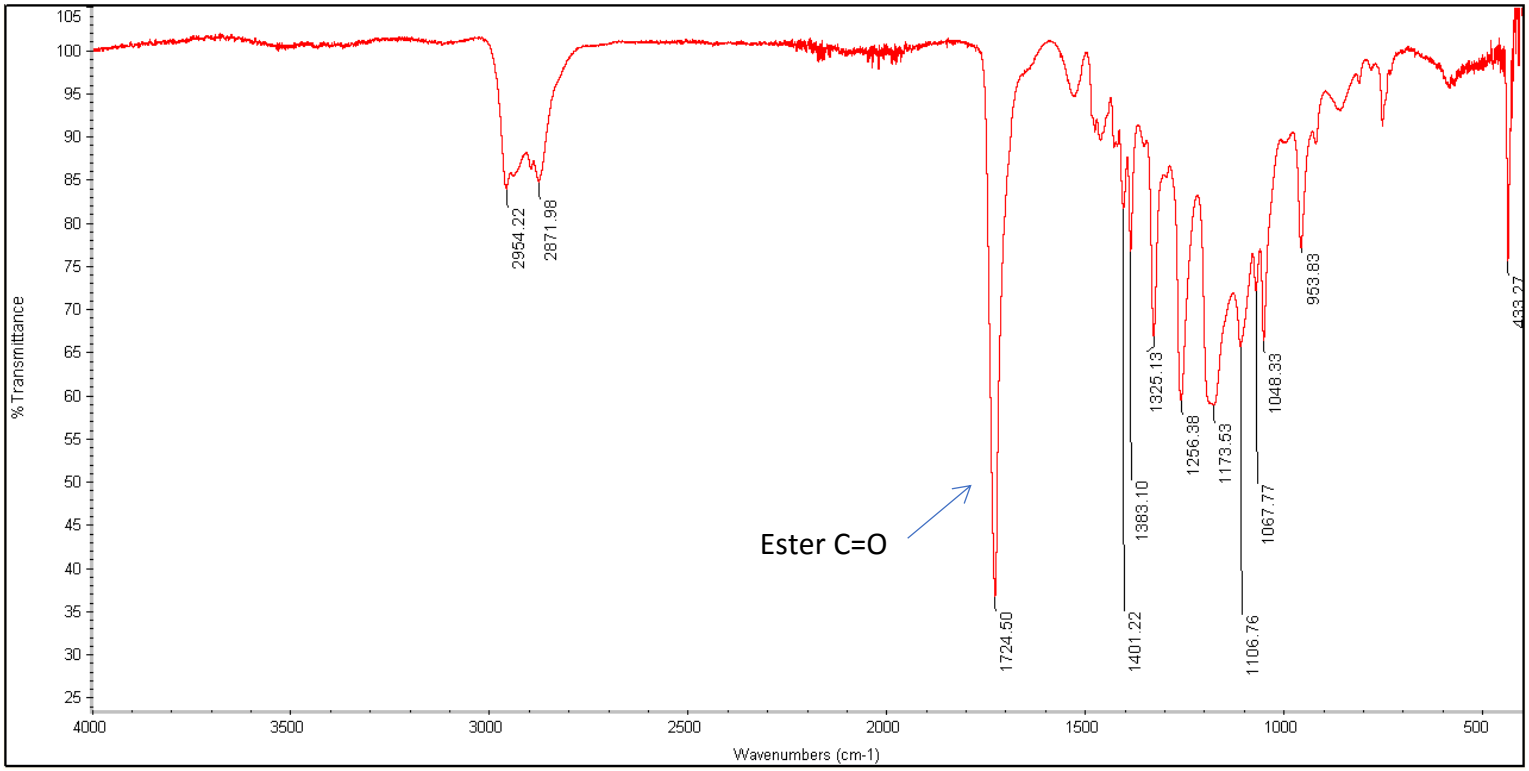

Figure 2-15: GPC analysis of PEG-PVL-PEG polymer

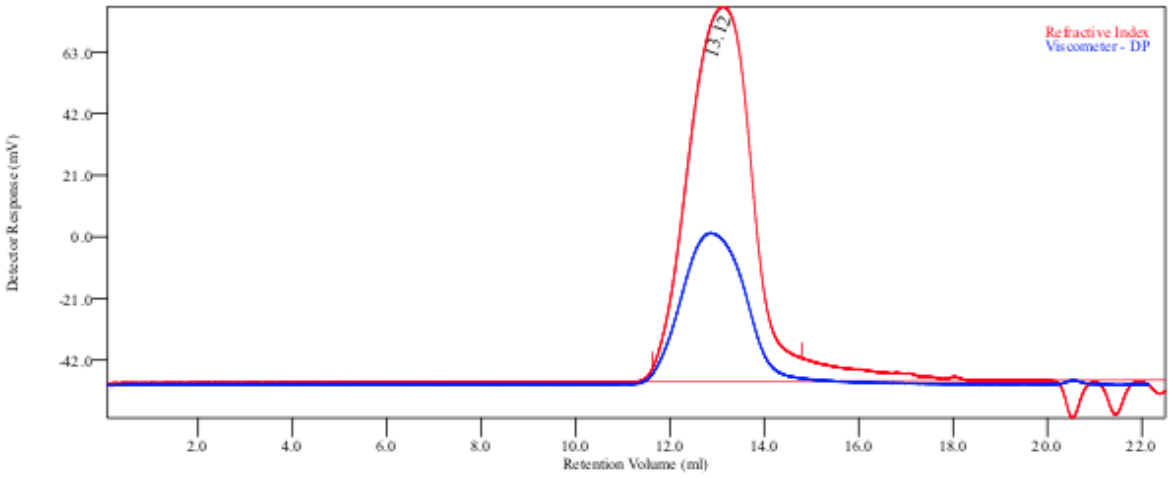

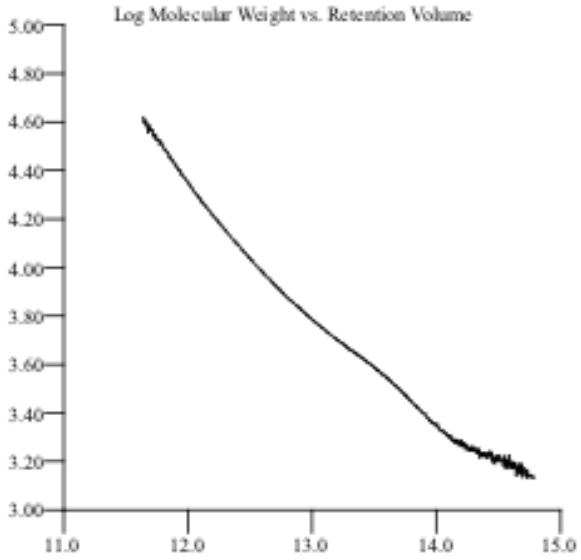

Figure 2-16: Sol-gel diagrams of the three PPLA-PEG-PPLA polymers at various concentrations. Gelation temperatures are found to be concentration dependent for all three polymers.

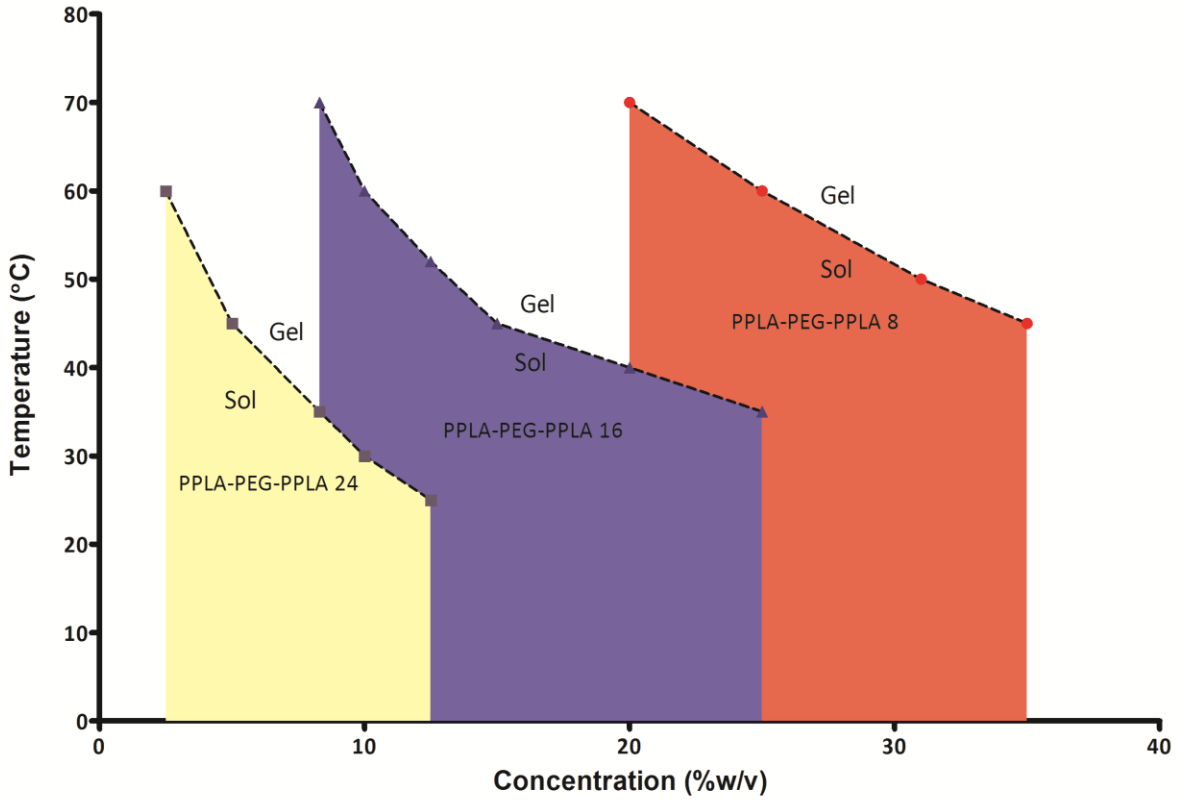

Figure 2-17: Cryo TEM images of PPLA-PEG-PPLA16 polymer at 0.5, 0.1, 1, and 5% in water

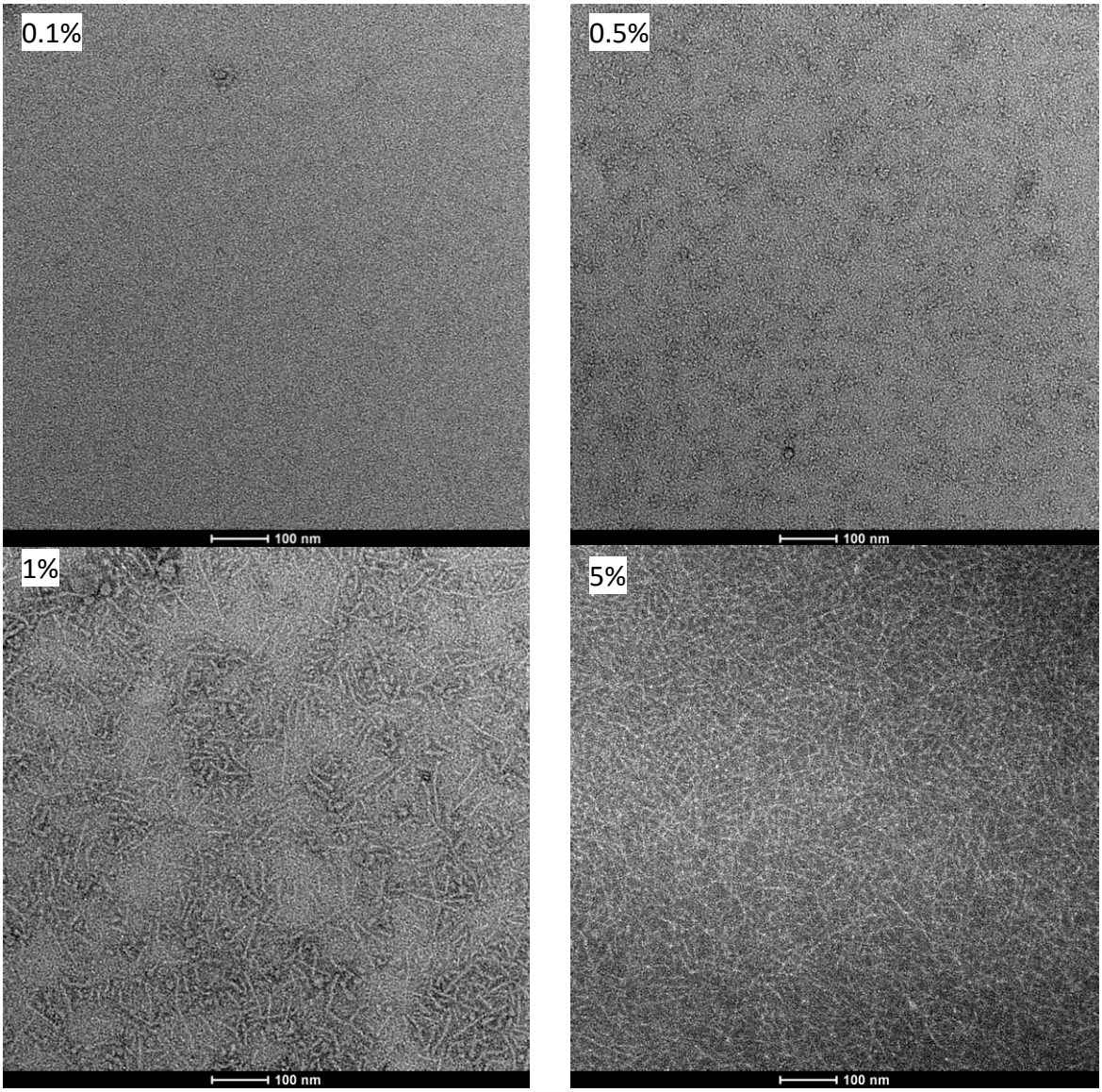

Figure 2-18: Rheological determination of Tg using TA AR200 rheometer. F127 18% in PBS is used for comparison. PPLA-PEG-PPLA16 at 25% in PBS has the same gelation temperature as F127. PPLA-PEG-PPLA24 starts gelling at around 25°C. And PPLA-PEG-PPLA8 gels at 45°C.

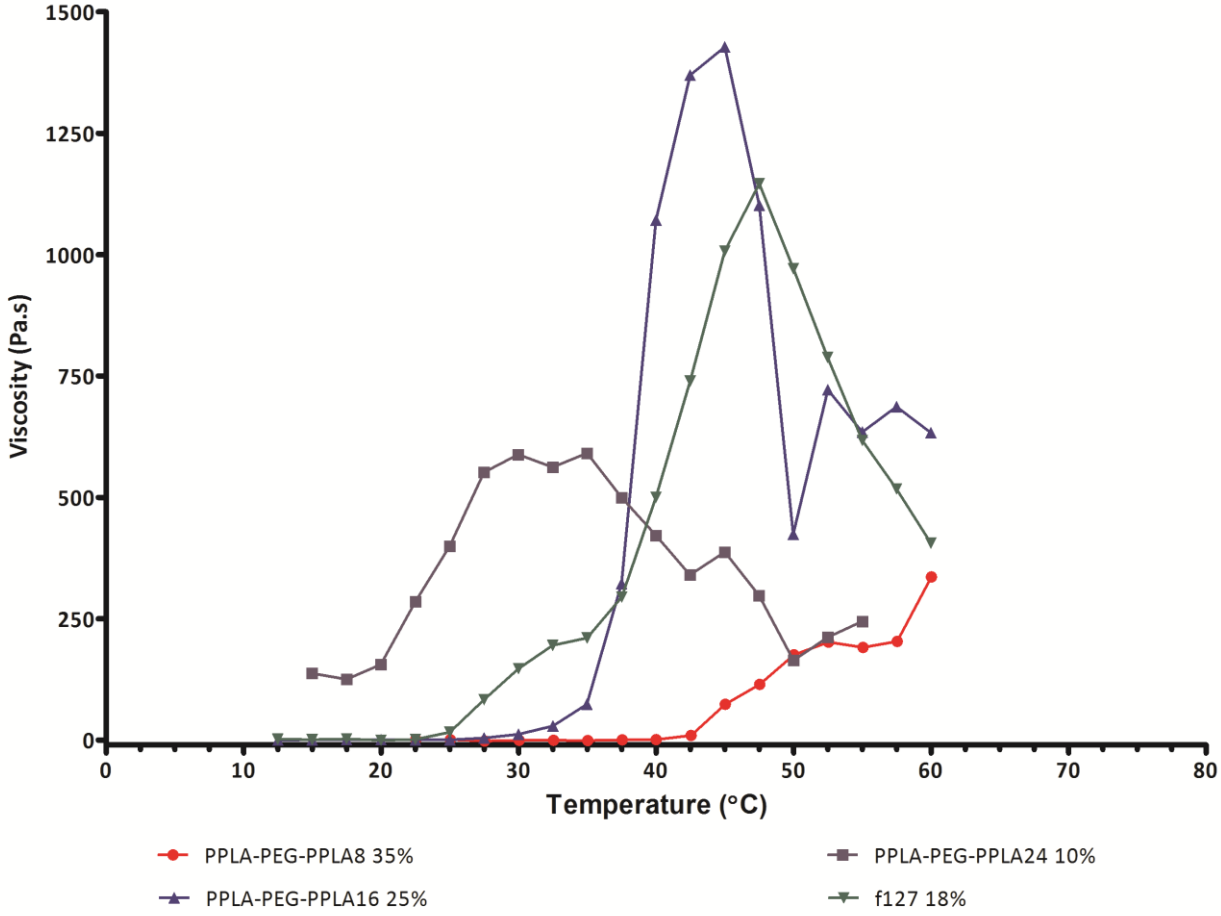

Figure 2-19: Cytotoxicity of PPLA-PEG-PPLA16 polymer. Values are reported relative to control, n = 5.

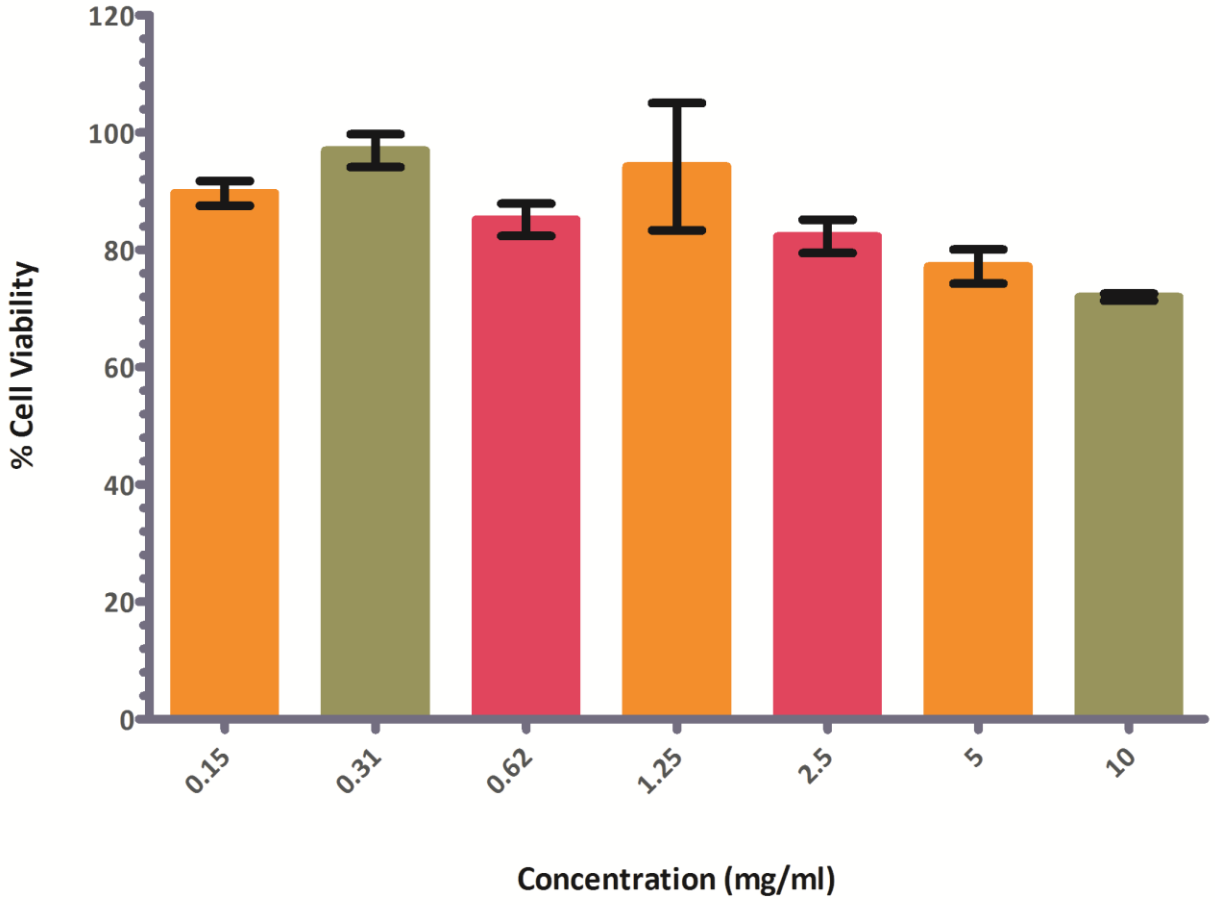

Figure 2-20: *in vitro* degradation of PPLA-PEG-PPLA16 hydrogel under the presence of proteinase K

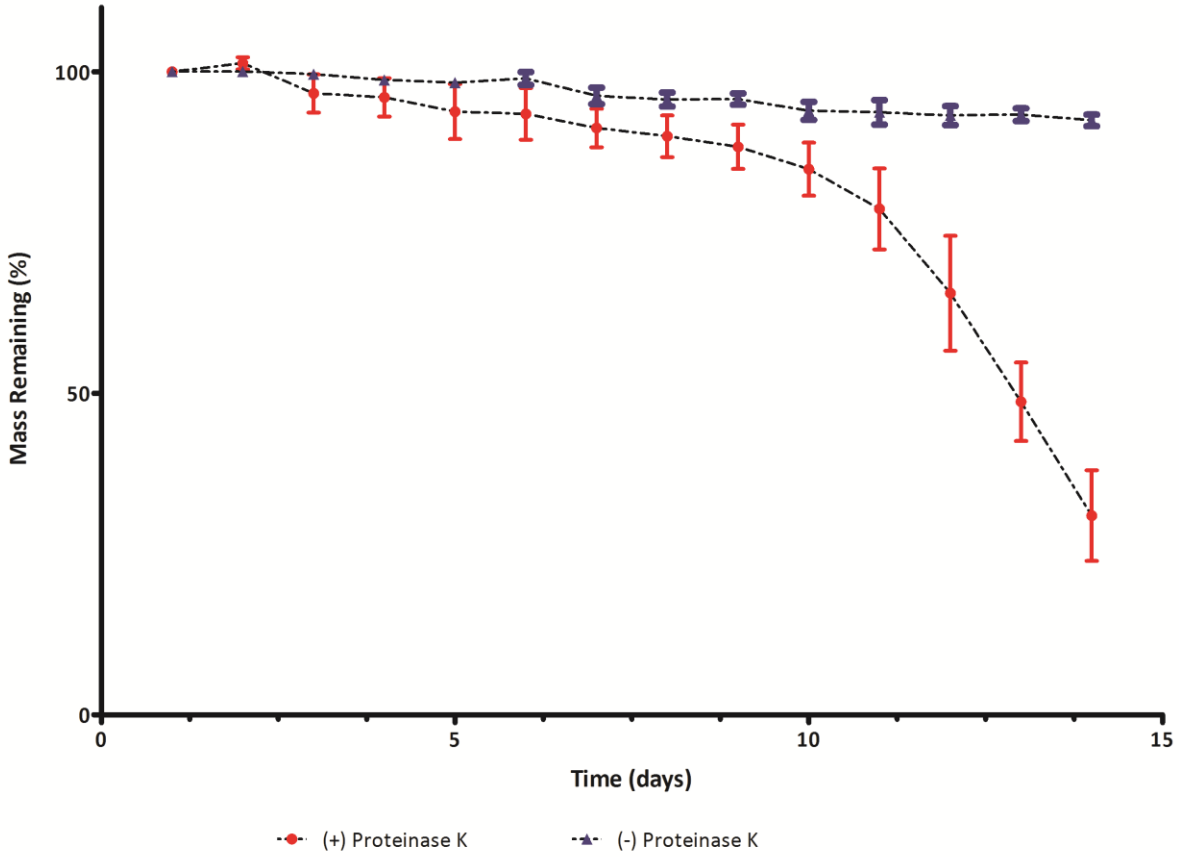

Figure 2-21: *in vivo* gelation of PPLA-PEG-PPLA16 polymer solution upon subcutaneous injection at days 1, 7, and 14.

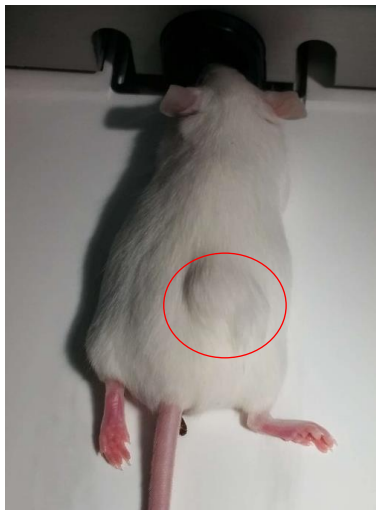

Day 1

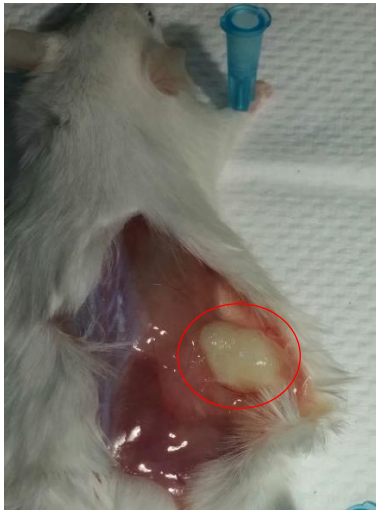

Day 7

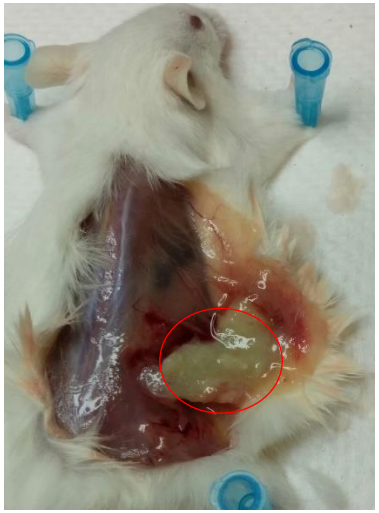

Day 14

Figure 2-22: Physical characterization of TAC-loaded nanoparticles. Drug loading efficiency (A), particle size (B), and PDI (C). Drug retention (D), particle size (E), and PDI (F) in storage at room temperature. Data is presented as Mean ± SD for four replicates.

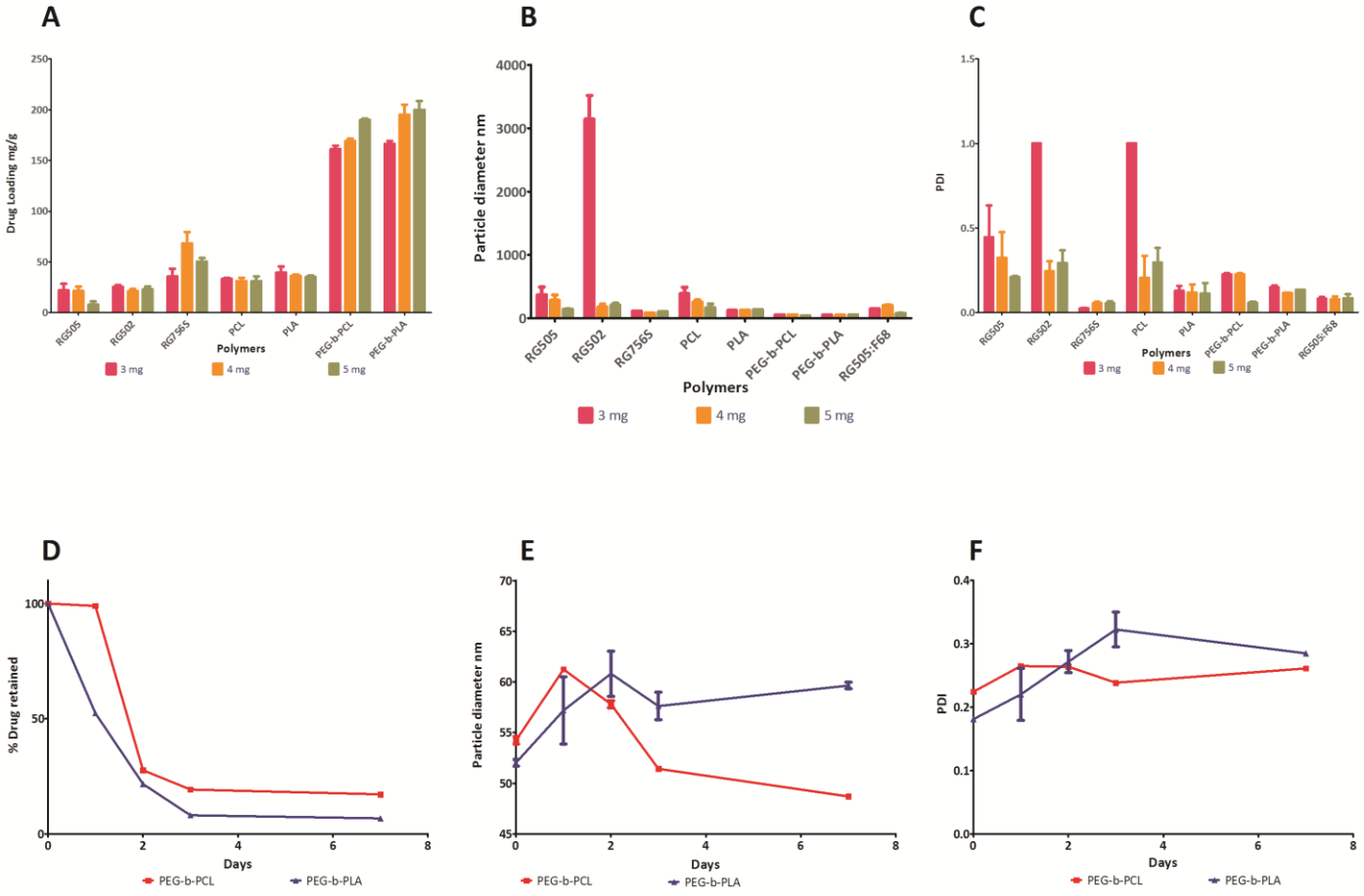

Figure 2-23: *In vitro* TAC released from PEG5k-b-PLA10k and PEG5k-b-PCL10k, nanoparticles. The dashed lines represent the one phase association curves.

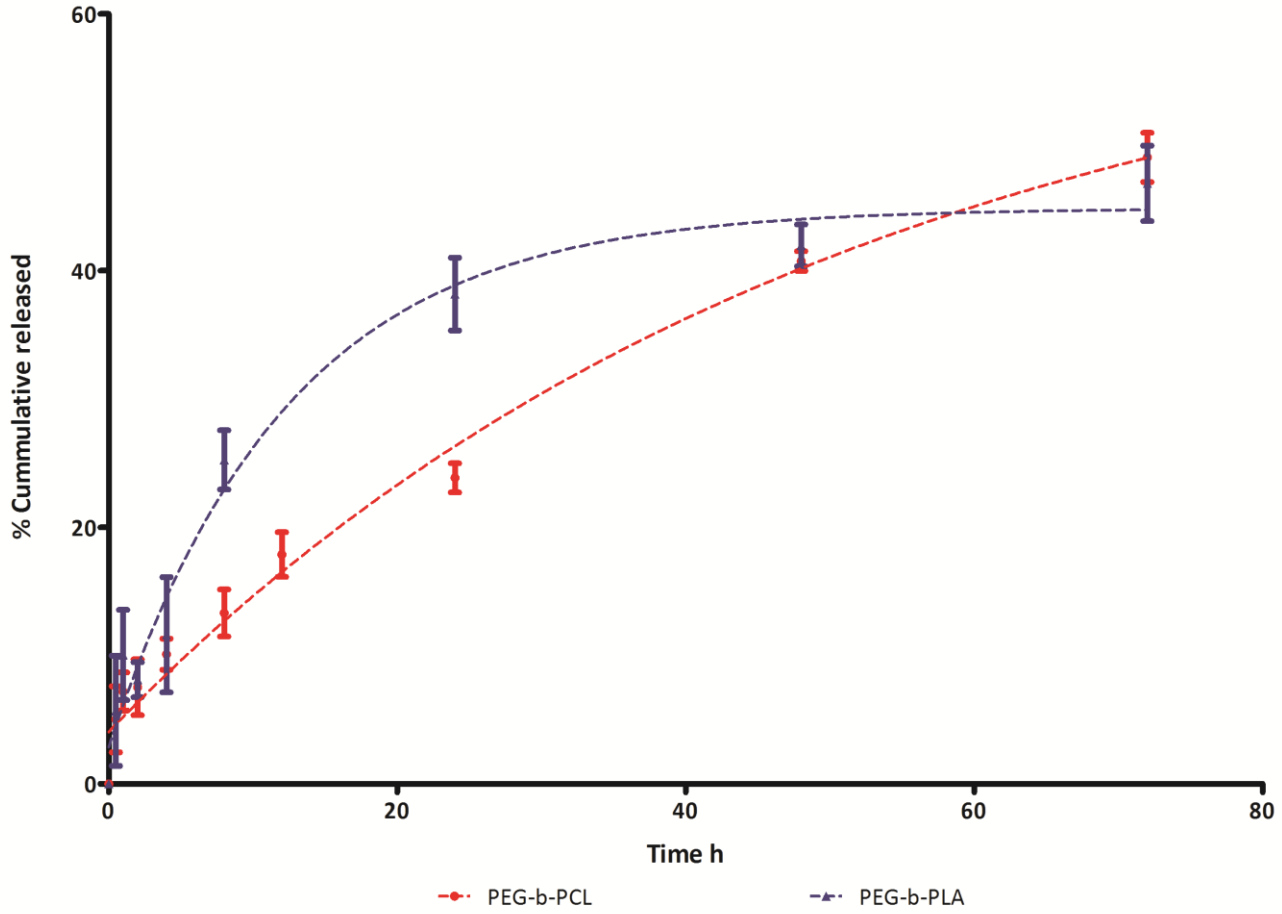

Figure 2-24: Cumulative amount and percent total TAC released from pvlGel (A and B) and aminoGel (C and D)

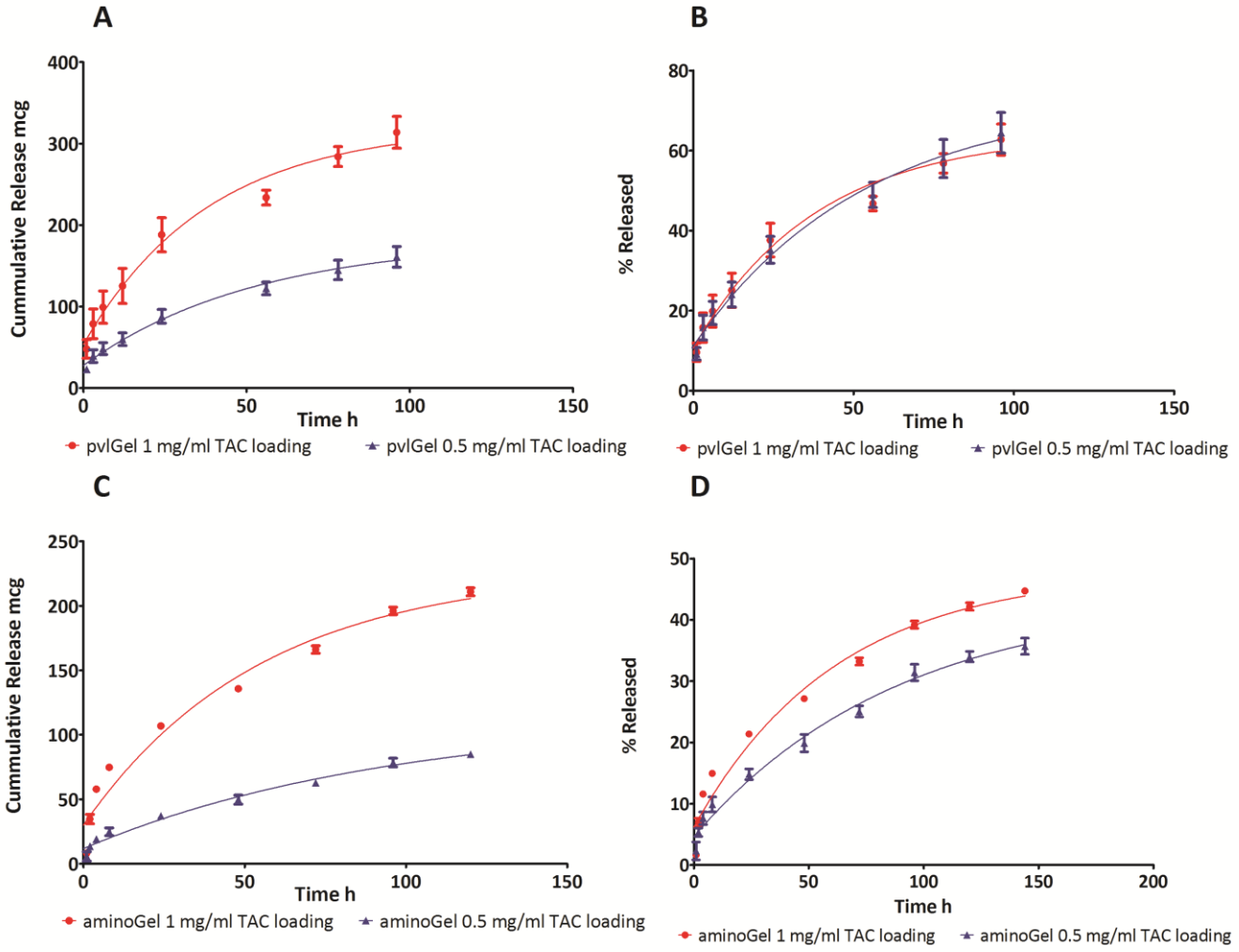

Figure 2-25: TAC release data are fitted into first order release kinetic and Higuchi models. A and B: 1st order and Higuchi model of pvlGel, respectively. C and D: 1st order and Higuchi model of aminoGel, respectively.

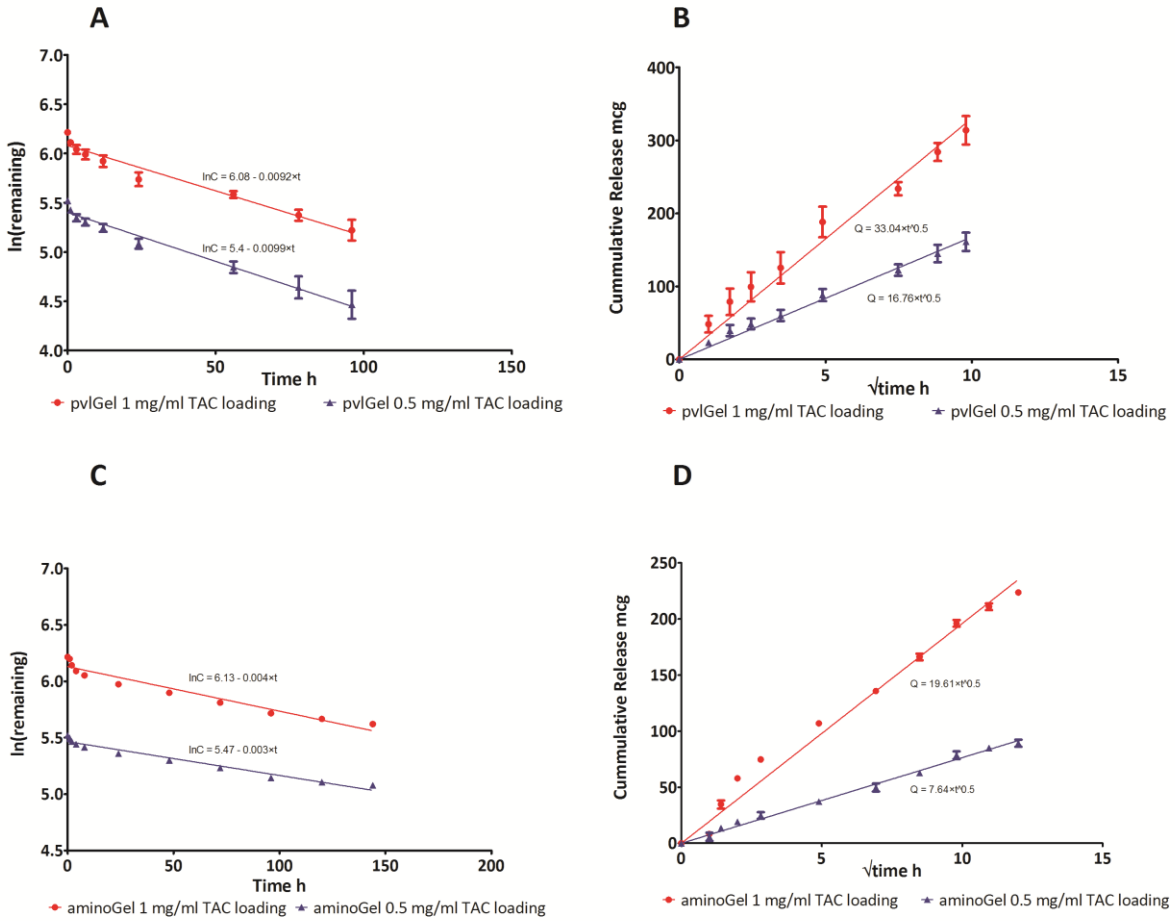

Figure 2-26: TAC whole blood levels of TAC-NP, pvlGel, TAC-NP-pvlGel, and aminoGel at 0.31 mg/kg dose. TAC concentrations are measured at 1, 2, 4, 8, 12, 24, and 48 hr post injection.

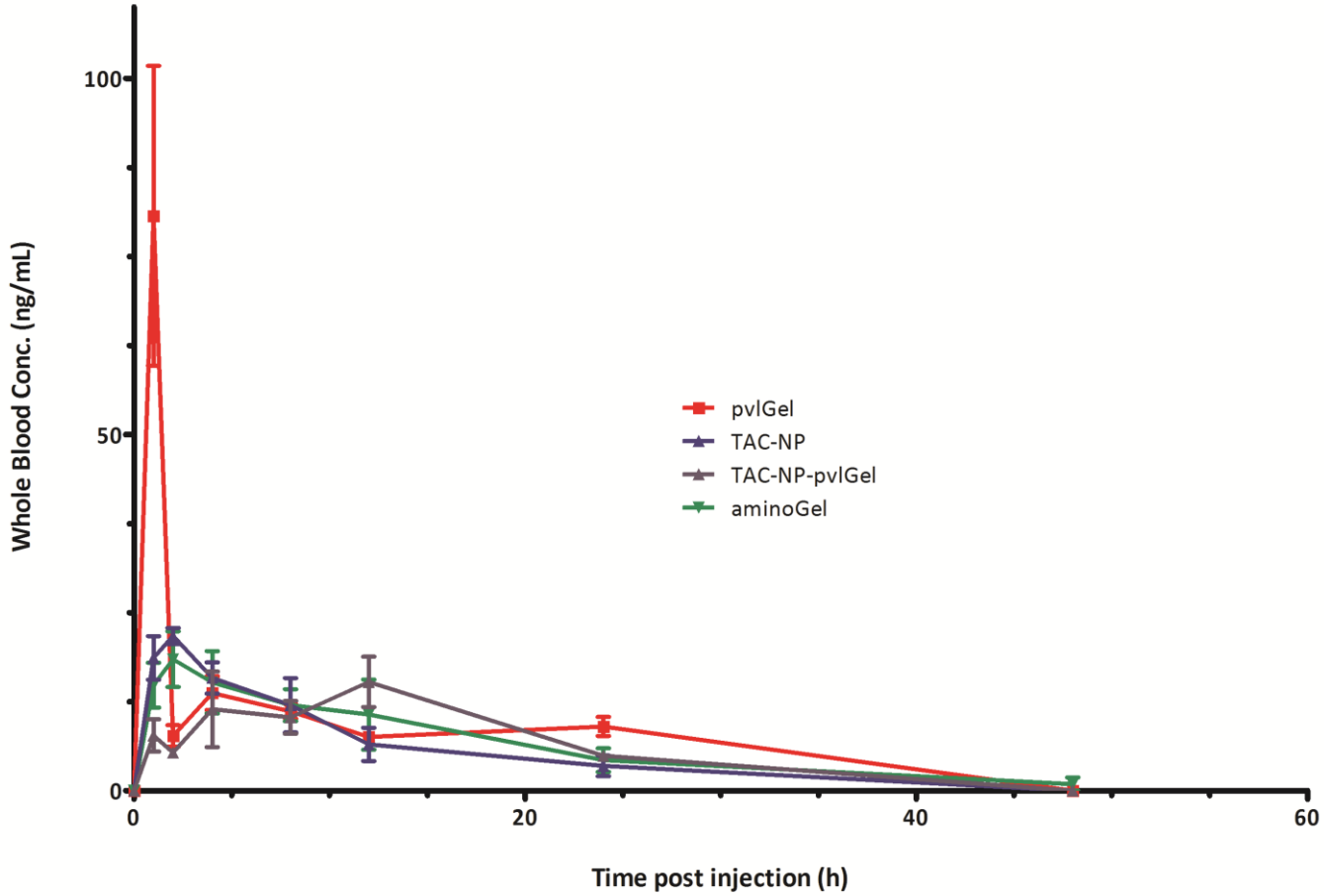

Figure 2-27: Whole blood concentration of TAC following subcutaneous injection of either TAC-NP-pvlGel or TAC-NP-aminoGel or aminoGel formulation. The dose is 1 mg/kg. TAC concentrations in whole blood are determined at 1, 2, 4, 8, 12, 24, and daily up to 9 days post injection.

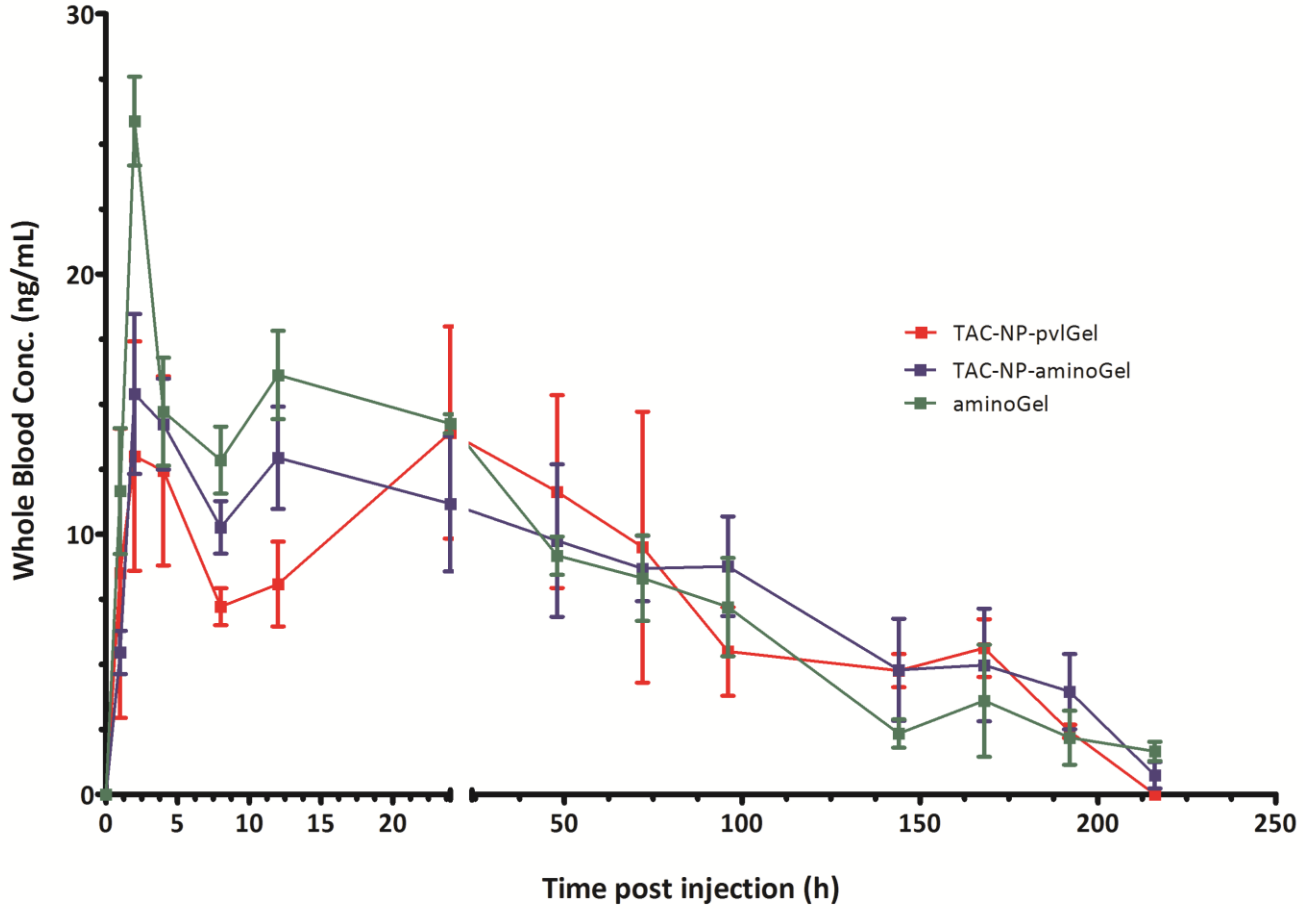

6. REFERENCES

1 Smith JM, Stablein DM, Munoz R, Hebert D, McDonald RA. Contributions of the Transplant Registry: The 2006 Annual Report of the North American Pediatric Renal Trials and Collaborative Studies (NAPRTCS). *Pediatr Transplant* 2007;**11**:366–73.

2 Chisholm-Burns MA, Spivey CA, Rehfeld R, Zawaideh M, Roe DJ, Gruessner R. Immunosuppressant therapy adherence and graft failure among pediatric renal transplant recipients. *Am J Transplant Off J Am Soc Transplant Am Soc Transpl Surg* 2009;**9**:2497–504.

3 2010 Annual Report of the U.S Organ Procurement and Transplantation Network and the Scientific Registry of Transplant Recipients: Transplant Data 1999-2008. US Department of Health and Human Services, Health Resources and Services Administratio, Healthcare Systems Bureau, Division of Transplantatio, ROckville, MD n.d.

4 Shemesh E, Shneider BL, Savitzky JK, Arnott L, Gondolesi GE, Krieger NR, *et al.* Medication adherence in pediatric and adolescent liver transplant recipients. *Pediatrics* 2004;**113**:825–32.

5 Yokoi H, Kinoshita T, Zhang S. Dynamic reassembly of peptide RADA16 nanofiber scaffold. *Proc Natl Acad Sci* 2005;**102**:8414–9.

6 Petka WA, Harden JL, McGrath KP, Wirtz D, Tirrell DA. Reversible hydrogels from self-assembling artificial proteins. *Science* 1998;**281**:389–92.

7 Nowak AP, Breedveld V, Pakstis L, Ozbas B, Pine DJ, Pochan D, *et al.* Rapidly recovering hydrogel scaffolds from self-assembling diblock copolypeptide amphiphiles. *Nature* 2002;**417**:424–8.

8 Hartgerink JD. Self-Assembly and Mineralization of Peptide-Amphiphile Nanofibers. *Science* 2001;**294**:1684–8.

9 Klok H-A. Protein-Inspired Materials: Synthetic Concepts and Potential Applications. *Angew Chem Int Ed* 2002;**41**:1509–13.

10 Jeong Y, Joo MK, Bahk KH, Choi YY, Kim H-T, Kim W-K, *et al.* Enzymatically degradable temperature-sensitive polypeptide as a new in-situ gelling biomaterial. *J Control Release Off J Control Release Soc* 2009;**137**:25–30.

11 Mishra GP, Kinser R, Wierzbicki IH, Alany RG, Alani AWG. In situ gelling polyvalerolactone-based thermosensitive hydrogel for sustained drug delivery. *Eur J Pharm Biopharm Off J Arbeitsgemeinschaft Für Pharm Verfahrenstechnik EV* 2014;**88**:397–405.

12 Daly WH, Poché D. The preparation of N-carboxyanhydrides of α-amino acids using bis(trichloromethyl)carbonate. *Tetrahedron Lett* 1988;**29**:5859–62.

13 Rao DA, Mishra G, Doddapaneni BS, Kyryachenko S, Wierzbicki IH, Ngyuen DX, *et al.* Combinatorial Polymeric Conjugated Micelles with Dual Cytotoxic and Antiangiogenic Effects for the Treatment of Ovarian Cancer. *Chem Mater* 2016;**28**:6068–79.

14 Siepmann J, Peppas NA. Higuchi equation: derivation, applications, use and misuse. *Int J Pharm* 2011;**418**:6–12.

15 Reis CP, Neufeld RJ, Ribeiro AJ, Veiga F. Nanoencapsulation I. Methods for preparation of drug-loaded polymeric nanoparticles. *Nanomedicine Nanotechnol Biol Med* 2006;**2**:8–21.
16 Jiang H, Sakuma S, Fujii Y, Akiyama Y, Ogawa T, Tamura K, *et al.* Tacrolimus versus cyclosporin A: a comparative study on rat renal allograft survival. *Transpl Int Off J Eur Soc Organ Transplant* 1999;**12**:92–9.
17 Nair AB, Jacob S. A simple practice guide for dose conversion between animals and human. *J Basic Clin Pharm* 2016;**7**:27–31.
18 Koop DR, Bleyle LA, Munar M, Cherala G, Al-Uzri A. Analysis of tacrolimus and creatinine from a single dried blood spot using liquid chromatography tandem mass spectrometry. *J Chromatogr B Analyt Technol Biomed Life Sci* 2013;**926**:54–61.
19 Huang J, Hastings CL, Duffy GP, Kelly HM, Raeburn J, Adams DJ, *et al.* Supramolecular hydrogels with reverse thermal gelation properties from (oligo)tyrosine containing block copolymers. *Biomacromolecules* 2013;**14**:200–6.
20 Zhang H, Yu L, Ding J. Roles of Hydrophilic Homopolymers on the Hydrophobic-Association-Induced Physical Gelling of Amphiphilic Block Copolymers in Water. *Macromolecules* 2008;**41**:6493–9.
21 Bae SJ, Suh JM, Sohn YS, Bae YH, Kim SW, Jeong B. Thermogelling Poly(caprolactone- *b* -ethylene glycol- *b* -caprolactone) Aqueous Solutions. *Macromolecules* 2005;**38**:5260–5.
22 Hwang MJ, Suh JM, Bae YH, Kim SW, Jeong B. Caprolactonic poloxamer analog: PEG-PCL-PEG. *Biomacromolecules* 2005;**6**:885–90.
23 Gong C, Shi S, Wu L, Gou M, Yin Q, Guo Q, *et al.* Biodegradable in situ gel-forming controlled drug delivery system based on thermosensitive PCL-PEG-PCL hydrogel. Part 2: sol-gel-sol transition and drug delivery behavior. *Acta Biomater* 2009;**5**:3358–70.
24 Jeong B, Kim SW, Bae YH. Thermosensitive sol-gel reversible hydrogels. *Adv Drug Deliv Rev* 2002;**54**:37–51.
25 Cheng Y, He C, Xiao C, Ding J, Cui H, Zhuang X, *et al.* Versatile biofunctionalization of polypeptide-based thermosensitive hydrogels via click chemistry. *Biomacromolecules* 2013;**14**:468–75.
26 Rughani RV, Salick DA, Lamm MS, Yucel T, Pochan DJ, Schneider JP. Folding, Self-Assembly, and Bulk Material Properties of a *De Novo* Designed Three-Stranded β-Sheet Hydrogel. *Biomacromolecules* 2009;**10**:1295–304.
27 Lu C, Wang X, Wu G, Wang J, Wang Y, Gao H, *et al.* An injectable and biodegradable hydrogel based on poly(α,β-aspartic acid) derivatives for localized drug delivery: Poly(α,β-aspartic acid) derivatives for localized drug delivery. *J Biomed Mater Res A* 2014;**102**:628–38.
28 Kwon GS. Diblock copolymer nanoparticles for drug delivery. *Crit Rev Ther Drug Carrier Syst* 1998;**15**:481–512.
29 Natarajan JV, Nugraha C, Ng XW, Venkatraman S. Sustained-release from nanocarriers: a review. *J Control Release Off J Control Release Soc* 2014;**193**:122–38.

30 Huang X, Brazel CS. On the importance and mechanisms of burst release in matrix-controlled drug delivery systems. *J Control Release Off J Control Release Soc* 2001;**73**:121–36.
31 Thoniyot P, Tan MJ, Karim AA, Young DJ, Loh XJ. Nanoparticle-Hydrogel Composites: Concept, Design, and Applications of These Promising, Multi-Functional Materials. *Adv Sci Weinh Baden-Wurtt Ger* 2015;**2**:1400010.
32 Hoare TR, Kohane DS. Hydrogels in drug delivery: Progress and challenges. *Polymer* 2008;**49**:1993–2007.
33 Venkataramanan R, Swaminathan A, Prasad T, Jain A, Zuckerman S, Warty V, *et al.* Clinical pharmacokinetics of tacrolimus. *Clin Pharmacokinet* 1995;**29**:404–30.
34 Christiaans M, van Duijnhoven E, Beysens T, Undre N, Schäfer A, van Hooff J. Effect of breakfast on the oral bioavailability of tacrolimus and changes in pharmacokinetics at different times posttransplant in renal transplant recipients. *Transplant Proc* 1998;**30**:1271–3.
35 Andrews LM, Li Y, De Winter BCM, Shi Y-Y, Baan CC, Van Gelder T, *et al.* Pharmacokinetic considerations related to therapeutic drug monitoring of tacrolimus in kidney transplant patients. *Expert Opin Drug Metab Toxicol* 2017;**13**:1225–3

Chapter 3.

TRANSDERMAL DELIVERY OF TACROLIMUS USING MATRIX PATCH UTILIZING SYNERGISTIC PENETRATION ENHANCERS

Duc X. Nguyen, Vidhi Shah, Rosa Woo, Adel Al Fatease, Rohi Gheewala, and Adam Alani

(to be submitted to Journal of Pharmaceutical Research)

1. ABSTRACT

TAC is the most commonly used immunosuppressant in post transplantation maintenance therapy. Being a highly potent drug, it requires a strict control of trough concentration in whole blood to avoid side effects. Developing a transdermal drug delivery system for TAC can help improve its PK profile by bypassing the GI absorption and first pass effect. To deliver a large molecule such as TAC, we identify penetration enhancers that are capable of enhancing TAC's permeation across porcine ear skin using Franz diffusion cells. Two penetration enhancers, phenylpiperazine and TPGS, are commonly used in transdermal formulations and FDA approved are incorporated into our matrix patch. The matrix type transdermal patch using a Eudragit RL100 and PVP K30 at 2:8 ratio as matrix formers is developed to deliver TAC. When incorporated with 1% PP and 5% TPGS, the patch is found to deliver TAC across pig ear skin in Franz diffusion experiment. The permeation enhancing effect exhibits a positive synergy from combining two mechanistically different enhancers PP and TPGS. The final formulation is studied in rats to confirm the *in vivo* release rate. A linear relationship between the TAC concentration curve AUC and patch size is established indicating the patch can be cut to accommodate different dosing requirements.

2. INTRODUCTION

Each year there are approximately 800 kidney transplants performed annually in children under 18 years old in the United States[1]. Kidney transplantation is the treatment of choice for kidney failure in children and adolescents as it is the most advantageous treatment in terms of improved survival, physical and cognitive developmental potential, and quality of life[2]. However, despite introducing newer and improved immunosuppression medications, long term graft survival rates remain suboptimal. The current estimated 7-year and 10-year graft survival probabilities are 77% and 63% for recipients of living donor organs respectively. For recipients of deceased donor organs, the corresponding graft survival estimates are much lower 64% and 50%[1,3]. Following kidney transplantation, patients are put on a regimen of immunosuppressants to prevent graft rejection. Tacrolimus (TAC) is the most commonly prescribed immunosuppressant in renal transplant. However, complicated dosing and therapeutic monitoring is thought to be the main cause of non-adherence in the population using this medication[4]. When taken orally, TAC is a substrate of p-glycoprotein and is metabolized extensively by CYP3A4/5[5,6]. On top of that, TAC lipophilicity and its erratic oral absorption especially in the presence of food intake results in great intra- and interpatient pharmacokinetic variations[7]. Non-adherence to medication intake is the most important factor in kidney rejection especially among adolescents and young adults[8]. Furthermore, non-adherence in adolescent renal transplant recipients can negatively impact the successful transition to adult care and affect long term graft outcomes. Therefore, there is a need to simplify the medication regimen and lower the frequency of medication intake, as such a strategy has been proven to help with increased adherence to medication intake in this vulnerable population while being less likely to interfere with the daily schedule of the adolescents and young adults[9].

When once-daily TAC was introduced in 2007, the efficacy and safety of both formulations were considered similar. However, an increase in treatment adherence was observed in

patients switching to the sustained release TAC tablets[10]. As demonstrated in other chronic diseases such as hypertension, a decrease in pill burden could improve adherence[11]. Similarly, a prospective study in 125 liver and kidney transplantation patients showed a 50% improvement in overall adherence after switching from twice- to once-daily TAC dosing[12]. Also, patient quality of life was affected positively from the switch as indicated by a significant increase in overall satisfaction[13]. However, oral extended formulation of TAC still suffers the drawback of erratic pharmacokinetics caused by oral absorption, dietary interaction, hepatic first pass effect, and changes in patient development. To maintain TAC concentration within therapeutic window and avoid toxicity, patients have to consistently take TAC at the same time without food daily[14]. Therefore, although improved, the rate of nonadherence is still much higher in adolescents (30-53%) than adults (15-25%)[15]. Overall, recent studies have shown nonadherence to immunosuppressant is responsible for 47% of rejection-related graft failures[16].

Among many factors affecting medication adherence such as ease of drug administration, drug cost, severity of symptoms, and severity of side effects, dosing frequency appears to be another important component of adherence[17]. When weekly versus daily fluoxetine maintenance therapy over 3 months in 109 patients with depression were compared, weekly dosing regimen was found to increase adherence by 8.8-12%[17]. Similarly, in another study, adherence to a combined estrogen/progestin weekly patch increased by increase 9.5 % versus daily oral contraceptive in 1417 subjects over 6 cycles[17]. Therefore, we believe that a well-designed transdermal matrix patch that can sustain the drug trough concentration in the range required for the prevention of graft-versus-host disease, 3-15 ng/ml of whole blood, will offer similar if not better patient compliance while having tighter control of drug concentration than the oral formulations.

An ideal candidate for formulating into a transdermal drug delivery system (TDDS) should have the following properties: 1) molecular weight less than 1000 Da, ideally less than

500 Da; 2) an octanol/water partition coefficient between 1 and 4; 3) skin permeability $>0.5\times10^{-3}$ cm/hr; and 4) daily dosage less than 20 mg[18]. With regard to our drug of interest, TAC has a molecular weight of 804 Da, partition coefficient of 3.3, and skin permeability of 0.7×10^{3} cm/hr [19]. The upper maintenance dose for TAC in pediatric post renal transplantation is 2.5 mg/day [20]. Based on these characteristics, TAC is a possible candidate for formulating into a TDDS. However, the major challenge is the high molecular weight of TAC; large molecules have difficulty crossing the stratum corneum, the top most layer of the skin.

To enhance the penetration of drug molecules across the stratum corneum, chemical enhancers are often employed. According to Fick's law, the rate of diffusion across membrane is proportional to the difference in concentration on each side of the membrane or $J = \frac{K*D}{h} * C$. The flux can be affected by changing K, drug's partition coefficient, D, diffusion coefficient, and C, drug concentration in the TDDS. There are various methods to increase K and D, but generally speaking they fall into two categories. The first one is by mean of physical enhancers such as heat, ultrasound, iontopheresis, or microneedle to disrupt the stratum corneum. Heat, ultrasound and iontophoresis are not suitable for sustained delivery as they are best used for either bolus delivery or short duration, plus the devices are bulky and required special training to use. Microneedles on the other hand are designed to bypass the stratum corneum without affecting the nerves and underlying tissues. They do not require special administration or training to apply, cause no discomfort, and can be designed to control the flux[21]. The second way of enhancing the flux is by using chemicals to alter drug's partition coefficient, enhancing its skin solubility, or disrupting the lipid composition of the skin allowing the drug to diffuse quicker[21]. Several studies have suggested the combined use of chemical penetration enhancers from different mechanistic classes to achieve synergistic effect[22–24]. By combining different classes of enhancer, the permeation flus of the compound can be enhanced much greater than either component used alone. Large molecules such as

inulin, leuprolide acetate, sulforhodamine B, heparin, and leutinizing hormone releasing hormone have been delivered across the skin by using synergistic pair of penetration enhancers[23,25]. In this work we are exploring the use of chemical penetration enhancers of various class with different mechanism of action to improve the flux of TAC across the skin. We will incorporate these enhancers into a matrix type transdermal patch for sustained delivery of TAC. The final formulation will be characterized for their *in vivo* release kinetics in rats.

3. MATERIAL AND METHODS:

3.1. Material

Eudragit RL100 and RS100 are gifts from Evonik Corporation (Parsippany, NJ). TAC HCl is purchased from LC Labs (Woburn, MA). Polyvinylpyrrolidone K30 (PVP), isopropyl myristate (IPM), 1-dodecylazecycloheptan-2-one (azone), polysorbate 80 (Tween80®), dimethyl sulfoxide (DMSO), 1-phenylpiperazine (PP), dl-alpha-tocopherol polyethylene glycol 1000 succinate (TPGS), propylene glycol, dibutyl phthalate are purchased from VWR (Radnor, PA). Sylgard 184 silicone elastomer is from Dow Corning (Midland, MI). All other reagents are purchased from either VWR or Sigma Aldrich.

Fresh pig ears are purchased from local market, Fubonn (Portland, OR). The dorsal skin is isolated from the ear and cut to uniformed size and thickness using a surgical blade. The dermal side of the skin is thoroughly cleaned with distilled water to remove any adhering tissues or blood vessels, then stored at -80°C up to six months for later use.

Sprague-Dawley rat weights between 250-300 g are purchased from Charles River. The animals are treated in accordance with OHSU and OSU IACUC protocol.

3.2. Penetration enhancer screening

To select and optimize the chemical penetration enhancers for later incorporation into TAC transdermal patches, we study the *in vitro* permeability enhancing effects of various enhancers across porcine ear skin. Porcine ear skin pieces are equilibrated for an hour in

20% ethanol dissolution medium before starting the experiment. The skins are mounted on a Franz diffusion cell with constant magnetic stirrer (400 rpm) (Figure 3-1). The isolated porcine ear skin piece is mounted between the compartments of the diffusion cell, with the epidermis facing upward into the donor compartment. The receiver compartment is filled with 20% ethanol dissolution medium, 13 ml. The temperature of the cell is maintained at 32°C using a thermostatically controlled heater. Six penetration enhancers, IPM, Tween80®, DMSO, azone, PP, and TPGS at various concentrations (1, 3, 5, and 10%) are incorporated into an 18% F127 gel loaded with 10 mg of TAC. The gel formulation, 0.5 ml, with or without enhancer, is applied into the donor compartment. At predetermined time points, 1 ml of dissolution medium is removed for analysis on an Agilent 6100 LCMS system (Agilent Technologies, Santa Clara, CA), and an equal volume of fresh pre-warmed medium is replaced. A Thermo Acclaim C18, 4.6x150 mm, particle size 5μm is employed for separation. The binary mobile phase consists of 20% solvent A, LCMS grade water with 0.1% formic acid, and 80% solvent B, LCMS grade methanol with 0.1% formic acid. The flowrate is 0.5 ml/min, and the injection volume is 10 μl. TAC's retention time is 4 minute and the *m/z* 826.5 is monitored. The steady state flux (J_{ss}) is determined directly as the slope of the curve between the linear steady state values of the amount of drug permeated versus time. The permeability coefficients (K_p) and enhancement ratios are calculated. The obtained values are compared with control (no penetration enhancer) using unpaired t-test.

$$K_p = \frac{J_{ss}}{C_s}$$

$$ER = \frac{K_p \; with \; penetration \; enhancer}{K_p \; without \; penetration \; enhancer}$$

3.3. Preparation and characterization of TAC-loaded matrix films

Monolithic matrix system for transdermal delivery of TAC is developed using solvent evaporation method. A number of placebo transdermal films are developed to find an

optimum combination of polymer. The patches are prepared using different ratios of RL100, RS100, and PVP while keeping the concentration of TAC constant, 25 mg/g polymer (Table 3-1). A homogenous mixture of the polymer, plasticizer (dibutyl phthalate), and the drug is dissolved in solvent mixture (methanol and dichloromethane, 50:50). The solution is mixed overnight to allow for complete dissolution and relaxation of the polymers. The mixture is then degassed using a bath sonicator for 20 minutes, then 2 ml is casted into a well in a 6-well plate. Silicone elastomer, 1 ml, is precasted in the 6-well plate as backing layer. The assembly is allowed to air dry for 12 hr in the chemical hood. A thin aluminum foil is placed on one side of the film as a release liner. Then the dried film is wrapped in aluminum foil and stored in airtight containers at room temperature for later use.

The prepared patches are evaluated for thickness, weight uniformity, folding endurance, moisture content, and stability at room temperature.

The thickness of the patches is measured using a digital caliper. Four readings at difference area of each patch are recorded. Five patches from each polymer mixture are measured and the values are reported as mean$\pm$SD.

Weight uniformity of the patches is determined using a digital balance. The average values obtained from five patches for each formulation are reported.

The folding endurance is defined as the number of times the film can be folded at the same area without breaking. It is determined by repeatedly folding a patch at the same place until it cracks begin to appear on the fold.

Moisture content is determined by change in weight. The patches, n = 5, are accurately weighed then kept in a dessicator containing anhydrous calcium chloride. After 72 hr, the patches are removed and weighed again. Average percentage moisture losses are determined with the following formula:

$$Moisture\ content = \frac{Initial\ weight - Final\ weight}{Initial\ weight} \times 100$$

The drug content of each patch is determined by dissolving the patch in 2 ml of methanol. The solution is further diluted and injected into a Shimadzu HPLC system to determine the drug concentration. The Shimadzu HPLC system consists of LC-20 AT pump and SPD M20 a diode array detector. The analysis is performed on a Zorbax C18 Column (4.6×75 mm, 3.5 µm) in isocratic mode with methanol/water (85/15) containing 0.1% phosphoric acid and 1% methanol at a flow rate of 0.5 ml/min and an injection volume of 10 µL. Column temperature is maintained at 40°C. TAC peak is monitored at 254 nm at retention time of 4 minutes. The drug contents on day 7, 14, and 30 after casting are measured to determine the stability of the formulation.

3.4. In vitro drug release from polymeric matrix patches

The *in vitro* release of TAC from the patches is evaluated using Franz diffusion cells with surface area of 1.72 cm^2. The drug loaded patch with an aluminum foil as backing membrane is mounted on a regenerated cellulose dialysis membrane with molecular weight cut off of 10,000 and placed between compartments of the diffusion cell. The receiver compartment is filled with distilled water, and the donor compartment is exposed to atmosphere. The two compartments are held together using a clamp. The apparatus is equilibrated to 32°C with constant stirring at 400 rpm. The 1 ml sample is withdrawn and replenished with fresh medium at different time intervals up to 72 hr. TAC concentrations in the receiver compartment is measured using LCMS. Cumulative amount of TAC released from the patch is calculated and plotted against time. Release rate constants from the patch formulations are compared using unpaired t-test. The patch formulation with the highest release profile will be used in *ex-vivo* studies.

3.5. Ex-vivo skin permeation studies

Franz diffusion cell with a surface area of 1.72 cm^2 is used for the *ex-vivo* permeation studies (Figure 3-1). Excised pig ear skin is mounted between the compartments of the

Franz cell with the stratum corneum facing up toward the donor compartment. The transdermal patch is kept in contact with the stratum corneum side during the entire duration of the test. The receiver compartment contains 13 ml of dissolution medium composed of 20% ethanol. The two compartments are held together using a metal clamp. The conditions are kept under 32°C with constant stirring at 400 rpm. The amount of drug permeated is determined by withdrawing 1 ml of medium at preset time points up to 72 hr and replenishing with an equal volume of fresh medium. The samples are filtered using a 0.2μm syringe filter before injecting into an LCMS system for analyzing TAC concentration. The cumulative amount of drug permeated is calculated and plotted against time. The optimized penetration enhancers from previous studies are incorporated into the patch formulation. Permeation flux from patches with individual enhancers and combination are compared to control (no enhancer) using unpaired t-test.

3.6. Drug-excipient compatibility study

Fourier transform infrared (FTIR) technique is used to study the physical and chemical interaction between drug and excipients. The FTIR spectra of TAC, nondrug patch, drug-loaded patch are obtained using a Nicolet-100 Infrared Spectrophotometer (Thermo Fisher Scientific, Waltham, MA). The resolution is set at 4 sec-1, and 16 scans per sample. The samples are pressed on a KBr-diamond plate surface using a manual tablet press.

3.7. Pharmacokinetic studies in rats

The test formulations are tested for their bioavailability on four Sprague-Dawley rats. The rats are put under anesthesia, and hair on the upper dorsal area is removed using an electric clipper the day before the PK study. The patches are applied to the shaved region and secure in place using a Tegaderm® transparent adhesive (3M Corporation, St Paul, MN). The rats are kept in individual cages for the duration of the study to prevent them from removing the patches on each other back. Blood is collected from the saphenous vein at 2, 4, 8, 12, and 24 hr, then every day thereafter. The patch is removed on day 7.

Approximately 100 μl whole blood is collected from the saphenous vein and analyzed by LC-MS/MS for TAC concentrations.

Weights, grooming, and feeding behaviors are monitored daily as indicators of toxicity. Acute toxicity is described a s weight loss of ≥15%. WinNonLin software is used to analyze pharmacokinetic parameters. All animal work is conducted in compliance with NIH guidelines and Institutional Animal Care and Use Committee policy at Oregon Health and Sciences University.

3.8. LC-MS/MS analysis

TAC is analyzed using AB Sciex Triple Quad 3500 LC-MS/MS based on methods described by Koop et al[26]. TAC samples are processed by adding 200 mcl of 0.1 mM $ZnSO_4$ solution, vortexing for 4 seconds, followed by adding 500 mcl of acetonitrile containing 4 ng/ml ascomycin. The mixture is mixed for 1 minutes then centrifuged for 5 minutes at 16,000 g. A 10 mcl aliquot of the clear supernatant is injected into LC-MS/MS for analysis.

TAC and ascomycin are resolved on a Thermo C18 Accucore™ column (30 mm x 2.1 mm, 30 Å, 2.6 μm) maintained at 40 °C. The gradient mobile phase is consisted of two solvents: A, 2 mM ammonium acetate with 0.1% formic acid in water and B, 2 mM ammonium acetate with 0.1% formic acid in methanol. The gradient is 50% B for 0.3 min, increase to 100% B in 0.7 min and hold for 2 min, return to 50% B for 0.1 min, re-equilibrate at 50% B for 3 min. The flow rate is 0.4 mL/min. The LC system is interfaced to an AB Sciex 3500 triple-quadrupole (Foster City, CA) with multiple raction monitoring. The equipped TurboIonSpray® ESI source is operated in positive mode with the following setting: source voltage 2500 V, GS1 60 psi, GS2 60 psi, CUR 30, TEM 550°C. The MRM transitions monitored are *m/z* 821 -> 768.5, amd 821 -> 718.5 for TAC, and *m/z* 809 ->756.2, and 809 -> 564.1 for ascomycin[26]. The DP is 80 V for both TAC and ascomycin. The dwell time is 150 ms. The optimal instrument parameters for the 4 MRM transitions are: EP, 10 V; CXP (V), 20, 20, 15, and 15; CE (V), 30, 35, 30, and 34 respectively. The transitions

used for quantification are *m/z* 821 -> 768.5 for TAC and 809 -> 756.2 for ascomycin. Instrument control and data acquisition are done with Analyst® Software.

3.9. Statistical analyses

All statistical analyses are performed with GraphPad Prism version 5.04 for Windows, GraphPad Software, San Diego California USA.

4. RESULTS AND DISCUSSION

4.1. Penetration enhancers for TAC

We assess the permeation enhancing effects of six different chemical penetration enhancers on TAC to determine the enhancers with the highest enhancement ratio compared to control. Fresh porcine ear skin obtained from a local market is used for this study due to similarities to human skin. Anatomically, it has been shown that porcine ear skin is similar to human skin in terms of thickness, follicular structure, hair density, and tissue contents[27]. Moreover, biochemical similarities such as glycosphingolipids and ceramides and enzymes in human and pig epidermis were found[28]. The flux is deduced from the slope of the linear steady state portion of the release curve for each enhancer at the tested concentrations (Figure 3-2). From there the enhancement ratio is calculated by dividing the enhancer flux by the control (no enhancer) flux. The calculated permeation fluxes, permeability coefficient, and enhancement ratios are presented in (Table 3-2). Enhancement ratios are also presented graphically (Figure 3-3). Azone, PP, and TPGS are found to be most effective at enhancing TAC permeability across porcine skin. Our data indicates that azone is more effective at lower concentration. At 1% w/v, the permeability of TAC is enhanced by almost 30 folds. The enhancement effect drops at higher concentration of azone. This negative correlation between azone concentration and its permeation enhancing effect has been reported previously in literatures[29,30]. Azone was the first synthetically designed enhancer in the amide class. It is a highly lipophilic oily substance that is compatible with most organic solvents including alcohols and propylene glycol. Therefore, the incorporation of azone to most transdermal system can be done

with ease. Although azone has been investigated for more than 35 years, its mechanism of action as a penetration enhancer is still unclear. Azone is thought to insert itself between the stratum corneum lipids increasing the fluidity within the monolayers[30]. As a result, the diffusion of substance across the skin is enhanced. However, the FDA has not approved azone for topical use due to its self-absorption enhancement. After repeated application, azone can be absorbed into the blood stream[31].

Another enhancer that is found to significantly enhance the permeation of TAC is TPGS. At 1, 3, 5, and 10% w/v, TPGS enhances the permeation of TAC across porcine skin by 4.2, 6.5, 7.9, and 8.1 times, respectively (Table 3-2). The enhancement ratio increases at higher concentration of TPGS incorporated into the formulation. The enhancement ratio is found to increased linearly from 1% to 5% (r^2 = 0.981). However, there is no different in permeation enhancement between 10% and 5%. TPGS is a water-soluble synthetic derivative of vitamin E by esterification of d-α-tocopherol succinate with polyethylene glycol 1000[32]. It is an amphiphilic molecule comprising of a hydrophilic polar head and a lipophilic alkyl tail. TPGS can be functionalized as an excellent solubilizer, emulsifier, permeation and bioavailability enhancer of hydrophobic drugs. As the water content increases, TPGS acts as a surfactant and forms lamellar reverse micellar phase, hexagonal phase, and normal micellar phase[33]. It has been approved by the FDA as a safe pharmaceutical excipient for used topically[34].

PP is another chemical penetration enhancer that shows the ability to improve the flux of TAC across porcine skin in this study. We have found that 1% w/v of PP has the highest enhancing ratio, 16 folds compared to control. Similar to azone, PP exerts higher enhancing ability at lower concentration than at higher concentrations. At 3, 5, and 10% the enhancement ratios are approximately 12.5, 8.2, and 2.7, respectively. The mechanism of PP is less clear. Whitehead et al[35] has shown that PP can induce tight junction opening on Caco-2 cell culture. Similarly, Bzik et al[36] study has shown that PP induces tight junction opening in rat colonic mucosae enhancing the permeability. When

used in combination with sodium laureth sulfate, a nonionic surfactant, PP has been shown to enhance the skin permeability synergistically, allowing the passage of cyclosporine, insulin, and various other large molecules[23].

The results of our studies show IPM and DMSO not effective in enhancing the permeability of TAC across pig skin. Interestingly, DMSO at 3% and 6% is observed to lower the permeability of TAC. Tween80® at 1% and 3% show 1.7 and 1.4 folds increase in enhancement compared to control. Although having similar mechanism of action as TPGS, a surfactant, Tween80® is not as effective at enhancing the flux of TAC through pig skin.

4.2. Fabrication of TAC matrix patches

Two groups of polymeric matrix patches are investigated. The A group comprises of Eudragit RL100 and RS100 at different mixtures. The mixtures in B group utilize PVP, a hydrophilic polymer, in exchange for RS100. Acetone or a binary mixture of methanol and dichloromethane (MeOH:DCM) at 1:1 ratio is investigated as casting solvents. The thickness and weight per patch are investigated for all mixtures (Table 3-3). Dibutyl phthalate at 20% in combination with propylene glycol 10% is sufficient as plasticizer to soften the patches. The binary mixture of MeOH:DCM is more suitable than acetone as casting solvent. The weights and thicknesses of the patches casted using MeOH:DCM are more uniform which indicate better solvent compatibility and even rate of solvent evaporation. Low standard deviation values in the film ensure uniformity of the patches prepared by solvent casting using MeOH:DCM. Folding endurance of group A patches are in the range of 80±5, which is an improvement from the range of 40±5 obtained from using acetone as casting solvent. Group B's folding endurance remains the same for either solvent choice. The folding endurance test results indicate that the patches do not break and maintain their integrity with general skin folding when applied. This is a good property for a patch to have, especially when it has to be worn over extended period lasting days, during which body movement may affect the patch integrity.

4.3. In vitro drug release studies

Eudragit RL100 and RS100 are hydrophobic copolymers of acrylic and methacrylic acid esters. RL100 due to its high content of quaternary ammonium group is a more permeable component of the two[37]. By varying the ratio of RL100 and RS100 in the formulation we can control the release of the drug from the matrix. On the other hand, PVP K30 is a hydrophilic polymer that swells when absorbs moisture. Due to the highly hydrophobic nature of RL100 and RS100, the release of TAC from the group A patches is very slow, less than 10% after 72 hr even at the highest ratio, 80%, of the high permeable component RL100 (Figure 3-4). It is possible that TAC molecule might have interact with the Eudragit matrix and prolong the release from the patch. Group B formulations, however, release the drug faster. By replacing the hydrophobic, low permeable RS100 component with the hydrophilic PVP polymer in combination with a highly permeable but hydrophobic RL100 polymer, the patches in this group show a higher release rate of TAC especially at higher ratio of PVP (Figure 3-5). The release profiles of all three patch formulations in this group can be characterized as following two distinct phases. The first is a fast release phase where the rapid swelling of the PVP component pushes the drug molecules out of the patch matrix. This phase is followed by a slow and steady portion. The formulation containing 80% PVP shows 86.6% drug release over 48 hr due to the high hydrophilic component of the matrix. Whereas the 60% and 40% PVP patches shows 71.2% and 53.7% drug release in 48 hr, respectively. The release rate increases when the concentration of PVP increases in the formulations. This is because as the proportion of this hydrophilic polymer in the matrix increases, the amount of water uptake and hydration of the patch increase, and thus more drug is released. To compare the release rates of the three formulations in group B, we fit each release curve to first order release equation (Figure 3-6). The data are summarized in (Table 3-4). The release rate of formulation B3 is the highest in the group ($p<0.05$). It is important that we proceed with a formulation capable of releasing TAC rapidly. Such a formulation would allow the drug to be readily available on the interface between the epidermis and the patch. Thus, the drug molecule is ready

to cross the skin barrier, and the rate limiting factor would be the flux across the skin. Therefore later experiment is conducted using the RL100:PVP 2:8 matrix formulation.

4.4. Ex vivo skin permeation studies

The results of *ex vivo* drug permeation studies from B3 patches with either 1% PP, 5% TPGS, or a combination of both are shown in (

Table 3-5) and (Figure 3-7). The permeation of TAC from the control patch with no penetration enhancer is the lowest, less than 2% permeated. The flux of TAC from each formulation is estimated by calculating the slope of the linear portion of each release curve. The flux is in the order from lowest to highest is control < 5%TPGS < 1%PP < combined enhancers 5% TPGS plus 1%PP. The formulation that incorporates both penetration enhancers, 1% PP plus 5% TPGS, exhibits the greatest cumulative amount of drug permeated after 72 hr (23.33$\pm$3.7%, 410.61$\pm$65.2 $\mu g/cm^2$). The permeation flux of the patch with combination enhancers, 5.11±0.71$\mu g/cm^2$/hr, is significantly higher than all other patches ($p<0.05$). The enhancement ratio for each formulation is also calculated (

Table 3-5). Compared to control, the enhancement ratios of incorporating 5% TPGS, 1% PP, and combined 5% TPGS plus 1% PP are 1.34±0.19, 3.7±0.85, and 6.24±0.88, respectively. To determine whether the enhancement from using the two enhancers is synergistic, the enhancement ratios obtained are applied to the following equation to determine the synergy S [22,23].

$$S = \frac{E_{A+B}^{x,y}}{X \cdot E_A^y + (1-X) \cdot E_B^y}$$

This equation assesses the synergy in a binary system. $E_{A+B}^{x,y}$ is the enhancement ratio obtained from the formulation containing the combine enhancers A and B (TPGS and PP in our experiment). Y is the total % wt/vol concentration of both enhancers, and X is the weight fraction of A. E_A^y and E_B^y are the enhancement ratios obtained with only enhancer A or B in the formulation. The synergy, S, obtained from our experiment is 1.26, indicating positive synergy and superior skin permeabilization resulting from combining the two enhancers[22,23]. Thus the B3 formulation utilizing the combination of 1% PP and 5% TPGS is used for later pharmacokinetic investigation in rats.

4.5. Drug compatibility and formulation stability

Before studying our final formulation in animals, we characterize the drug compatibility and formulation stability. The FTIR spectra of TAC powder and the empty patch containing both enhancers are obtained (Figure 3-8). The additional result of combining the two spectra is compared to the TAC-loaded patch formulation. The addition spectrum and the spectrum of TAC-loaded patch are identical. No new bands or shift in characteristic peaks appeared indicating no interaction between the drug and the excipients used in the formulation.

The stability of the final formulation is assessed by storing four drug-loaded patches at room temperature. The drug content is determined by HPLC on day 7, 14, and 30 and compared to initial drug loading. The drug concentration in the patches remains above

90% by day 30, indicating stability of the formulation to at least one month at room temperature (Figure 3-9).

4.6. Pharmacokinetic studies in rats

The TAC-loaded transdermal patch incorporating two synergistic enhancers PP and TPGS at 1% and 5% respectively is cut into 1, 2.5, and 5 cm^2 and applied to three groups of Sprague-Dawley rats (n=4 each). Whole blood from the saphenous vein is collected daily, and the patches are removed on day 7. To secure the patch in place, a Tegaderm® adhesive is employed. The rats are also housed individually to avoid them removing each other patches. The TAC concentration profiles are presented in (

Figure 3-10). For all three experiments, the concentration of TAC in whole blood reaches steady state by 24 hr. The *in vivo* permeation flux of the formulation is determined using the PK profile of the 5 cm^2 patch experiment. Assuming a steady state concentration of 35±5 ng/ml achieved after 24 hr of patch application, the flux is derived by applying the following equation:

$$Flux = Elimination = Css \cdot Cl \cdot Wt$$

The clearance (Cl) of TAC injected intravenously to Sprague-Dawley rats is 42 ml/min*kg[38]. The average weight of rats in our experiment is 0.3 kg. The flux is therefore estimated to be 4.5-6.0 μg/cm^2/hr, which is similar to the estimated *ex vivo* flux (5.11±0.71 μg/cm^2/hr). Following the removal of the patch on day 7, the concentration of TAC in whole blood gradually clears and completely eliminated by day 9. The skin area where the patch applied is observed. No irritation or redness is observed on rat skin where the patch is applied (Figure 3-12).

The area under the curve (AUC) from day 0 to 9 of the three patch experiments are computed and plotted vs patch size (Figure 3-11). The AUCs are found to follow a linear relationship to patch size, indicating that our patch can be cut to accommodate different dosing requirement or scaling to other animal species. By utilizing the synergistic effect of combining two penetration enhancers, PP and TPGS, belonging to two mechanistic classes, we are able to deliver TAC, a large molecule. Without such synergy, the delivery of TAC across the skin barrier would be nonsignificant as demonstrated in the *ex vivo* studies. Our experiment shows for the first time the possibility of developing a transdermal delivery system for TAC in the maintenance phase of immunosuppressant therapy post transplantation.

The clinical implication of this patch formulation of TAC is two folds. First, we have demonstrated the ability of control TAC concentration within its narrow therapeutic window with the 2.5 cm^2 patch where the C_{max} and C_{min} do not exceed 30 ng/ml or drop

below 5 ng/ml, respectively. Second, the PK variability is minimized. The variations in AUC of each tested patch size are 8.4%, 13.5%, and 17.5% for 5, 2.5, and 1 cm^2 patches respectively. When compared to reported AUC variations of oral once-a-day TAC regimens which range from 21% to 35% [39], PK variability has been minimized with the patch formulation. Speculatively, the introduction of a weekly transdermal patch for TAC maintenance therapy to adolescents would improve the treatment adherence rates similar to that observed when Alzheimer's patients switch to transdermal patches. The adolescent and geriatric populations share similar nonadherence characteristics such as forgetfulness, avoidance of adverse events and refusal of treatment. In a study looking at adherence rate in Alzheimer's patient, at 6 months after switching to transdermal patch, the adherence rate went up to 85.9% from 69.2% at baseline, a 24% improvement[40]. Applying this to adolescent renal transplant patients where nonadherence rate was found to be 30% (n = 586) [8], a 24% improvement rate would result in an increase of >98 patients (16.8%) into the adherence group. It would be interesting to see how this translate to improvement in long-term graft survival rates in future studies.

5. CONCLUSION

We have successfully developed a matrix type transdermal patch using a Eudragit RL100 and PVP K30 at 2:8 ratio as matrix formers. When incorporated with 1% PP and 5% TPGS, the patch is found to deliver TAC across pig ear skin in Franz diffusion experiment. The permeation enhancing effect is due to the synergistic effect from combining two mechanistically different enhancers PP and TPGS. The final formulation is studied in rats to confirm the *in vivo* release rate. A linear relationship between the TAC concentration curve AUC and patch size is established indicating the patch can be cut to accommodate different dosing requirements.

Table 3-1: Composition of polymeric matrix patches

Code	Drug (mg)	Polymer (g)			n-Dibutyle phthalate (w/w)	Propylene glycol (w/w)	Solvent acetone or methanol:dichloro methane (ml)
		RS100	RL100	PVP			
A1	50	3	2		20%	10%	25
A2	50	2	3		20%	10%	25
A3	50	1	4		20%	10%	25
B1	50		3	2	20%	10%	25
B2	50		2	3	20%	10%	25
B3	50		1	4	20%	10%	25

Table 3-2: Permeation fluxes, permeability coefficient, and enhancement ratios obtained from various penetration enhancers. All values are expressed as mean ± SD (n = 4).

Name	Transdermal flux µg/cm^2/hr	Permeability coefficient cm/hr	Enhancement ratio
Control	0.865±0.04	0.173E-03±0.008	1
IPM 1%	0.683±0.041	0.137E-03±0.008	0.79±0.048
IPM 3%	0.494±0.063	0.0989E-03±0.013	0.57±0.072
IPM 6%	0.576±0.065	0.115E-03±0.013	0.67±0.076
IPM 10%	0.468±0.04	0.0935E-05±0.008	0.54±0.046
Tween 80 1%	1.603±0.207	0.321E-04±0.041	1.71±0.144
Tween 80 3%	1.303±0.09	0.261E-03±0.002	1.43±0.012
DMSO 3%	0.146±0.027	0.0292E-03±0.005	0.17±0.031
DMSO 6%	0.405±0.046	0.0809E-03±0.009	0.47±0.053
DMSO 10%	0.291±0.048	0.0583E-03±0.01	0.34±0.055
Azone 1%	25.757±0.033	5.15E-03±0.007	29.78±0.038
Azone 3%	1.297±0.054	0.259E-03±0.011	1.5±0.063
Azone 5%	0.933±0.021	0.187E-03±0.004	1.08±0.025
Azone 10%	0.379±0.012	0.0757E-03±0.002	0.44±0.013
TPGS 1%	3.669±0.275	0.734E-03±0.055	4.24±0.317
TPGS 3%	5.631±0.816	1.13E-03±0.016	6.51±0.943
TPGS 5%	6.836±0.959	1.37E-03±0.019	7.9±1.109
TPGS 10%	6.988±0.86	1.40E-03±0.017	8.08±0.994
PP 1%	13.883±1.827	2.78E-03±0.037	16.05±2.112
PP 3%	10.81±0.719	2.16E-03±0.014	12.5±0.831
PP 5%	7.07±0.832	1.41E-03±0.017	8.17±0.962
PP 10%	2.324±0.043	0.465E-03±0.009	2.69±0.049

Table 3-3: Physicochemical properties of TAC patches. All values are expressed as mean ± SD (n=5).

Casting solvent: acetone						
Code	Polymer ratio			Weight (mg)	Thickness (µm)	Folding Endurance (folds)
	RL100	RS100	PVP K30			
A1	40	60		547±13	331±19	55±5
A2	60	40		537±19	332±12	40±5
A3	80	20		545±18	330±13	40±5
B1	60		40	537±12	325±10	100±5
B2	40		60	537±13	332±15	100±5
B3	20		80	538±16	332±13	100±5

Casting solvent: methanol:dichloromethane 1:1							
Code	Polymer ratio			Weight (mg)	Thickness (µm)	Folding Endurance (folds)	Drug content (mg)
	RL100	RS100	PVP K30				
A1	40	60		544±3	334±5	75±5	10.5±0.2
A2	60	40		544±4	332±5	80±5	10.7±0.3
A3	80	20		544±4	329±5	80±5	10.4±0.2
B1	60		40	532±4	326±3	100±5	10.6±0.3
B2	40		60	538±2	333±4	100±5	10.5±0.2
B3	20		80	539±4	326±4	100±5	10.6±0.3

Table 3-4: *in vitro* release rate constant K of each formulation in Group B as fitted to first-order release kinetic. N = 4

Formulation	K (± SD)	R^2
B1	-0.017±0.002	0.995
B2	-0.026±0.002	0.924
B3	-0.042±0.004	0.969

Table 3-5: *Ex vivo* permeation studies using pig ear skin. Cummulative % of the drug released Q, cumulative amount of drug released M, transdermal flux J_{ss}, permeability coefficient K_p, and enhancement ratio ER of TAC transdermal patches. N = 3. Values represent as mean $\pm$ SD

Formulation	Q (%)	M ($\mu g/cm^2$)	J_{ss} ($\mu g/cm^2/hr$)	K_p ($cm/hr*10^{-2}$)	ER
B3	1.81±0.25	31.78±4.37	0.54±0.08	0.81±0.11	1
B3+5% TPGS	4.62±0.60	81.3±10.65	1.08±0.16	1.61±0.23	1.34±0.19
B3+1% PP	12.27±2.66	215.98±46.8	2.98±0.68	4.45±1.02	3.7±0.85
B3+1%PP & 5% TPGS	23.33±3.7	410.61±65.2	5.11±0.71	7.62±1.06	6.34±0.88

Figure 3-1: Franz diffusion cell set up for *in vitro* release and *ex vivo* permeation studies

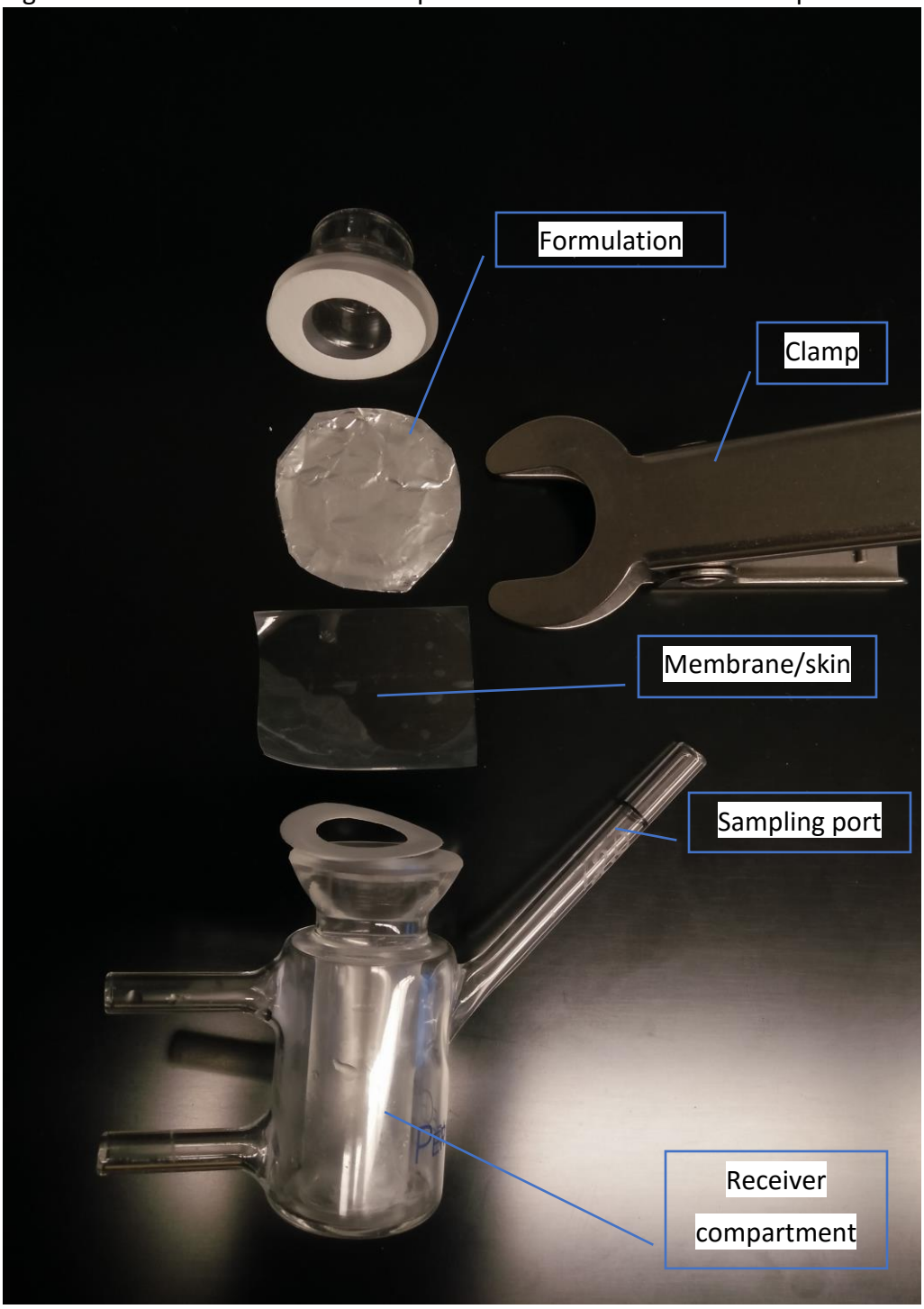

Figure 3-2: TAC permeation across excised porcine ear skin. Six penetration enhancers are tested and compared to vehicle with no enhancer. N = 4 each

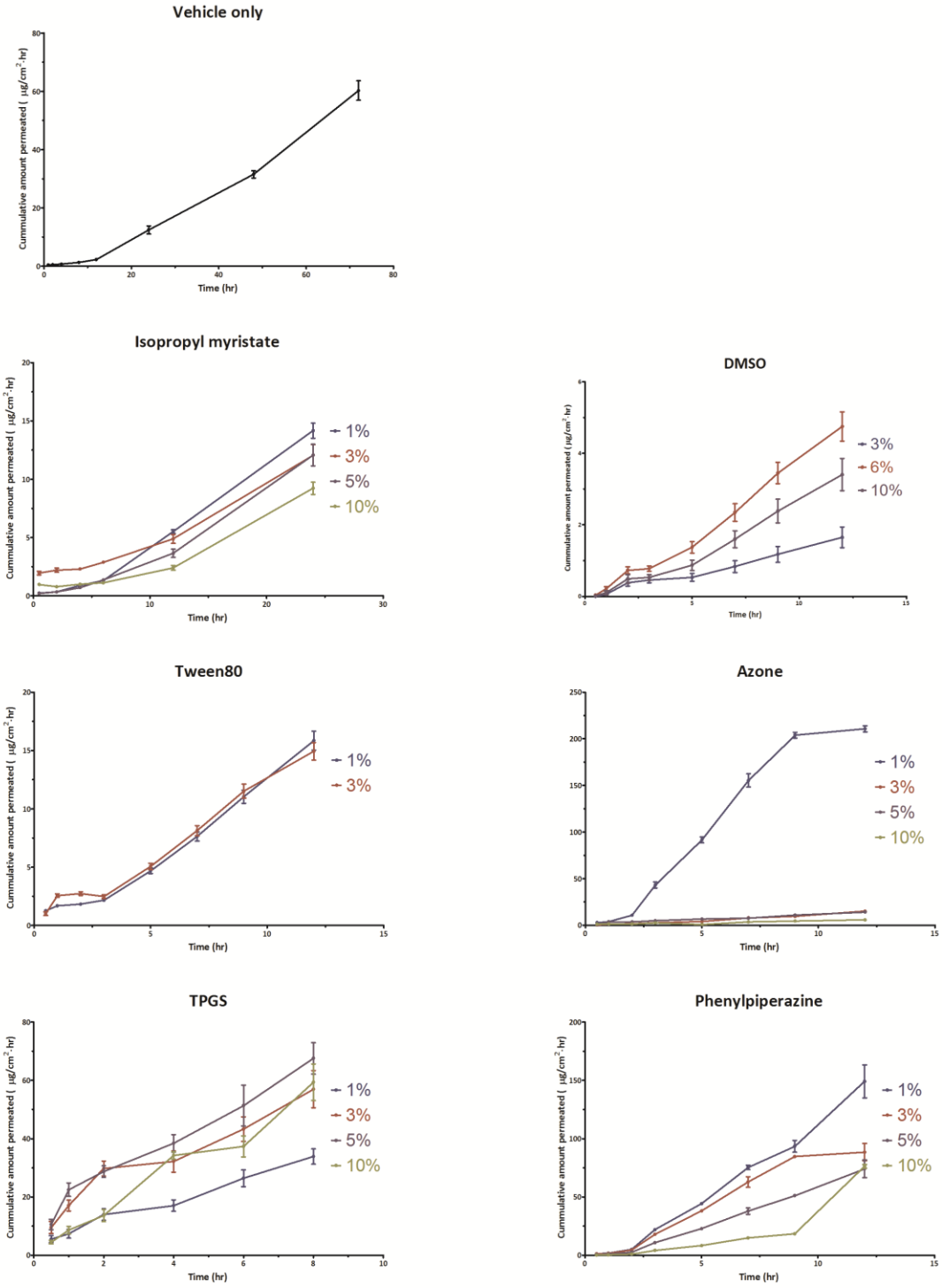

Figure 3-3: Permeation coefficient of six penetration enhancers at various concentration. N = 4 each

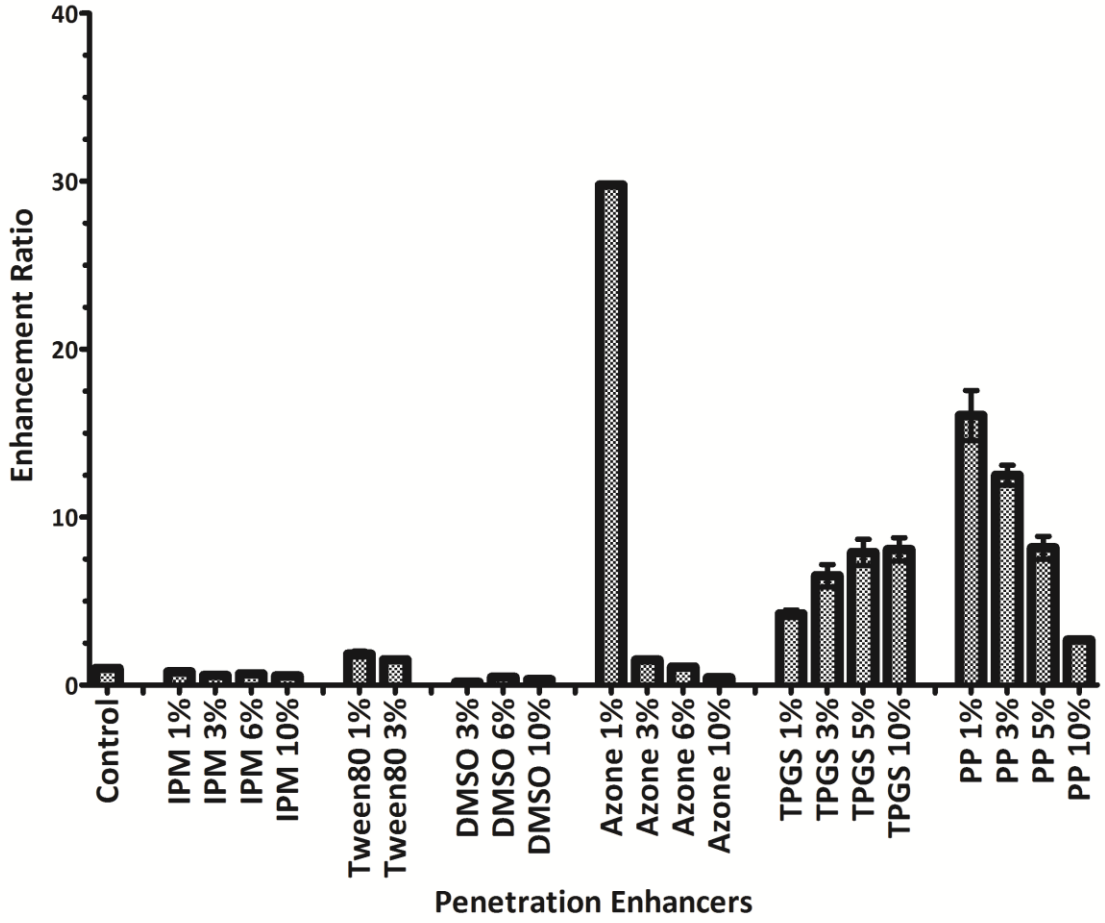

Figure 3-4: *in vitro* TAC release from Group A matrix patches. These patches are composed of RL100 and RS100 at different ratios.

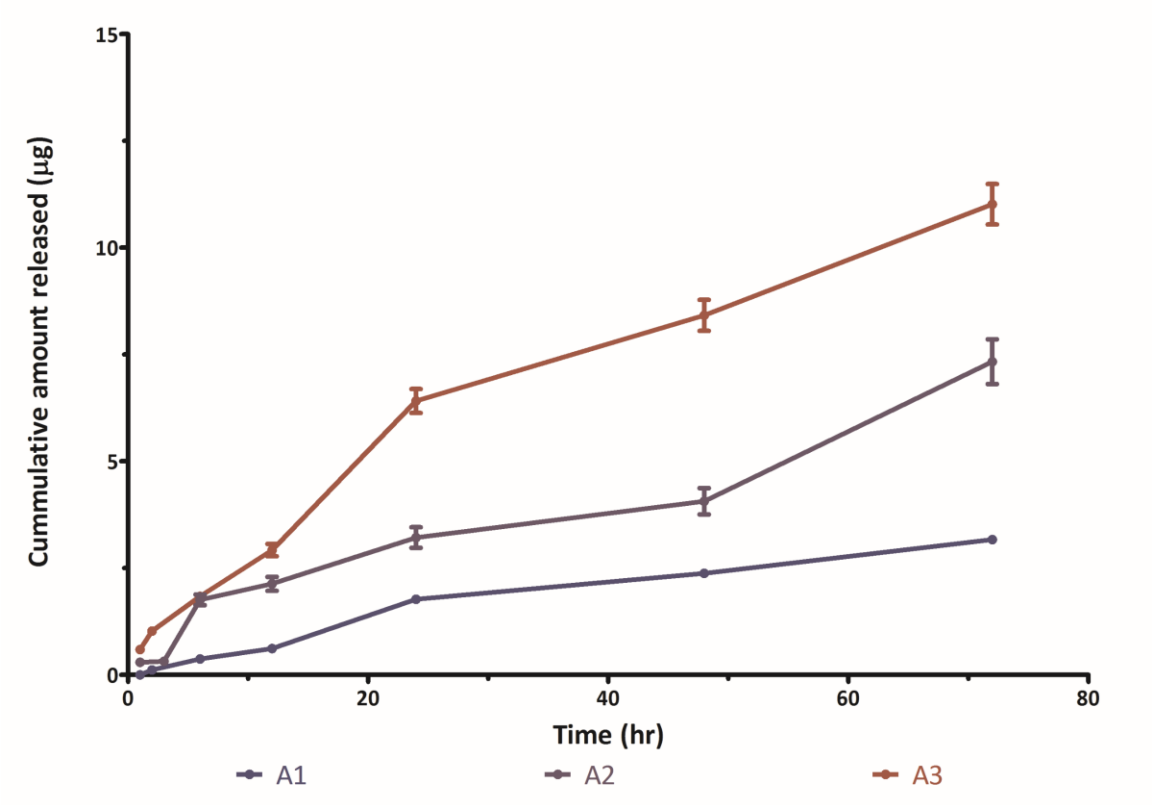

Figure 3-5: *in vitro* TAC release from Group B matrix patches. These patches are composed of RL100 and PVP at different ratios. N = 4 each.

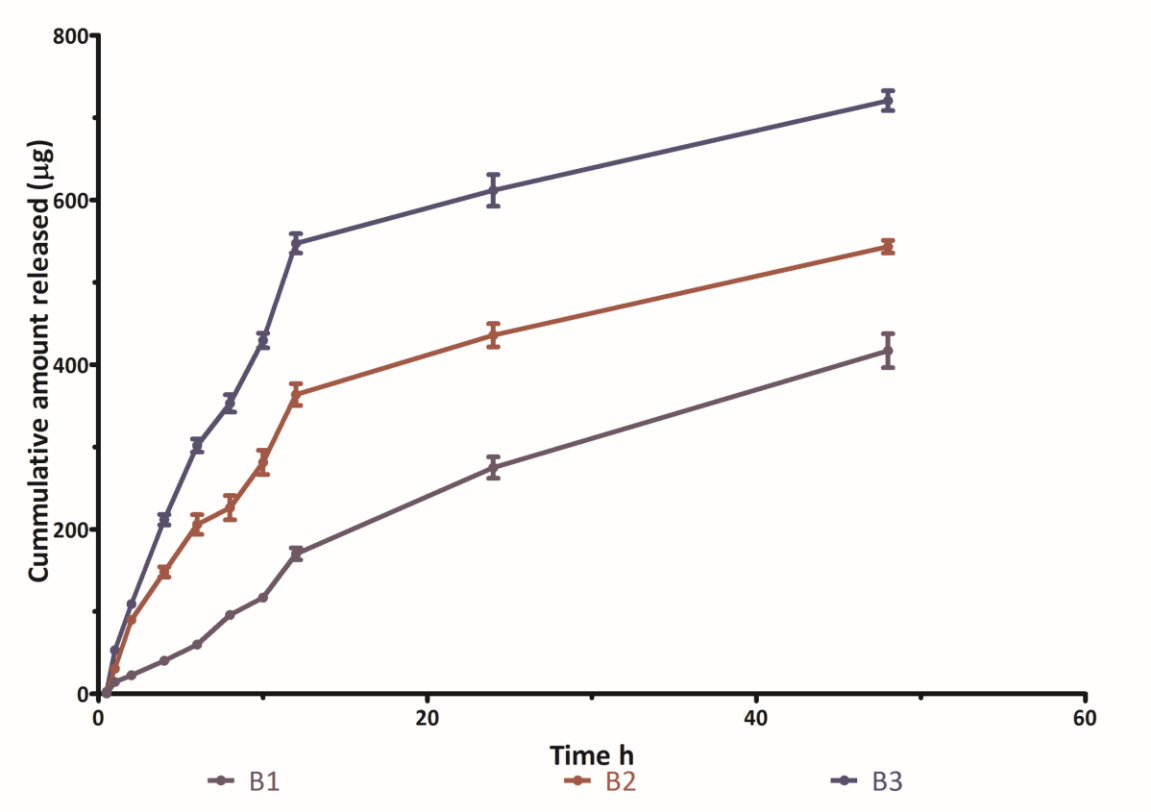

Figure 3-6: *in vitro* TAC release from Group B matrix patches fitted to first order release kinetic. These patches are composed of RL100 and PVP at different ratios. Log of remaining amount at time t is plotted against time.

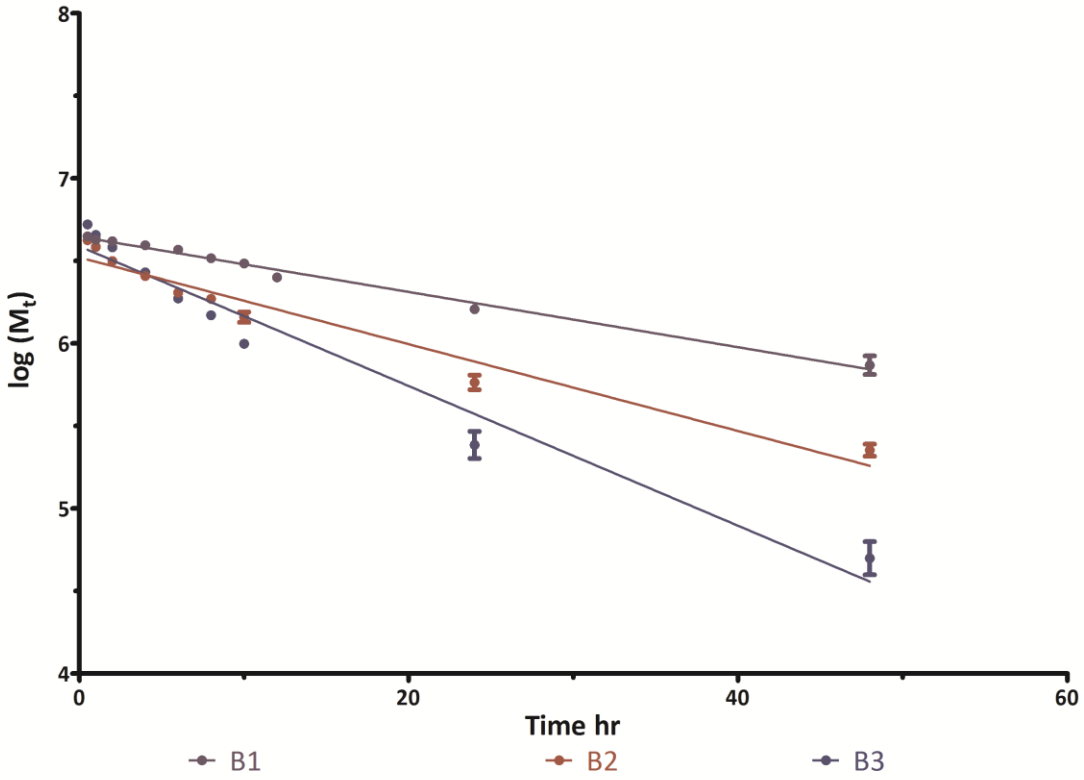

Figure 3-7: *Ex vivo* skin permeation studies. Four formulations, TAC-loaded patch with no penetration enhancer, TAC patch with 5% TPGS, TAC patch with 1% PP, and TAC patch with 1% PP and 5% TPGS are studied. Following the lag period, the slopes of the linear portion are estimated and compared. N = 4 each.

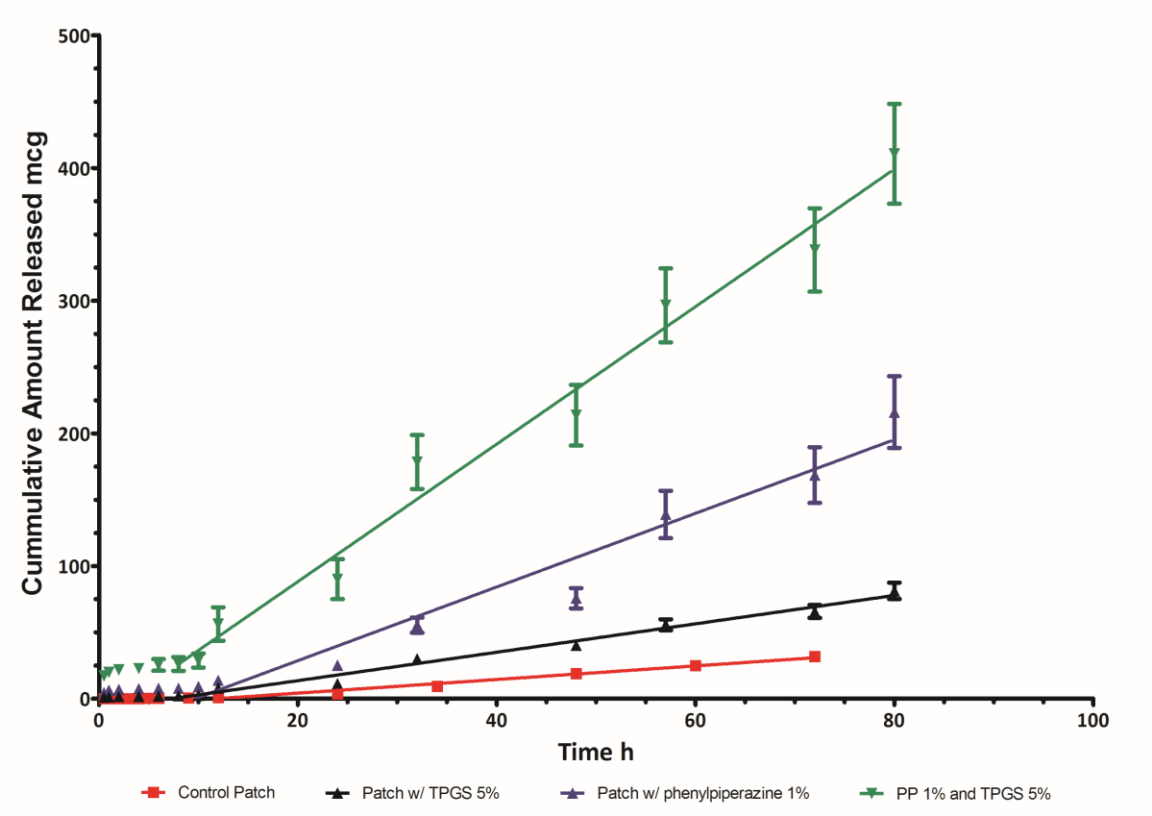

Figure 3-8: Drug compatibility study using FTIR. The FTIR spectra of the final formulation without TAC, TAC powder, and the addition spectrum are compared to TAC-loaded patch spectrum.

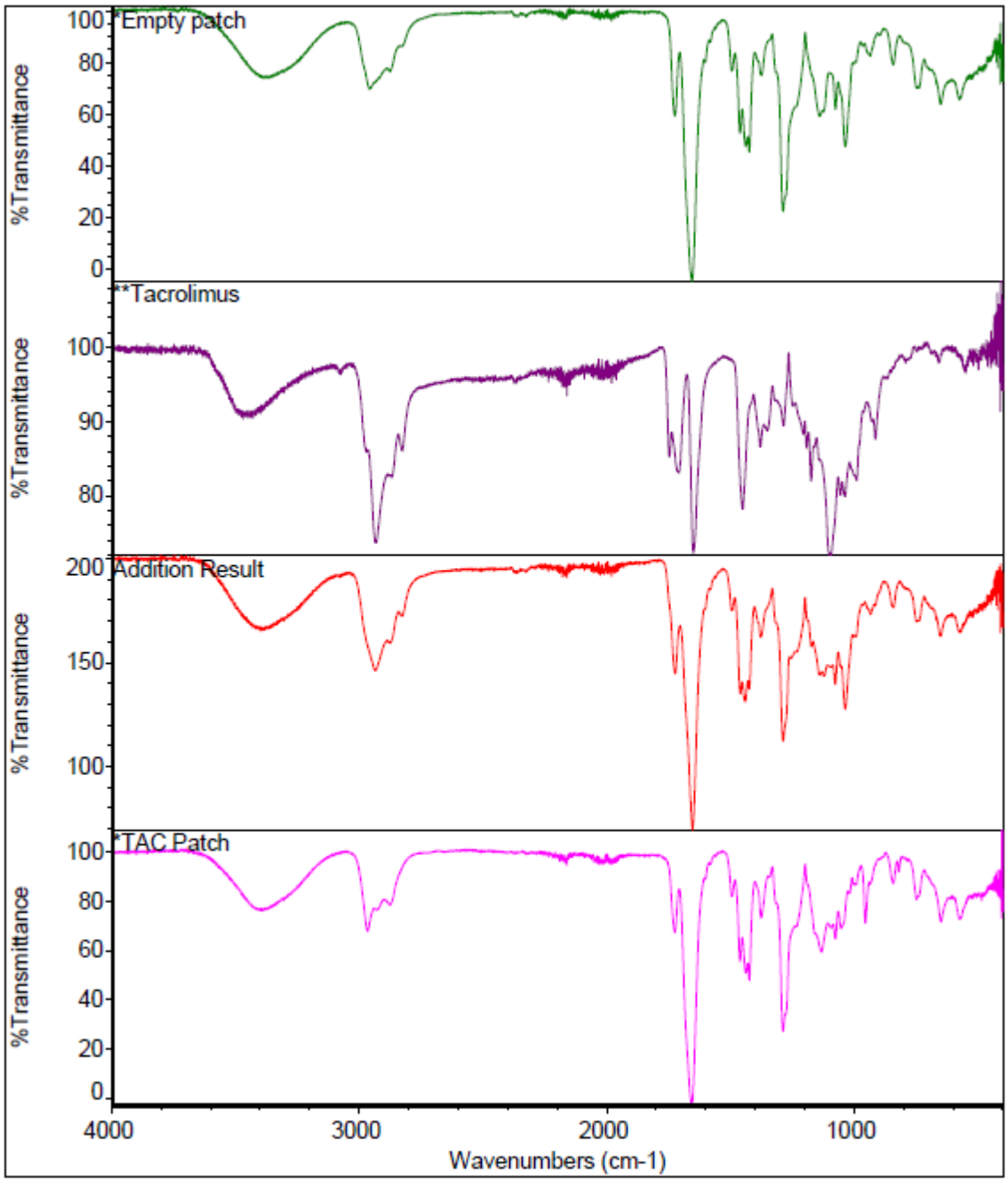

Figure 3-9: Stability of drug loaded patch stored at room temperature for 1 month

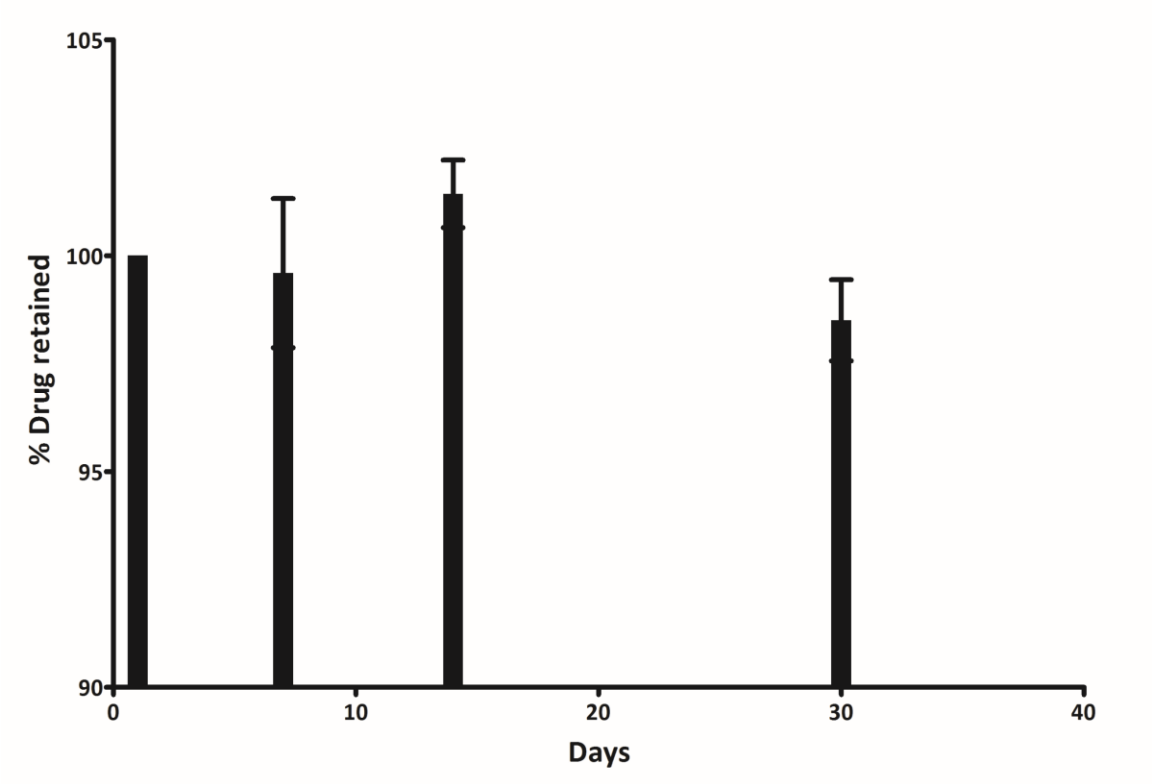

Figure 3-10: TAC concentration profiles in rats with 1, 2.5, and 5 cm^2 patches. N = 4 each.

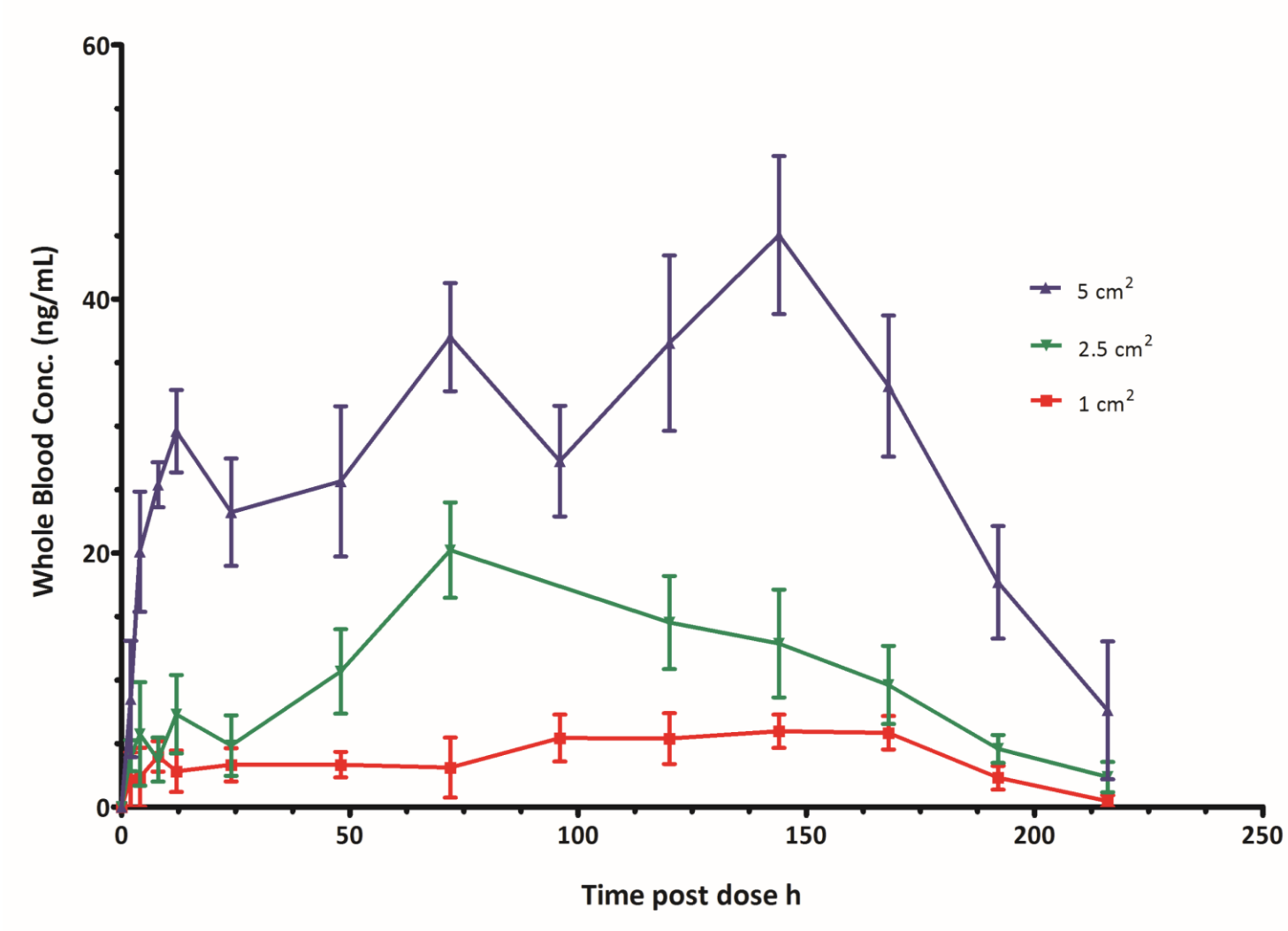

Figure 3-11: Area under the curve obtained from the PK profiles of the three patch sizes. N = 4 each.

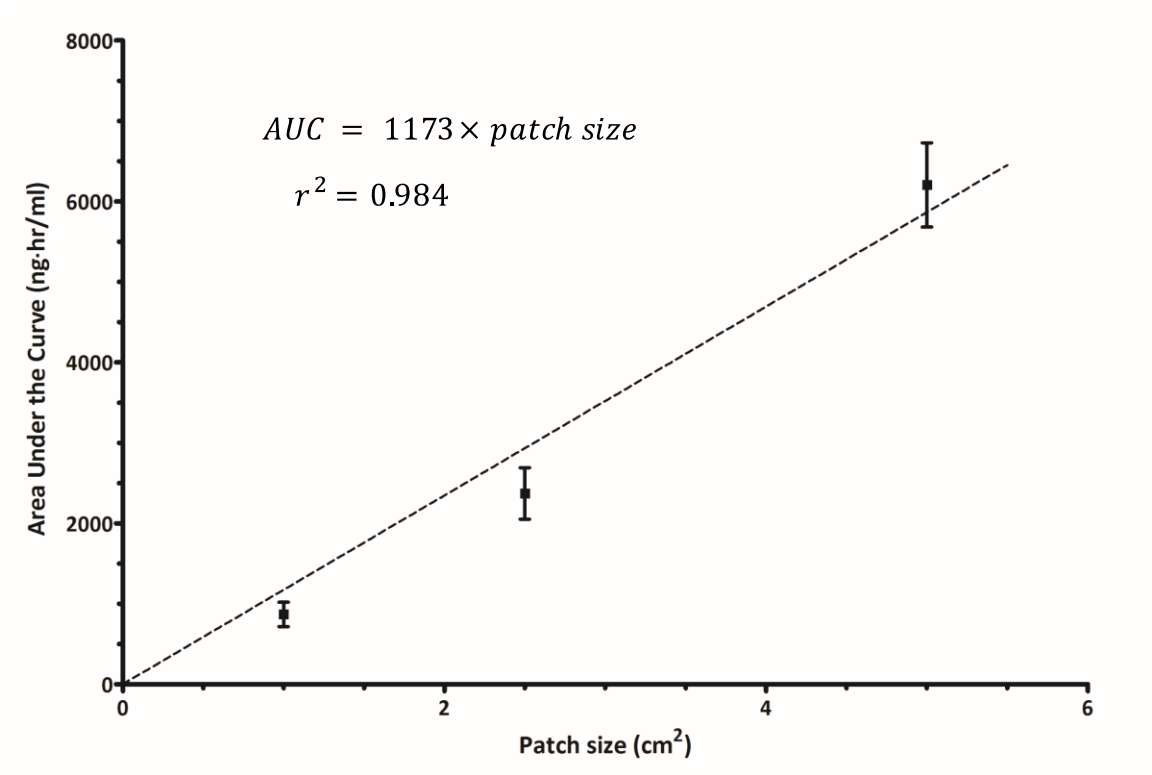

Figure 3-12: Application of transdermal patch to rat (A). Rat skin is inspected for irritation after patch is removed (B)

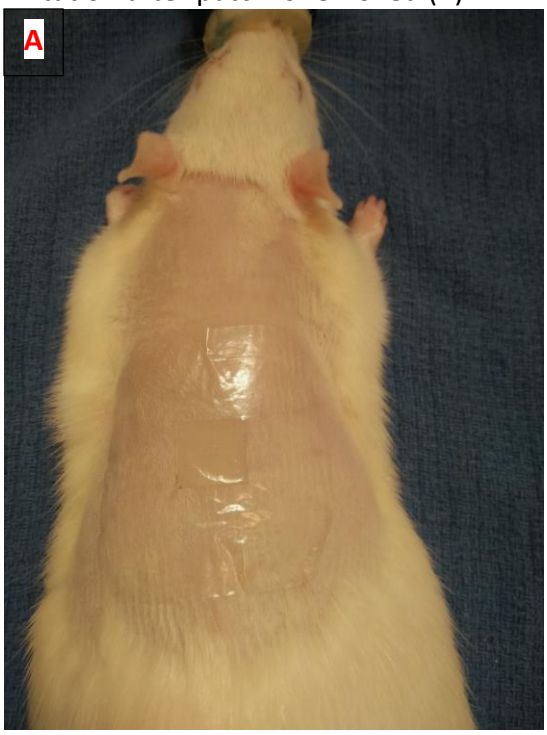

6. REFERENCES

1 North American Pediatric Renal Trials and Collaborative Studies, 2014 Annual Report. Available from: https://www.naprtcs.org. An overview of the current state of pediatric kidney transplantation across the United States. The data provide future directions for changing practices and guiding research to improve outcomes in pediatric kidney transplantation. n.d.

2 Horslen S, Barr ML, Christensen LL, Ettenger R, Magee JC. Pediatric transplantation in the United States, 1996-2005. *Am J Transplant Off J Am Soc Transplant Am Soc Transpl Surg* 2007;**7**:1339–58. https://doi.org/10.1111/j.1600-6143.2007.01780.x.

3 2010 Annual Report of the U.S Organ Procurement and Transplantation Network and the Scientific Registry of Transplant Recipients: Transplant Data 1999-2008. US Department of Health and Human Services, Health Resources and Services Administratio, Healthcare Systems Bureau, Division of Transplantatio, ROckville, MD n.d.

4 Pinsky BW, Takemoto SK, Lentine KL, Burroughs TE, Schnitzler MA, Salvalaggio PR. Transplant outcomes and economic costs associated with patient noncompliance to immunosuppression. *Am J Transplant Off J Am Soc Transplant Am Soc Transpl Surg* 2009;**9**:2597–606. https://doi.org/10.1111/j.1600-6143.2009.02798.x.

5 Yokogawa K, Takahashi M, Tamai I, Konishi H, Nomura M, Moritani S, *et al.* P-glycoprotein-dependent disposition kinetics of tacrolimus: studies in mdr1a knockout mice. *Pharm Res* 1999;**16**:1213–8.

6 Hu Y-F, Qiu W, Liu Z-Q, Zhu L-J, Liu Z-Q, Tu J-H, *et al.* Effects of genetic polymorphisms of CYP3A4, CYP3A5 and MDR1 on cyclosporine pharmacokinetics after renal transplantation. *Clin Exp Pharmacol Physiol* 2006;**33**:1093–8. https://doi.org/10.1111/j.1440-1681.2006.04492.x.

7 Steiner RW, Feist AA. The 'generic' effect of food on tacrolimus pharmacokinetics. *Clin Transplant* 2011;**25**:334–5. https://doi.org/10.1111/j.1399-0012.2010.01387.x.

8 Chisholm-Burns MA, Spivey CA, Rehfeld R, Zawaideh M, Roe DJ, Gruessner R. Immunosuppressant therapy adherence and graft failure among pediatric renal transplant recipients. *Am J Transplant Off J Am Soc Transplant Am Soc Transpl Surg* 2009;**9**:2497–504. https://doi.org/10.1111/j.1600-6143.2009.02793.x.

9 Shemesh E, Shneider BL, Savitzky JK, Arnott L, Gondolesi GE, Krieger NR, *et al.* Medication adherence in pediatric and adolescent liver transplant recipients. *Pediatrics* 2004;**113**:825–32.

10 Coilly A, Calmus Y, Chermak F, Dumortier J, Duvoux C, Guillaud O, *et al.* Once-daily prolonged release tacrolimus in liver transplantation: Experts' literature review and recommendations. *Liver Transplant Off Publ Am Assoc Study Liver Dis Int Liver Transplant Soc* 2015;**21**:1312–21. https://doi.org/10.1002/lt.24228.

11 Eisen SA, Miller DK, Woodward RS, Spitznagel E, Przybeck TR. The effect of prescribed daily dose frequency on patient medication compliance. *Arch Intern Med* 1990;**150**:1881–4.

12 Beckebaum S, Iacob S, Sweid D, Sotiropoulos GC, Saner F, Kaiser G, *et al.* Efficacy, safety, and immunosuppressant adherence in stable liver transplant patients converted from a twice-daily tacrolimus-based regimen to once-daily tacrolimus extended-release formulation. *Transpl Int Off J Eur Soc Organ Transplant* 2011;**24**:666–75. https://doi.org/10.1111/j.1432-2277.2011.01254.x.

13 Hatakeyama S, Fujita T, Yoneyama T, Yoneyama T, Koie T, Hashimoto Y, *et al.* A switch from conventional twice-daily tacrolimus to once-daily extended-release tacrolimus in stable kidney transplant recipients. *Transplant Proc* 2012;**44**:121–3. https://doi.org/10.1016/j.transproceed.2011.11.022.

14 Akchurin OM, Melamed ML, Hashim BL, Kaskel FJ, Del Rio M. Medication adherence in the transition of adolescent kidney transplant recipients to the adult care. *Pediatr Transplant* 2014;**18**:538–48. https://doi.org/10.1111/petr.12289.

15 Fredericks EM, Zelikovsky N, Aujoulat I, Hames A, Wray J. Post-transplant adjustment - The later years. *Pediatr Transplant* 2014;**18**:675–88. https://doi.org/10.1111/petr.12366.

16 Sellarés J, de Freitas DG, Mengel M, Reeve J, Einecke G, Sis B, *et al.* Understanding the causes of kidney transplant failure: the dominant role of antibody-mediated rejection and nonadherence. *Am J Transplant Off J Am Soc Transplant Am Soc Transpl Surg* 2012;**12**:388–99. https://doi.org/10.1111/j.1600-6143.2011.03840.x.

17 Kruk ME, Schwalbe N. The relation between intermittent dosing and adherence: Preliminary insights. *Clin Ther* 2006;**28**:1989–95. https://doi.org/10.1016/j.clinthera.2006.12.011.

18 Chandrashekar NS, Shobha Rani RH. Physicochemical and pharmacokinetic parameters in drug selection and loading for transdermal drug delivery. *Indian J Pharm Sci* 2008;**70**:94–6. https://doi.org/10.4103/0250-474X.40340.

19 Zadeh B, Yazdani M, Rezai S, Salimi E. The Effect of Chemical Enhancers on Tacrolimus Permeation through Rat Skin. *J Pharm Res* 2012;**5**:1309–12.

20 Mehta P, Beltz S, Kedar A, Graham-Pole J, Wingard JR. Increased clearance of tacrolimus in children: need for higher doses and earlier initiation prior to bone marrow transplantation. *Bone Marrow Transplant* 1999;**24**:1323–7. https://doi.org/10.1038/sj.bmt.1702053.

21 Prausnitz MR, Langer R. Transdermal drug delivery. *Nat Biotechnol* 2008;**26**:1261–8. https://doi.org/10.1038/nbt.1504.

22 Ng KW, Lau WM, Williams AC. Synergy Between Chemical Penetration Enhancers. In: Dragicevic N, Maibach HI, editors. *Percutaneous Penetration Enhanc. Chem. Methods Penetration Enhanc.* Berlin, Heidelberg: Springer Berlin Heidelberg; 2015. p. 373–85.

23 Karande P, Mitragotri S. Enhancement of transdermal drug delivery via synergistic action of chemicals. *Biochim Biophys Acta* 2009;**1788**:2362–73. https://doi.org/10.1016/j.bbamem.2009.08.015.

24 Paudel KS, Milewski M, Swadley CL, Brogden NK, Ghosh P, Stinchcomb AL. Challenges and opportunities in dermal/transdermal delivery. *Ther Deliv* 2010;**1**:109–31.

25 Karande P, Jain A, Mitragotri S. Discovery of transdermal penetration enhancers by high-throughput screening. *Nat Biotechnol* 2004;**22**:192–7. https://doi.org/10.1038/nbt928.

26 Koop DR, Bleyle LA, Munar M, Cherala G, Al-Uzri A. Analysis of tacrolimus and creatinine from a single dried blood spot using liquid chromatography tandem mass spectrometry. *J Chromatogr B Analyt Technol Biomed Life Sci* 2013;**926**:54–61. https://doi.org/10.1016/j.jchromb.2013.02.035.

27 Kong R, Bhargava R. Characterization of porcine skin as a model for human skin studies using infrared spectroscopic imaging. *The Analyst* 2011;**136**:2359–66. https://doi.org/10.1039/c1an15111h.

28 Gray GM, White RJ. Glycosphingolipids and ceramides in human and pig epidermis. *J Invest Dermatol* 1978;**70**:336–41.

29 Jampilek J, Brychtova K. Azone analogues: classification, design, and transdermal penetration principles. *Med Res Rev* 2012;**32**:907–47. https://doi.org/10.1002/med.20227.

30 Sugibayashi K, Nakayama S, Seki T, Hosoya K, Morimoto Y. Mechanism of skin penetration-enhancing effect by laurocapram. *J Pharm Sci* 1992;**81**:58–64.

31 López-Cervantes M, Márquez-Mejía E, Cázares-Delgadillo J, Quintanar-Guerrero D, Ganem-Quintanar A, Angeles-Anguiano E. Chemical enhancers for the absorption of substances through the skin: Laurocapram and its derivatives. *Drug Dev Ind Pharm* 2006;**32**:267–86. https://doi.org/10.1080/03639040500518708.

32 Yang C, Wu T, Qi Y, Zhang Z. Recent Advances in the Application of Vitamin E TPGS for Drug Delivery. *Theranostics* 2018;**8**:464–85. https://doi.org/10.7150/thno.22711.

33 Guo Y, Luo J, Tan S, Otieno BO, Zhang Z. The applications of Vitamin E TPGS in drug delivery. *Eur J Pharm Sci Off J Eur Fed Pharm Sci* 2013;**49**:175–86. https://doi.org/10.1016/j.ejps.2013.02.006.

34 *TPGS Regulatory Status*. n.d. URL: http://tpgs.com/tpgs-technical-info/tpgs-regulatory-status/.

35 Whitehead K, Mitragotri S. Mechanistic analysis of chemical permeation enhancers for oral drug delivery. *Pharm Res* 2008;**25**:1412–9. https://doi.org/10.1007/s11095-008-9542-2.

36 Bzik VA, Brayden DJ. An Assessment of the Permeation Enhancer, 1-phenyl-piperazine (PPZ), on Paracellular Flux Across Rat Intestinal Mucosae in Ussing Chambers. *Pharm Res* 2016;**33**:2506–16. https://doi.org/10.1007/s11095-016-1975-4.

37 Thakral S, Thakral NK, Majumdar DK. Eudragit: a technology evaluation. *Expert Opin Drug Deliv* 2013;**10**:131–49. https://doi.org/10.1517/17425247.2013.736962.

38 Okabe H, Hashimoto Y, Inui KI. Pharmacokinetics and bioavailability of tacrolimus in rats with experimental renal dysfunction. *J Pharm Pharmacol* 2000;**52**:1467–72.

39 Staatz CE, Tett SE. Clinical Pharmacokinetics of Once-Daily Tacrolimus in Solid-Organ Transplant Patients. *Clin Pharmacokinet* 2015;**54**:993–1025. https://doi.org/10.1007/s40262-015-0282-2.

40 Molinuevo JL, Arranz FJ. Impact of transdermal drug delivery on treatment adherence in patients with Alzheimer's disease. *Expert Rev Neurother* 2012;**12**:31–7. https://doi.org/10.1586/ern.11.178.

Chapter 4.

GENERAL CONCLUSION

TAC is the most commonly used immunosuppressant in post transplantation maintenance therapy. Being a highly potent drug, it requires a strict control of trough concentration in whole blood to avoid side effects. My work has demonstrated the feasibility of controlled release of TAC utilizing two dosage forms for two different routes of administration. The first is an injectable thermosensitive hydrogel formulation, and the second is a transdermal patch incorporating synergistic penetration enhancers.

My work on injectable thermosensitive hydrogels has resulted in two hydrogel platforms capable of delivering TAC within therapeutic window for up to 7 days. Current hydrogel platforms on the market, especially ester-based ones are susceptible to initial burst release when a lipophilic drug molecule is loaded in the formulation. This burst effect presents a significant challenge to delivery of potent compound such as TAC. The burst effect is thought to be the result of the crystallization of the micellar core when the polymer solution undergoes thermogelation. To overcome this burst effect, I have loaded TAC into a nanoparticle platform. By loading TAC into PEG_{5k}-*b*-PCL_{10k} nanoparticle, the stable formulation also allows the incorporation of TAC into the hydrogel solution without using toxic organic solvent. The TAC-NP-PVL hydrogel composite demonstrates no burst effect when compares to the TAC-loaded PVL hydrogel alone. The TAC-NP-PVL hydrogel composite formulation is capable of sustaining TAC concentration within the 5-15 ng/ml in rat PK studies.

The second thermosensitive hydrogel formulation is based on polyamino polymers. I have successfully synthesized and characterized a library of polyaspartate- and polyglutamate-based polymers for their gelation properties. Three polyaspartate polymers are identified to be able to undergo thermosensitive gelation, where the transition temperature is dependent on the polymer concentration and hydrophobicity. The gelation mechanism is shown to be due to aggregation of β-sheet formation of the polymer. This phenomenon allows a smaller burst release of TAC from the gel demonstrated both *in vitro* and *in vivo*. The aminoGel formulations show a sustained release profile of TAC over a 7-day period

in rats. The future direction for the two hydrogel platforms is to reproduce their PK profiles in human clinical trials. Both platforms can be utilized in either induction or maintenance phase of TAC immunosuppression therapy post solid organ transplantation.

Another formulation that has been developed for TAC in my studies is a transdermal patch incorporating synergistic penetration enhancers. TAC is a large molecule beyond the ideal molecular size for transdermal delivery. Here we have demonstrated the feasibility of delivering such molecule across the skin barrier using a pair of synergistic enhancers, phenylpiperazine and TPGS. By incorporating the drug and penetration enhancers into a matrix type transdermal patch using Eudragit RL100 and PVP K30 at 2:8 ratio as matrix formers, the patch is found to deliver TAC across pig ear skin in Franz diffusion experiment at a rate of 5.11±0.71 $\mu g/cm^2/hr$. The release rate is confirmed in rat PK studies. The patch size of 2.5 cm^2 is shown to be able to maintain TAC concentration within the therapeutic range for up to 7 days. The patch size can be cut to accommodate different release rates, allowing for customized dosing based on weight and scaling to other animal models.

Overall, the formulations developed from our studies would add into the repertoires of available formulations for transplantation clinicians. These formulations can be used to maintain patients who demonstrate difficulties in adhering to their oral TAC regimens or variability in their absorption following TAC administration.